

In presenting the dissertation as a partial fulfillment of the requirements for an advanced degree from the Georgia Institute of Technology, I agree that the Library of the Institute shall make it available for inspection and circulation in accordance with its regulations governing materials of this type. I agree that permission to copy from, or to publish from, this dissertation may be granted by the professor under whose direction it was written, or, in his absence, by the Dean of the Graduate Division when such copying or publication is solely for scholarly purposes and does not involve potential financial gain. It is understood that any copying from, or publication of, this dissertation which involves potential financial gain will not be allowed without written permission.

7/25/68

A SIMPLE MODEL OF DYNAMIC CLEAVAGE

A THESIS

Presented to

The Faculty of the Graduate Division

by

Han Pin Kan

In Partial Fulfillment

of the Requirements for the Degree

Doctor of Philosophy


in the School of Engineering Science and Mechanics

Georgia Institute of Technology

August 1971

A SIMPLE MODEL OF DYNAMIC CLEAVAGE

Approved:


Chairman

Date approved by Chairman: August 21, 1971

ACKNOWLEDGEMENTS

The author wishes to express his appreciation, very sincerely, to his thesis advisors, Dr. W. W. King and Dr. J. M. Anderson, for suggesting the topic and giving continuous guidance and encouragement throughout this work. Appreciation is also extended to Dr. M. Stallybrass for his service as a member of the reading committee. The author is grateful to Dr. M. E. Ravielle, Director of the School of Engineering Science and Mechanics, for his arrangement of the author's plan of study at the Georgia Institute of Technology.

The work in this thesis has been supported by the National Science Foundation under Grant Number GK-5529.

TABLE OF CONTENTS

	Page
ACKNOWLEDGEMENTS	ii
LIST OF TABLES	iv
LIST OF ILLUSTRATIONS.	v
SUMMARY.	viii
Chapter	
I. INTRODUCTION.	1
II. A SIMPLE MECHANICAL MODEL	9
The Properties and Construction of the Model	
The Equation of Motion	
Foundation Laws	
III. ANALYSIS OF THE EQUATION OF MOTION.	18
Nondimensionalization of the Equation of Motion	
Static Solutions	
The Method of Characteristics	
IV. NUMERICAL RESULTS	35
Disturbed Mobile Equilibrium Crack	
Suddenly Applied Load	
Initial Velocity Problem	
Periodic Loading	
Effects of Small Damping	
V. SUMMARY AND CONCLUSIONS	94
APPENDIX	100
LITERATURE CITED	110
VITA	112

LIST OF TABLES

Table	Page
1. Analytical Expression of Foundation Laws	17
2. Effect of Damping on the Pattern of Crack Propagation.	94

TABLE OF ILLUSTRATIONS

Figure	Page
1. An Idealized Atomic Structure Near the Tip of a Cleavage Crack	2
2. A General Form of the Force-separation Law	3
3. Proposed Simple Mechanical Model	11
4. A Segment of the Deflected String.	13
5. The Foundation Laws.	16
6. String in Equilibrium Under External Load, $P(X)$, and Foundation Reaction, $Q_1 + Q_2$	22
7. Critical Equilibrium Load Versus Crack Length, $b=\infty$	25
8. Critical Equilibrium Load Versus Crack Length, $b=20$	27
9. a. Distribution of Foundation Reaction and Applied Load b. Critical Equilibrium Profile of the String	29
10. A General Characteristic Net and its Interior Element.	33
11. Region of Integration and its Elements	36
12. Crack Length Versus Time, $b=\infty$	40
13. Velocity of Crack Propagation, $b=\infty$	41
14. Displacement Profiles of the String at Selected Time. $a(0) = 5, b = \infty, \epsilon = 0.01$	42
15. Displacement Profiles of the String at Selected Time. $a(0) = 10, b = \infty, \epsilon = 0.01$	43
16. Displacement History at Selected Points on the String. $a(0) = 5, b = \infty, \epsilon = 0.01$	44
17. Displacement History at Selected Points on the String. $a(0) = 10, b = \infty, \epsilon = 0.01$	45

Figure	Page
18. Crack Length Versus Time. $b=20$	46
19. Velocity of Crack Propagation. $b=20$	47
20. Unstable Crack Propagation. $a(0) = 5, b=\infty$	48
21. Stable Crack Propagation. $a(0) = 5, b=20$	49
22. Stable Crack Propagation. $a(0) = 10, b=20$	50
23. Displacement Profiles of the String at Selected Time . $a(0) = 5, b=20, \epsilon = 0.01$	51
24. Displacement Profiles of the String at Selected Time . $a(0) = 10, b=20, \epsilon = 0.01$	52
25. Displacement History at Selected Points on the String . $a(0) = 5, b=20, \epsilon = 0.05$	53
26. Displacement History at Selected Points on the String . $a(0) = 10, b=20, \epsilon = 0.05$	54
27. Region of Integration and its Elements.	56
28. Displacement History of the Initial Crack Tip . $a(0) = \infty$	60
29. Location of the Cracks. $a(0) = \infty, P = 0.95$	61
30. Displacement Profiles of the String at Selected Time . $a(0) = \infty, P = 0.95$	62
31. Successive Displacement Profiles Show Forming of a Secondary Crack. $a(0) = \infty, P = 0.95$	63
32. Displacement History at Selected Points on the String . $a(0) = \infty, P = 0.95$	64
33. Location of the Cracks. $a(0) = 5, P = 0.95$	65
34. Location of the Cracks. $a(0) = 10, P = 0.95$	66
35. Location of the Cracks. $a(0) = 20, P = 0.95$	67
36. Decomposition of Displacement History . $a(0) = \infty, P = 0.95, X = 10$	68

Figure	Page
37. Decomposition of Displacement History . $a(0) = \infty$, $P = 0.95$, $X = 30$	69
38. Displacement History of the Initial Crack Tip . $a(0) = \infty$	72
39. Location of the Cracks. $a(0) = \infty$, $V_0 = 0.67$	73
40. Displacement Profiles of the String at Selected Time . $a(0) = \infty$, $V_0 = 0.67$	74
41. Displacement History at Selected Points on the String . $a(0) = \infty$, $V_0 = 0.67$	75
42. Location of the Cracks. $a(0) = 5$, $V_0 = 0.67$	76
43. Location of the Cracks. $a(0) = 10$, $V_0 = 0.67$	77
44. Pattern of Secondary Cracks Under Varying Load Ratios . $\omega = 1$, $T = 80$	81
45. Pattern of Secondary Cracks Under Varying Driving Frequencies. $P/P_{cr} = 0.95$, $T = 80$	82
46. Location of the Cracks. $P/P_{cr} = 0.95$	83
47. Displacement Profiles of the String at Selected Time . $\omega = 0.4$, $P/P_{cr} = 0.95$	84
48. Displacement History at Selected Points on the String . $\omega = 0.4$, $P/P_{cr} = 0.95$	85
49. A Modified Model Showing Material Damping Effect.	87
50. Displacement History at Selected Points on the String . $\beta = 0.01 \beta_{cr}$, $P/P_{cr} = 0.95$	89
51. Displacement Profiles of the String at Selected Time . $P/P_{cr} = 0.95$	90
52. Displacement History at $X = 20$. $P/P_{cr} = 0.95$	91
53. Effect of Damping on the Pattern of Secondary Cracks . $P/P_{cr} = 0.95$	92
A-1. Region of Integration for Equation (A-8).	103
A-2. The Path of the Crack Tip Divides R into S_1 and S_2	106

SUMMARY

In this thesis a simple mechanical model is proposed for the study of dynamic cleavage. The model consists of a taut string supported by an elastic but fracturable foundation. The foundation reaction is governed by a nonlinear law patterned in form after the force-separation law for two isolated atoms.

The equation governing the string motion is a one-dimensional wave equation. Because of the foundation law, this equation is essentially nonlinear. The equation of motion is solved numerically by the method of characteristics, and results are presented for a series of initial-boundary value problems. These results describe the effects of four different loading histories - quasi-static, suddenly applied and maintained, impulsive and periodic - and considers some of the consequences of introducing damping in the model.

Results of this study show that an initial crack in the foundation may propagate in significantly different ways, depending on how the transverse load is applied. The initial crack propagates continuously when the string is brought to its mobile equilibrium position quasi-statically and then disturbed slightly. However, when the load is applied dynamically, the extension of the initial crack is accompanied by the formation of new and separate cracks - secondary cracks. The formation of secondary cracks persists when small viscous damping is introduced in the model.

CHAPTER I

INTRODUCTION

Cleavage is the act of **splitting** a material, usually along a natural line of division. In a crystalline solid, for example, cleavage can only occur on certain planes called cleavage planes. Thus the two new surfaces produced are more or less smooth.

Cleavage of a crystal occurs when it is deformed so severely as to break the interatomic bonds across a cleavage plane. However, these bonds are not broken simultaneously over the whole plane. An essential feature in the cleavage of a crystalline solid is the successive separation of atoms at the tip of a cleft or crack. To illustrate this, an idealized atomic structure near the tip of a cleavage crack is shown in Figure 1.

When remote forces are applied that tend to extend the crack, atoms on opposite sides of the cleavage plane begin to separate in accordance with a force-separation law having the general form indicated in Figure 2. In so far as the interior of the solid is concerned, the separation is most acute near the tip of the crack and increases as the remote forces increase. The interatomic forces opposing the separation increase until they reach a maximum; these forces then diminish rapidly with further increase in separation. Finally the pair of atoms at the crack tip move "out-of-range" as to their mutual attraction. At this time, they become part of the new crack surface and the next pair enters the final stages of separation. These then move out of range and so on.

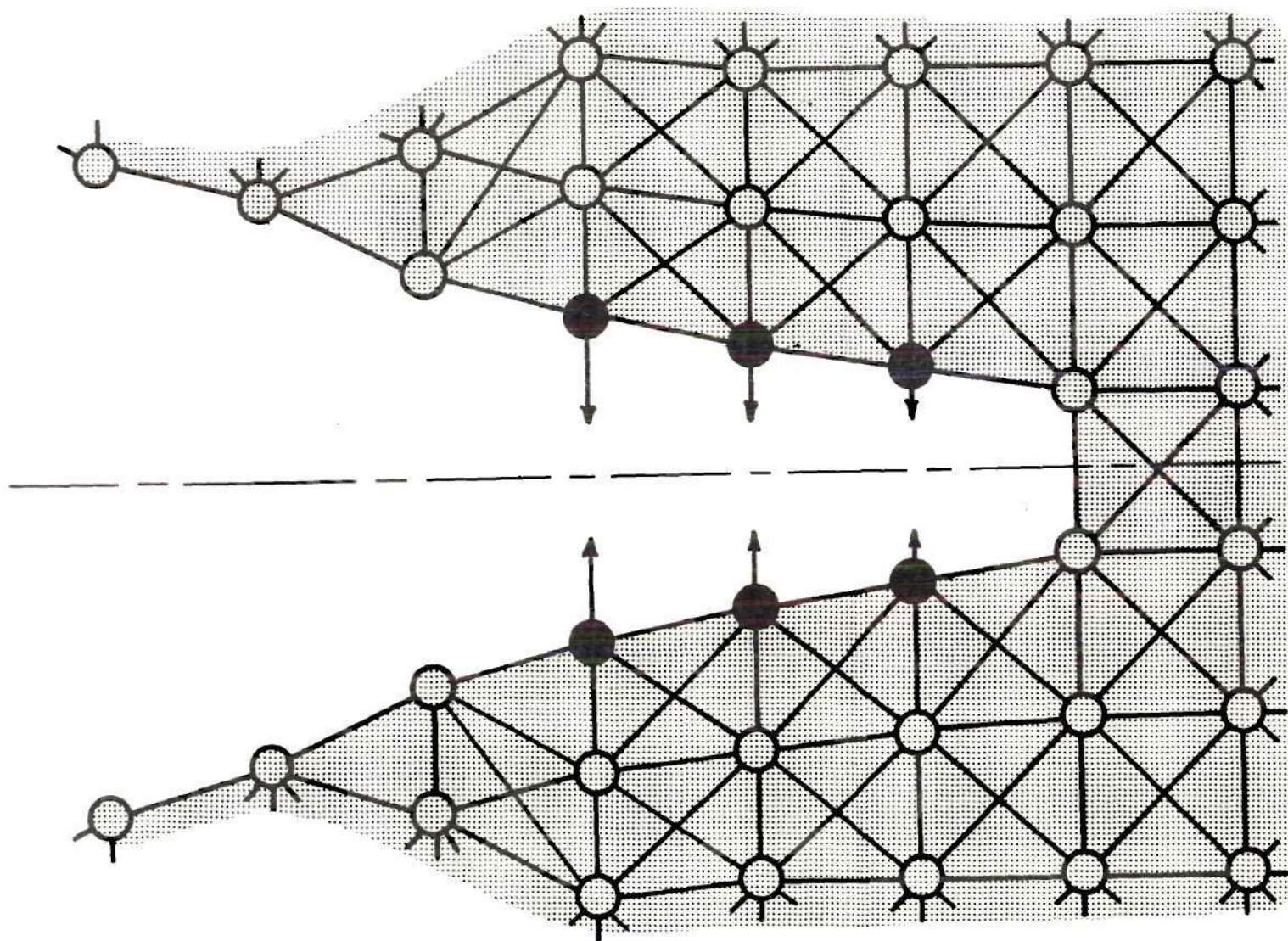


Figure 1. An Idealized Atomic Structure Near the Tip of a Cleavage Crack.

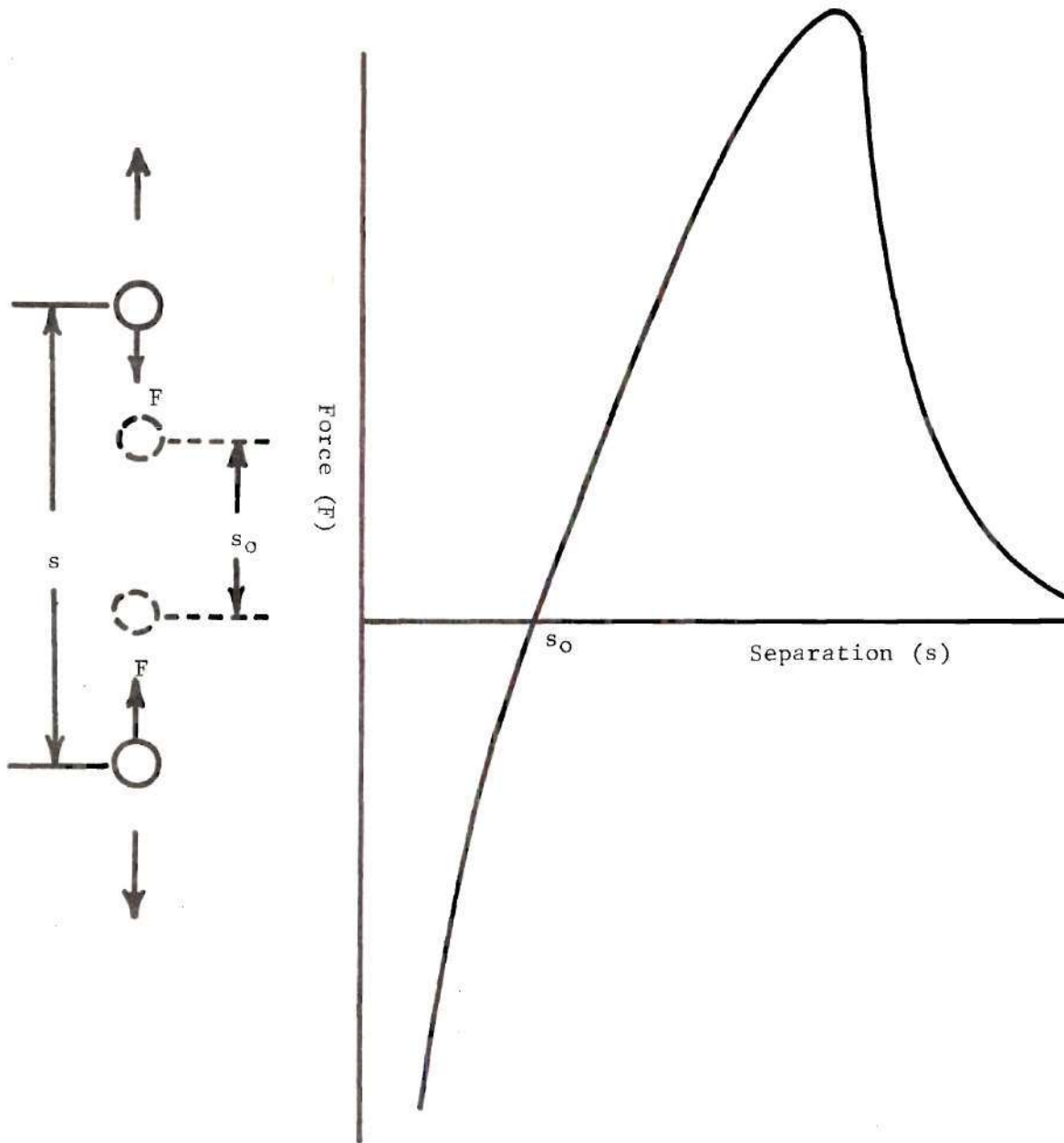


Figure 2. A General Form of the Force-separation Law.

If the remote forces are applied gradually, the initial stage of cleavage, when the interatomic forces remain on the rising branch of the curve in Figure 2, can be regarded as a quasi-static process. In fact, the inherent nonlinearity of cleavage is not manifested in the initial stage. However, as the separation at the crack tip approaches the value corresponding to maximum interatomic attraction, it increases very rapidly with any increase in remote forces, no matter how gradually applied. In this stage of cleavage, inertia effects and nonlinearity cannot be reasonably ignored.

Just over fifty years ago, Griffith [1]⁽¹⁾ made the first fruitful effort to model cleavage. Griffith's model represents an initial crack in a solid by a vanishingly thin slit in an infinite, linearly-elastic continuum. Points on the prolongation of the slit are assumed to remain fixed as a remote tension perpendicular to the slit is applied. The solution to this problem was already available to Griffith; it had been found earlier by Inglis [2] subject to the usual assumption of small deformations. Griffith used Inglis's solution to compute the strain energy stored in the solid, and by incorporating surface energy in an energy balance, he obtained the remote tension required for an imagined quasi-static and infinitesimal extension of the slit. The stresses (and strains) used by Griffith in his calculation are singular at the ends of the slit and consequently represent a local violation of the assumption of small deformations. In spite of its more obvious shortcomings⁽²⁾,

(1) Numbers inside brackets refer to references on p.110.

(2) For a comprehensive and detailed critique of Griffith's theory see J. N. Goodier [3,p.18].

the Griffith theory has dominated subsequent efforts to model and analyze the cleavage process.

The Griffith theory of cleavage assumes a perfectly brittle material. Irwin [4] and Orowan [5] have extrapolated Griffith's result to include plastic deformation confined to a small region just ahead of the crack tip by introducing an "effective surface energy".

A recent paper by Barenblatt [6] gives a more realistic description of the crack tip. Barenblatt's theory rests on the following two hypotheses: "the first is that the area of the part of the crack surface acted upon by the [nonlinear] forces of cohesion can be considered as negligibly small compared to the entire area of the crack surface ... second ... [when the crack is at the point of extending] the form of the crack surface (and consequently, the local distribution of the forces of cohesion) near the edges ... does not depend on the applied load." Using these hypotheses in conjunction with the methods of linear elasticity, Barenblatt obtained a criterion for crack extension. This criterion is equivalent to that of Griffith by proper interpretation of Barenblatt's limiting distribution of cohesive forces in terms of surface tension.

In order to examine Barenblatt's hypotheses for Griffith's original problem, Goodier and Kanninen [7] introduced a model in which the forces across the cleavage plane are replaced by the reaction of nonlinear springs. Stresses to either side of the cleavage plane are taken to be those found in a linearly elastic solid. This model allows the essential nonlinearity of the cleavage process to be dealt with directly. Results obtained with the Goodier-Kanninen model lend support to Barenblatt's hypotheses.

For the three models so far discussed, the remote forces leading to crack extension must be applied slowly enough to warrant the neglect of inertia forces. Indeed in Griffith's theory, the crack extension is assumed to occur so slowly that no kinetic energy is developed. In less ideal situations, once a crack begins to extend, it may continue to do so at an alarming rate, and in such cases, the inertia of the material near the crack tip cannot be ignored.

Using dimensional analysis and estimating velocities from the quasi-static displacement field, Mott [8] considered consequences of including the kinetic energy in Griffith's energy balance. In analyzing Griffith's problem, Mott concluded with the suggestion that the velocity of propagation of a crack in a brittle material will tend towards a value of the order of the velocity of sound in the material, and which is independent of the stress applied or of the atomic cohesive forces across the cleavage plane.

Yoffe [9] obtained the first solution to the field equations of dynamic elasticity theory which satisfied boundary conditions appropriate (in the Griffith sense) to a moving crack. She considered a Griffith crack of constant length travelling through an infinite elastic plate subjected to uniform remote tension. The crack was presumed to move at a constant speed in a straight line collinear with its length. The stress field established near the crack tip is such that if the prescribed crack speed exceeds a certain value, the direction of maximum tensile stress is no longer perpendicular to the assumed propagation direction-- indicating a possible limiting speed for the propagation of a straight crack. Broberg [10] and Craggs [11] later also obtained

exact solutions to similar problems involving the steady propagation of a crack. Their conclusions are in agreement with Yoffe's regarding possible branching of the crack. Moreover, Craggs points out that the forces required to maintain a steady crack speed decrease as the speed increases.

Ang [12] investigated an unsteady field of stresses and strains by considering the transient response of an infinite elastic plate when a force applied on and normal to the crack surface suddenly moves with constant speed away from the tip of a semi-infinite crack. Baker [13] has obtained the transient response of a stretched infinite elastic plate when a semi-infinite crack suddenly appears and extends at a constant speed.

The present information concerning the nature of unsteady crack propagation is very limited. Erdogan [14] emphasized this in a recent review paper by stating that we need "a solution for an accelerating crack for the simplest possible case". To this end the unsteady crack propagation problems that have received the most attention to date are the so-called anti-plane or "shear crack" problems, which require the solution of only one wave equation. Such problems have been treated analytically by Kostrov [15] and Eshelby [16].

The preceding brief review of certain investigations into the nature of dynamic crack propagation indicates that the investigators have either assigned a constant crack speed or treated anti-plane strain problems. In all cases, the model used is that of a slit running through a linearly elastic continuum so that the inherent nonlinearity of the process is confronted only to the extent of applying Barenblatt-type

hypotheses.

The following study proposes a relatively simple mechanical model which exhibits the more significant features of crack propagation. The model is a taut string resting on an elastic but fracturable foundation; it will be discussed in detail in Chapter II. Such a model allows a defect (crack) to grow at a rate dictated not by the analyst but by the intrinsic separation properties of the foundation. The inertia forces and nonlinearity can be taken into account due to the relative simplicity of mathematical formulation presented in Chapter III.

By using the method of characteristics, the numerical solutions of various initial-boundary value problem are obtained and discussed in Chapter IV. These results describe the kinetics of the crack tip and the wave effects on the other parts of the string during the process of crack extension. It will be seen that the model, in responding to a variety of dynamic loads, predicts the formation of secondary cracks in addition to the simple extension of the primary crack.

CHAPTER II

A SIMPLE MECHANICAL MODEL

In the preceding chapter, we discussed the cleavage of a crystalline solid, and in describing the essential features of the process, we used the lattice or particle model to represent the solid. While this model is useful for just such discussions and descriptions, it is beset with severe mathematical difficulties which make the model impractical for quantitative analysis. On the other hand, using a continuum model to represent the solid, we reduce the mathematical difficulties but at a cost of making indistinguishable precisely those features of cleavage we wish to study in detail. A hybrid model, such as the one proposed by Goodier and Kanninen, would seem a reasonable compromise for studying quasi-static or steady crack propagation, but to determine and analyze the unsteady response of such a complex model seems too ambitious for a first effort.

The Properties and Construction of the Model

In this chapter, we set ourselves the problem of constructing a mechanical model which will be simple enough to be mathematically tractable and yet elaborate enough to exhibit what we have described as the essential features of dynamic cleavage. Such a model's properties would necessarily include:

- (i) a sufficiently simple analytical description to facilitate at least a numerical solution to a meaningful initial-boundary value problem;

- (ii) a capacity for the accelerated growth of a defect (crack);
- (iii) an intrinsic mechanical criterion for the formation and growth of such a defect;
- (iv) the capacity for propagating mechanical disturbances.

One of the simpler mechanical systems having these properties consists of a taut string supported by an elastic but fracturable foundation. Figure 3 shows the proposed model. The two-sided foundation is piecewise continuous and is represented in the figure by a dense array of springs. The spring law is patterned in form after the force-separation law for two isolated atoms (see Figure 2). This feature makes the foundation fracturable; it also makes the problem of determining the response of this model necessarily nonlinear.

When there are no transverse loads applied to the string, it takes the level equilibrium position with no reaction from either side of the foundation. If a transverse load is applied which causes points on the string to be displaced vertically upwards, the springs comprising the lower side of the foundation are stretched by varying amounts, and the springs of the upper side are compressed by corresponding amounts. In continuing this description and in all that follows, it will be convenient to refer to the lower and upper sides of the foundation as the tensile and compressive foundations respectively.

Both foundations continue to oppose any increase in vertical displacement until a specified critical displacement is exceeded by some segment of the string. The corresponding segment of the tensile foundation is then recognized as being fractured. This means that over

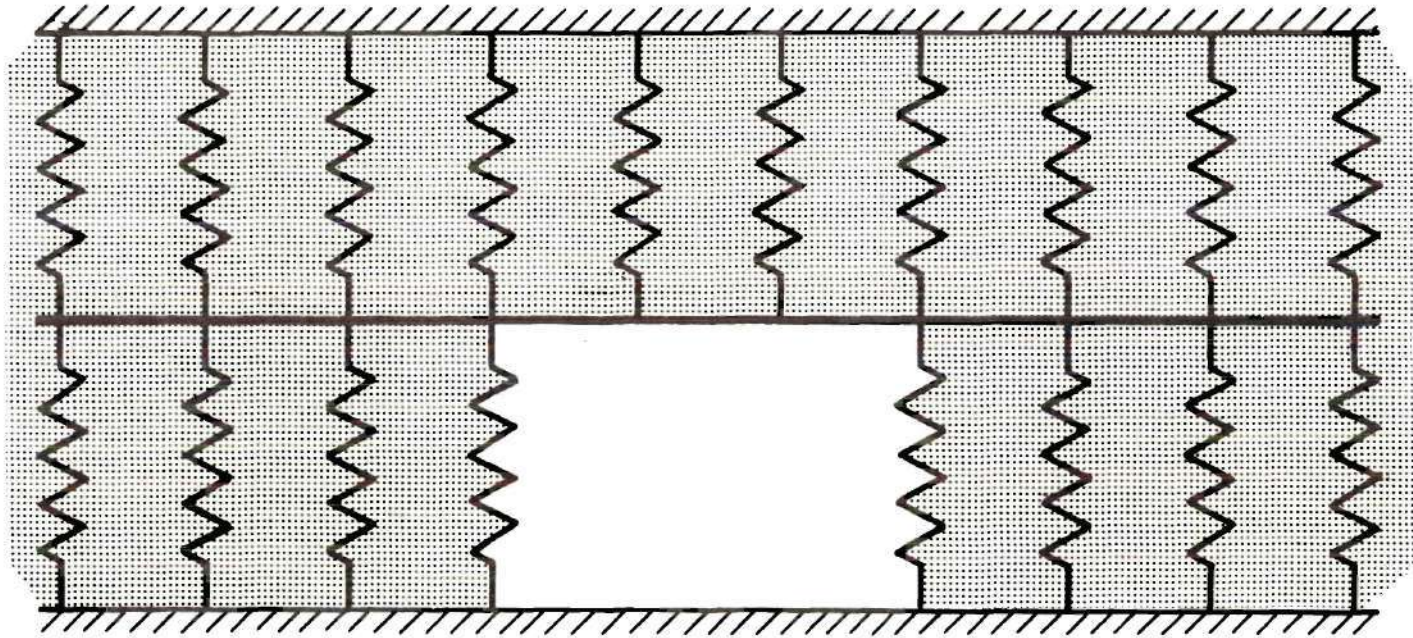


Figure 3. Proposed Simple Mechanical Model.

the extent of the fracture, the tensile foundation is incapable of exerting any force on the string even if the displacement should subsequently become less than critical. With the reader's indulgence, we shall refer to such a fractured segment of the tensile foundation as a "crack" and to its ends as "crack tips".

The Equation of Motion

Figure 4 shows an infinitesimal segment of the deflected string stretched by a constant tension S . The mass per unit length of the string is denoted by the constant ρ . The spatial, x , axis is coincident with the equilibrium position of the unloaded string, and t is the time. Assuming the transverse displacement $w(x,t)$ is everywhere small during the motion, we can write Newton's equation of motion in the transverse direction of the string as

$$S \frac{\partial^2 w}{\partial x^2} + f(w,x,t) = \rho \frac{\partial^2 w}{\partial t^2}, \quad (1)$$

where $f(w,x,t)$ is the total transverse force per unit length acting on the string. Equation (1) is a one-dimensional wave equation.

The function $f(w,x,t)$ includes the reactions of the tensile and compressive foundations and any externally applied load. If we denote these three components of $f(w,x,t)$ by $-q_1(w)$, $-q_2(w)$ and $p(x,t)$ respectively, the equation of motion becomes

$$S \frac{\partial^2 w}{\partial x^2} - \rho \frac{\partial^2 w}{\partial t^2} = q_1(w) + q_2(w) - p(x,t);$$

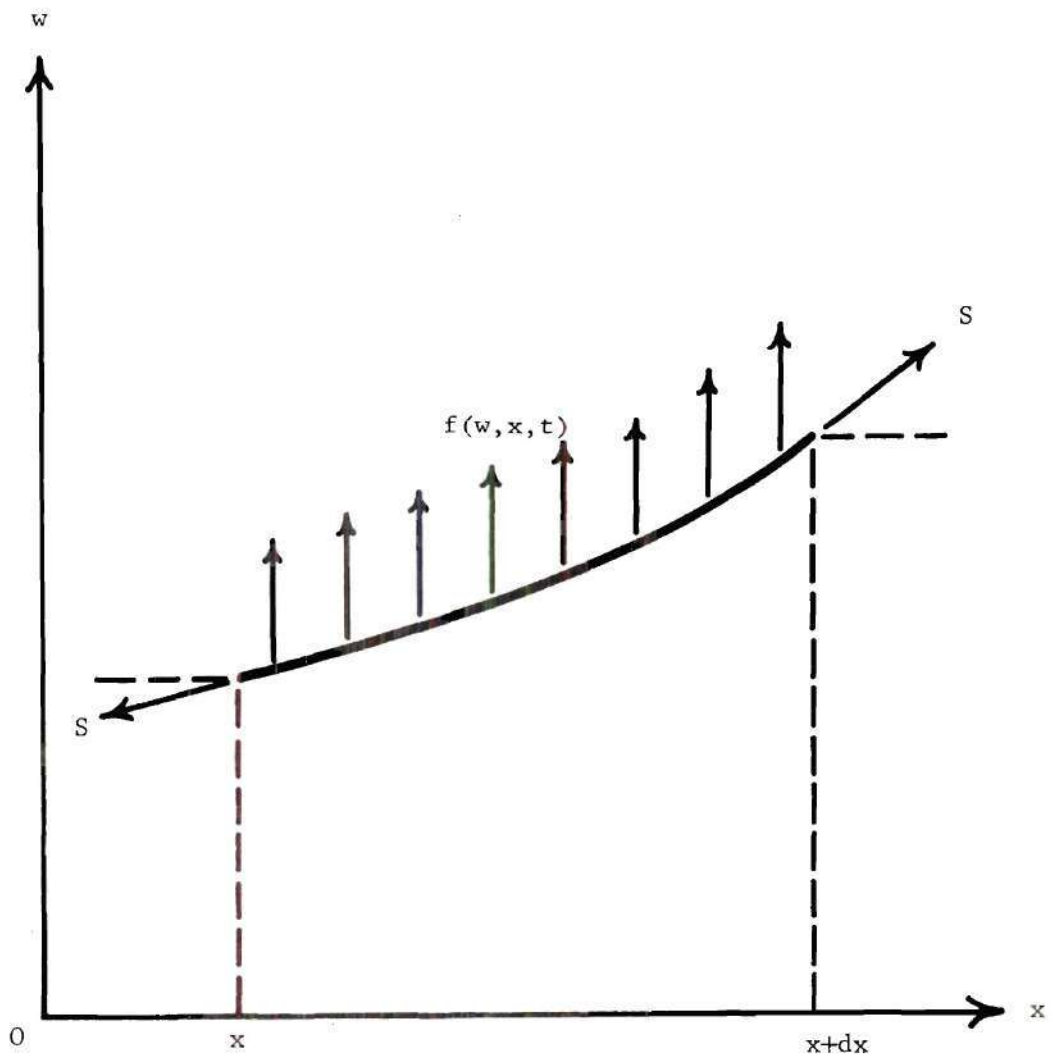


Figure 4. A Segment of the Deflected String.

this is usually written

$$\frac{\partial^2 w}{\partial x^2} - \frac{1}{c^2} \frac{\partial^2 w}{\partial t^2} = \frac{1}{S} [q_1(w) + q_2(w) - p(x,t)] ,$$

where

$$c^2 = \frac{S}{P} \quad (3)$$

is the sound speed of the string. Although not immediately apparent, Equation (2) is essentially nonlinear, since, in order that the tensile foundation be fracturable, q_1 is necessarily a nonlinear function of w .

Solutions of (2) for selected functions q_1 and q_2 are obtained in the following two chapters. Details of q_1 and q_2 are specified in the following section.

Foundation Laws

As mentioned earlier in this chapter, we shall pattern the spring law for the foundation in our model after the force-separation law for two isolated atoms indicated in Figure 2. While the precise shape of the curve shown there is not known, two of its features have been identified with two mechanical properties of the crystalline solid. The slope of the curve at the equilibrium separation is related to the modulus of elasticity, and the area under the upper portion of the curve is related to the work of separation or surface energy.

The curve has been represented by a number of qualitatively similar functions selected to form analytically convenient laws and usually written in terms of the two parameters mentioned above. The most common use of such laws has been in estimating the theoretical strength

of a crystal⁽¹⁾. Hence more attention has been paid to the representation of the upper portion of the curve where the forces between atoms are attractive than to the lower portion where they are repulsive. Some functions that have been used in the past are a linear-with-cut-off or "sawtooth" law, a sine law, an exponential law and an inverse power law. Of these, only the inverse power law represents both the upper and lower portions of the curve.

Any of these functions would be satisfactory for our purposes. Since we are concerned here with studying the effect of nonlinearity rather than the particular kind of nonlinearity, we shall use only the linear-with-cut-off and sine laws. We choose two in order to determine in limited measure the sensitivity of our results to the particular kind of nonlinearity considered.

The two spring laws for the tensile foundation are shown in Figure 5 as functions $q(w)$. They have common initial slopes⁽²⁾ k and areas-under-tension A . The relation in compression is taken to be a smooth and linear continuation of the upper portion of each curve. Hence the curves are coincident in compression. Each of the laws determines a maximum lineal force q^* and a critical displacement w^* in terms of k and A . The analytical expression of each law including q^* and w^* is presented in Table 1.

The compressive foundation is completely linear (unfracturable) with spring modulus k in tension and compression.

(1) See for instance A. H. Cottrell, "The Mechanical Properties of Matter." Wiley, New York, 1964, pp. 270-271.

(2) The unstretched length of the spring is the "equilibrium separation".

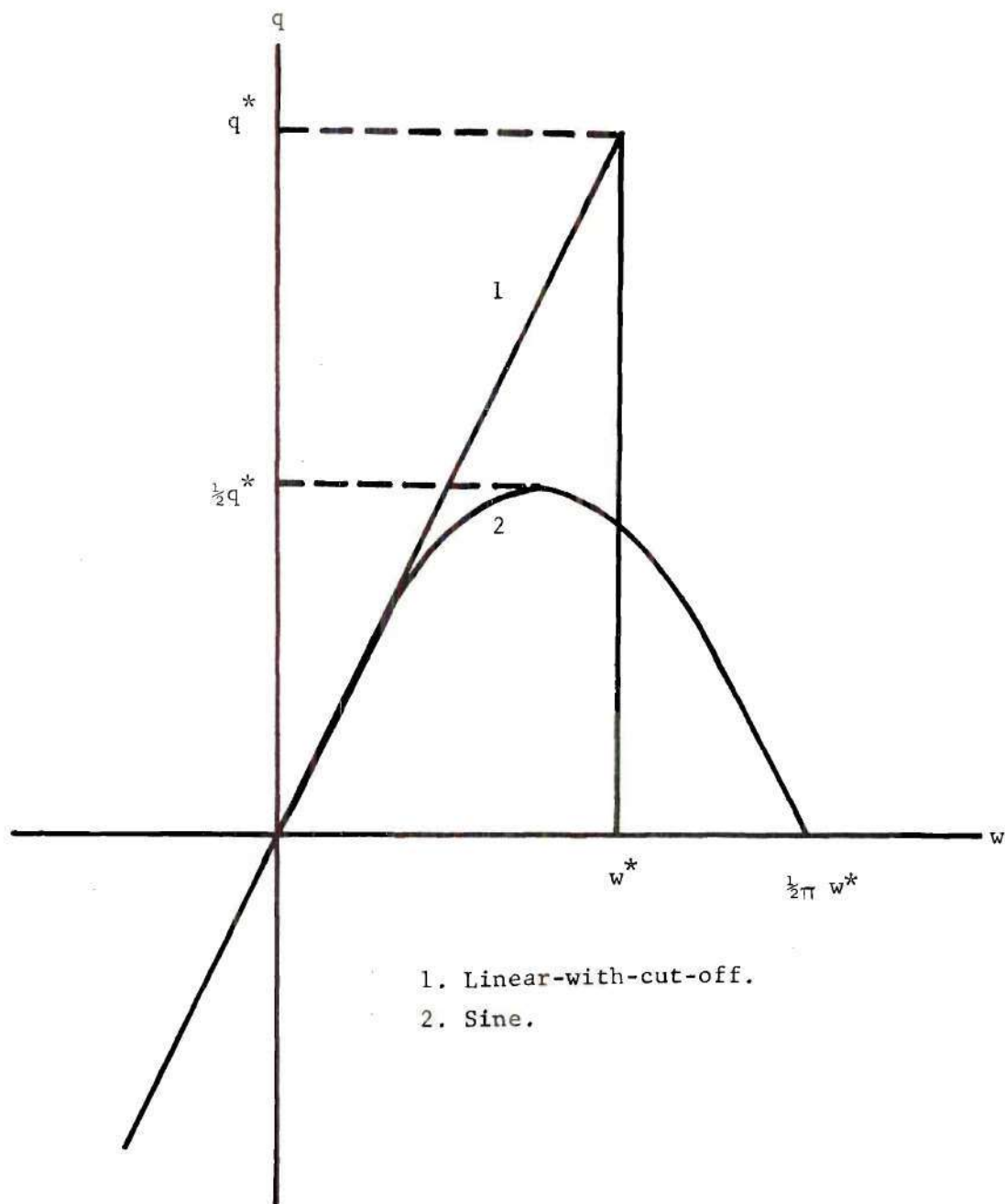


Figure 5. The Foundation Laws.

Table 1. Analytical Expression of Foundation Laws.

Foundation Law	q	Range of w ⁽¹⁾	q _{max}	w _{max}
Linear-with-cut-off	kw 0	$0 \leq w < w^*$ $w^* > w^*$	kw [*]	w [*]
Sine	$\frac{1}{2}kw^* \sin \frac{2w}{w^*}$ 0	$0 \leq w < \frac{\pi}{2}w^*$ $w^* > \frac{\pi}{2}w^*$	$\frac{1}{2}kw^*$	$\frac{1}{2}\pi w^*$
Compressive	kw	all w	—	—

(1) The symbols \leq^* and $>^*$ mean "has never exceeded" and "has ever exceeded" respectively.

CHAPTER III

ANALYSIS OF THE EQUATION OF MOTION

In this chapter we prepare to solve the nonlinear partial differential equation governing the motion of the string of our model. Details of this preparation are presented only for the linear-with-cut-off spring law because the corresponding work for the sine law is very similar.

Nondimensionalization of the Equation of Motion

As a first step toward putting (2) into a dimensionless form, we introduce dimensionless independent variable X and T related to the real space and time variables through

$$X = \frac{x}{\ell} \quad \text{and} \quad T = \frac{ct}{\ell}, \quad (4)$$

where ℓ is a characteristic length whose value and meaning will be discussed later. Under this transformation, the sound speed of the string in the XT plane is unity.

With k replaced by q^*/w^* , the linear-with-cut-off spring law in Table 1 becomes

$$q_1 = \begin{cases} \frac{q^*}{w^*} w, & w \leq w^* \\ 0, & w > w^* \end{cases},$$

which suggests

$$W = \frac{w}{w^*} \quad \text{and} \quad Q = \frac{q}{q^*} \quad (5)$$

as natural choices for dimensionless displacement and foundation reaction respectively. In (5), Q and q represent general foundation reactions which can be either tensile or compressive. As before, indices distinguish the foundation reactions; i.e. Q_1 and Q_2 represent the dimensionless tensile and compressive foundation reactions respectively.

In order that X and W be measured on the same basis, we now choose the characteristic length ℓ equal to w^* . Finally, we put the applied lineal force into dimensionless form by writing

$$P = \frac{P}{q^*} . \quad (6)$$

Upon substituting (4) - (6) into (2), we find that the equation of motion becomes

$$\frac{\partial^2 W}{\partial X^2} - \frac{\partial^2 W}{\partial T^2} = \frac{q^* w^*}{S} [Q_1(W) + Q_2(W) - P(X,T)]$$

or

$$\frac{\partial^2 W}{\partial X^2} - \frac{\partial^2 W}{\partial T^2} = M^2 [Q_1(W) + Q_2(W) - P(X,T)] , \quad (7)$$

where

$$M^2 = \frac{q^* w^*}{S} \quad (8)$$

is a dimensionless parameter.

In terms of the dimensionless variables, the spring laws for the tensile and compressive foundations are

$$Q_1(W) = \begin{cases} W , & W \leq 1 \\ 0 , & W > 1 \end{cases} \quad (9)$$

and

$$Q_2(W) = W \quad (10)$$

respectively.

In its new form, the only parameter appearing in the equation of motion is M^2 . According to (8), M^2 depends directly on the spring law through the product $q w^{**}$ and inversely on the string tension S .

Whenever possible, we shall develop solutions of (7) in terms of M^2 ; i.e. without specifying its value in advance. In the following section, for instance, we obtain certain static or equilibrium solutions in terms of M^2 . In Chapter IV, however, where we obtain solutions of (7) by numerical integration, M^2 must be specified in advance, and some consideration must be given to the value assigned to it.

Taking $M^2 \ll 1$ would bias (7) in favor of the slope-tension force $\frac{\partial^2 W}{\partial X^2}$ and the inertia force $\left(-\frac{\partial^2 W}{\partial T^2}\right)$ at the expense of the foundation reactions $Q_1(W) + Q_2(W)$ and the applied lineal force $P(X,T)$. On the other hand, specifying $M^2 \gg 1$ merely reverses the bias and makes (7) more nearly singular. In order to study the interaction of all the forces represented in (7) and at the same time to expedite the numerical analysis, we shall assign the value $\frac{1}{4}$ to M^2 when it must be specified in advance.

Static Solutions

One of the initial-boundary value problems we wish to investigate concerns the response of our model when the applied load is increased slightly after a quasi-static loading to the greatest load that can be supported for a given initial crack. With this intention, it is natural

to require a solution to an equilibrium problem. In this section, we obtain such solutions in closed form including the expression for the critical static load.

Consider an imperfect tensile foundation with an initial crack of length $2a$. Let the string be displaced quasi-statically to its final equilibrium position $W(X)$ under an applied load whose final distribution is $P(X)$. By setting the inertia force in (7) equal to zero, we obtain

$$\frac{d^2 W}{dX^2} - M^2 [Q_1(W) + Q_2(W) - P(X)] = 0 \quad (11)$$

for determining the final equilibrium position of the string. It is assumed, of course, that $P(X)$ has been applied in such a way as to prohibit stretching any of the springs in the tensile foundation past their critical displacement.

If we take the origin of the X axis to be the midpoint of the initial crack and consider only loads $P(X)$ that are even functions of X , then only the semi-infinite string $X \geq 0$ need be considered (see Figure 6). In particular, if the external load is of constant intensity and applied only over the central part of the string, then the loading function is

$$P(X) = \begin{cases} P \text{ (constant)} , & 0 \leq X \leq b \\ 0 & , \quad X > b \end{cases}$$

and the linear foundation reactions can be written as

$$Q_1(W) + Q_2(W) = \begin{cases} 2W , & X \geq a \\ W , & X < a \end{cases}$$

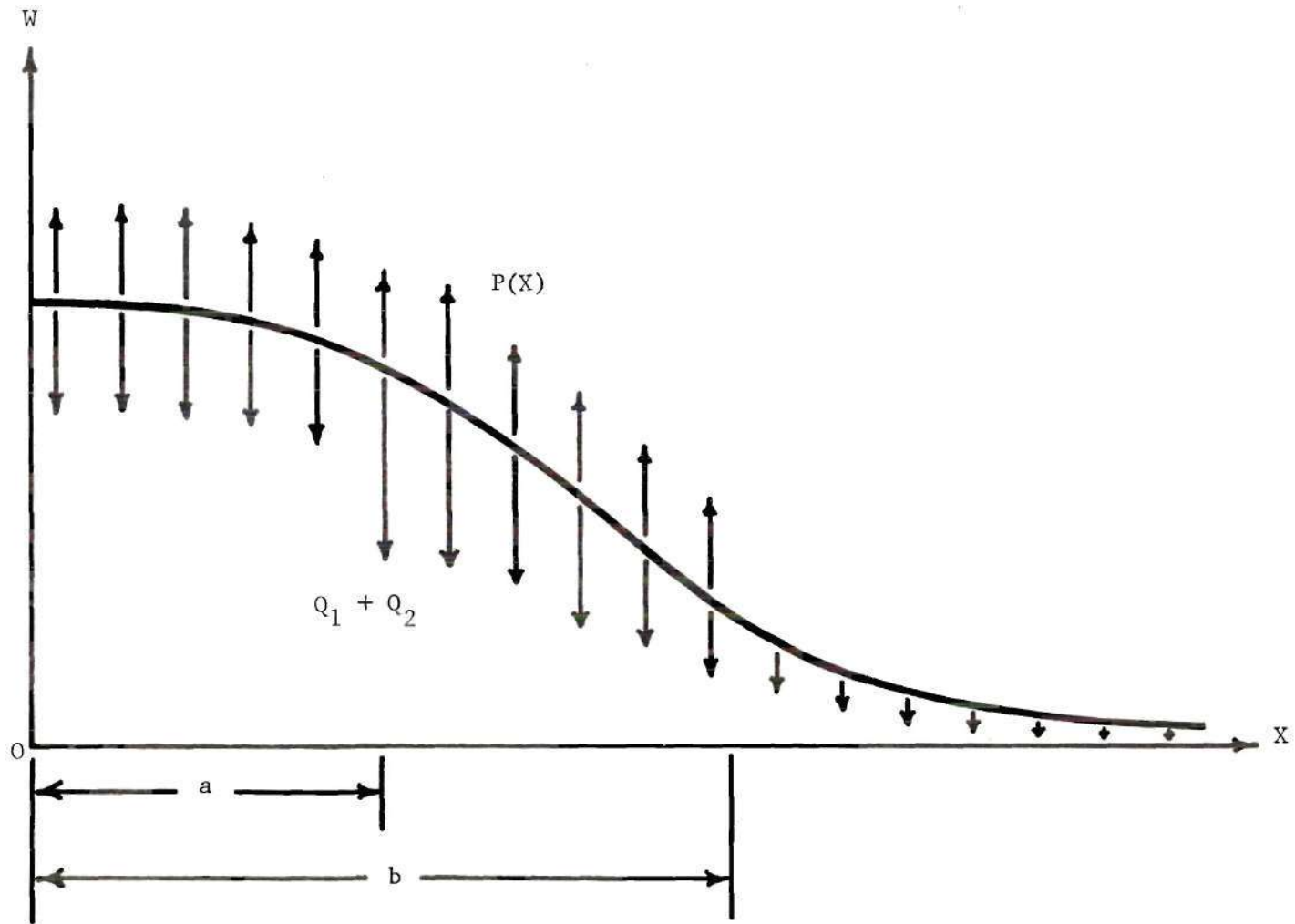


Figure 6. String in Equilibrium Under External Load, $P(X)$, and Foundation Reaction, Q_1+Q_2 .

Now the equilibrium equation (11) can be readily solved, and the equilibrium load can be determined in terms of the crack tip displacement $W(a)$. We shall denote by P_{cr} that value of P bringing the initial crack just to the point of extending; i.e. that value of P corresponding to $W(a) = 1$. A crack which is opened to such an equilibrium configuration has been called a "mobile equilibrium crack" by Barenblatt. We shall consider separately the loading cases of $a \leq b$ and $a > b$.

$a \leq b$:

In this case, the equilibrium equations written for the various segments of the string are:

$$\begin{aligned} W'' - M^2 W + M^2 P_{cr} &= 0, & 0 \leq X < a; \\ W'' - 2M^2 W + M^2 P_{cr} &= 0, & a \leq X \leq b; \\ W'' - 2M^2 W &= 0, & x > b. \end{aligned} \quad (12)$$

Prime (') indicates the derivative of a function with respect to its argument. In addition to (12), the following conditions must be satisfied;

$$\begin{aligned} W'(0) &= 0; \\ W(a) &= 1; \\ \lim_{X \rightarrow \infty} W(X) &\text{ exists;} \end{aligned} \quad (13)$$

$W(X)$ and $W'(X)$ are continuous on $0 \leq X < \infty$.

The first condition is due to the symmetry of the string, foundation and load with respect to $X = 0$. The second condition identifies the applied load as the critical load. The third condition follows from the stipulation that under finite loading, the displacement should remain

finite everywhere. The last condition is an obvious requirement for any string free of concentrated lateral loads.

A solution satisfying (12) and (13) is

$$\frac{1 - P_{cr}}{e^{Ma} + e^{-Ma}} (e^{MX} + e^{-MX}) + P_{cr} , \quad 0 \leq X < a$$

$$W(X) = A_1 e^{\sqrt{2MX}} + B_1 e^{-\sqrt{2MX}} + \frac{P_{cr}}{2} , \quad a \leq X \leq b , \quad (14a)$$

$$C_1 e^{-\sqrt{2MX}} , \quad X > b$$

where the integration constants A_1 , B_1 and C_1 are given by

$$A_1 = - \frac{P_{cr}}{4} e^{-\sqrt{2Mb}} ,$$

$$B_1 = \frac{1}{2} \left(1 - \frac{P_{cr}}{2} - \frac{1 - P_{cr}}{2} \tanh Ma \right) e^{\sqrt{2Ma}} \quad (14b)$$

and

$$C_1 = B_1 + \frac{P_{cr}}{4} e^{\sqrt{2Mb}}$$

with

$$P_{cr} = \frac{(2 + \sqrt{2} \tanh Ma) e^{\sqrt{2M(b-a)}}}{(1 + \sqrt{2} \tanh Ma) e^{\sqrt{2M(b-a)}} - 1} . \quad (14c)$$

When the load is applied over the entire string ($b \rightarrow \infty$), the critical load is

$$P_{cr} = \frac{2 + \sqrt{2} \tanh Ma}{1 + \sqrt{2} \tanh Ma} . \quad (15)$$

Equation (15) is plotted in Figure 7 for $M = \frac{1}{2}$.

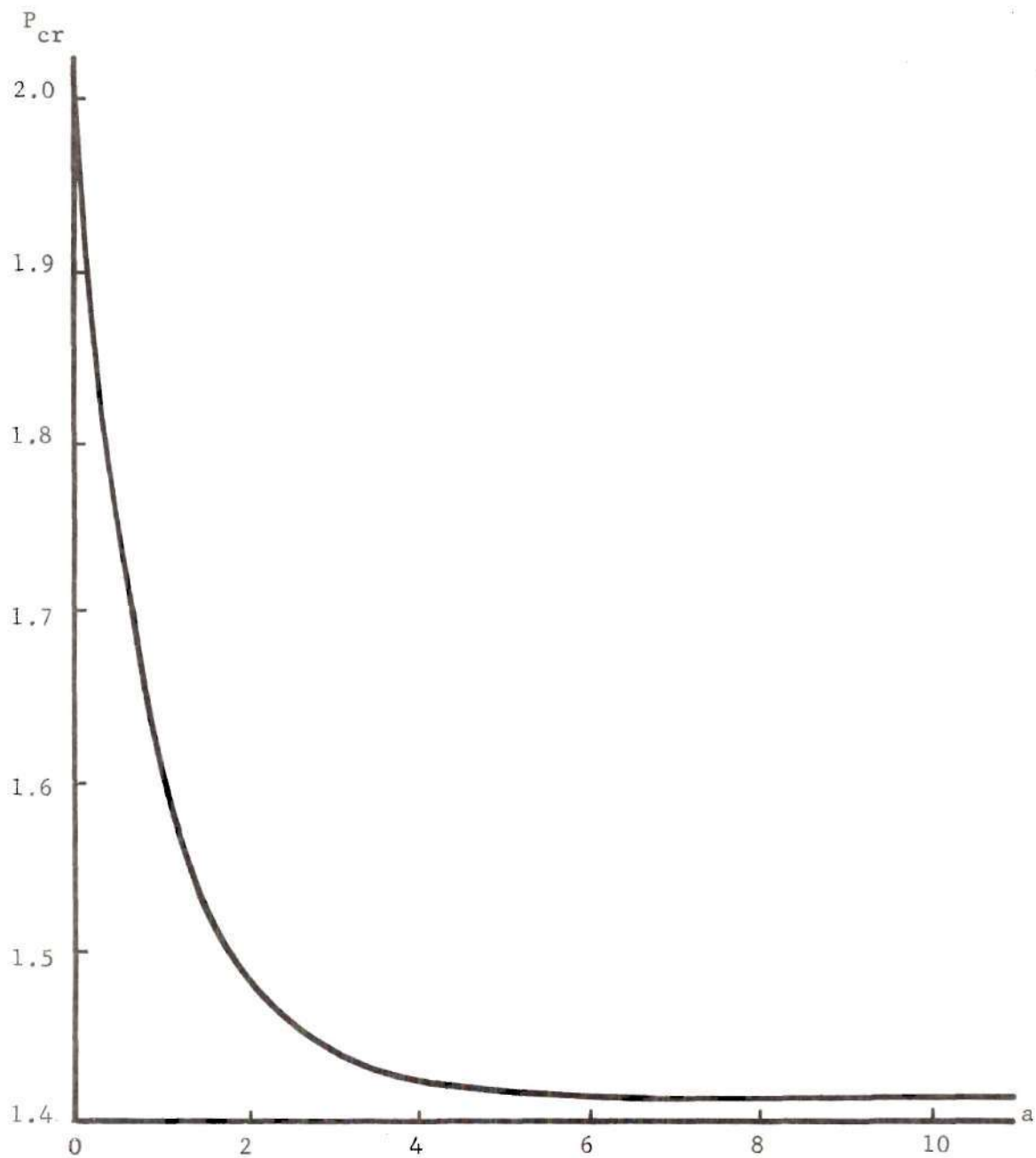


Figure 7. Critical Equilibrium Load Versus Crack Length. $b = \infty$

$a > b$:

When the load is applied only over a part of the segment corresponding to the initial crack, the equilibrium equations are:

$$\begin{aligned} W'' - M^2 W + M^2 P &= 0, & 0 \leq X \leq b; \\ W'' - M^2 W &= 0, & b < X < a; \\ W'' - 2M^2 W &= 0, & X \geq a. \end{aligned} \quad (16)$$

A solution satisfying (16) subject to the same conditions (13) as before is

$$\begin{aligned} A_2(e^{MX} + e^{-MX}) + P_{cr}, & \quad 0 \leq X < b \\ W(X) = \frac{1}{2} [(1 - \sqrt{2}) e^{M(X-a)} + (1 + \sqrt{2}) e^{M(a-X)}], & \quad b \leq X \leq a, \\ e^{\sqrt{2}M(a-X)}, & \quad X > b \end{aligned} \quad (17a)$$

where

$$A_2 = \frac{1}{2(e^{Mb} - e^{-Mb})} [(1 - \sqrt{2}) e^{M(b-a)} - (1 + \sqrt{2}) e^{M(a-b)}] \quad (17b)$$

and

$$P_{cr} = \frac{1}{\sinh Mb} (\sqrt{2} \cosh Ma + \sinh Ma). \quad (17c)$$

Equations (14c) and (17c) are equivalent when $a = b$.

As an example to illustrate the relation between critical load and crack length, a curve is drawn in Figure 8 showing $P_{cr}(a)$ for $b = 20$ and $M = \frac{1}{2}$. For $a \leq b$ we plot (14c); for $a > b$ (17c). The curve shows that as a varies from zero, the value of P_{cr} first decreases with increasing

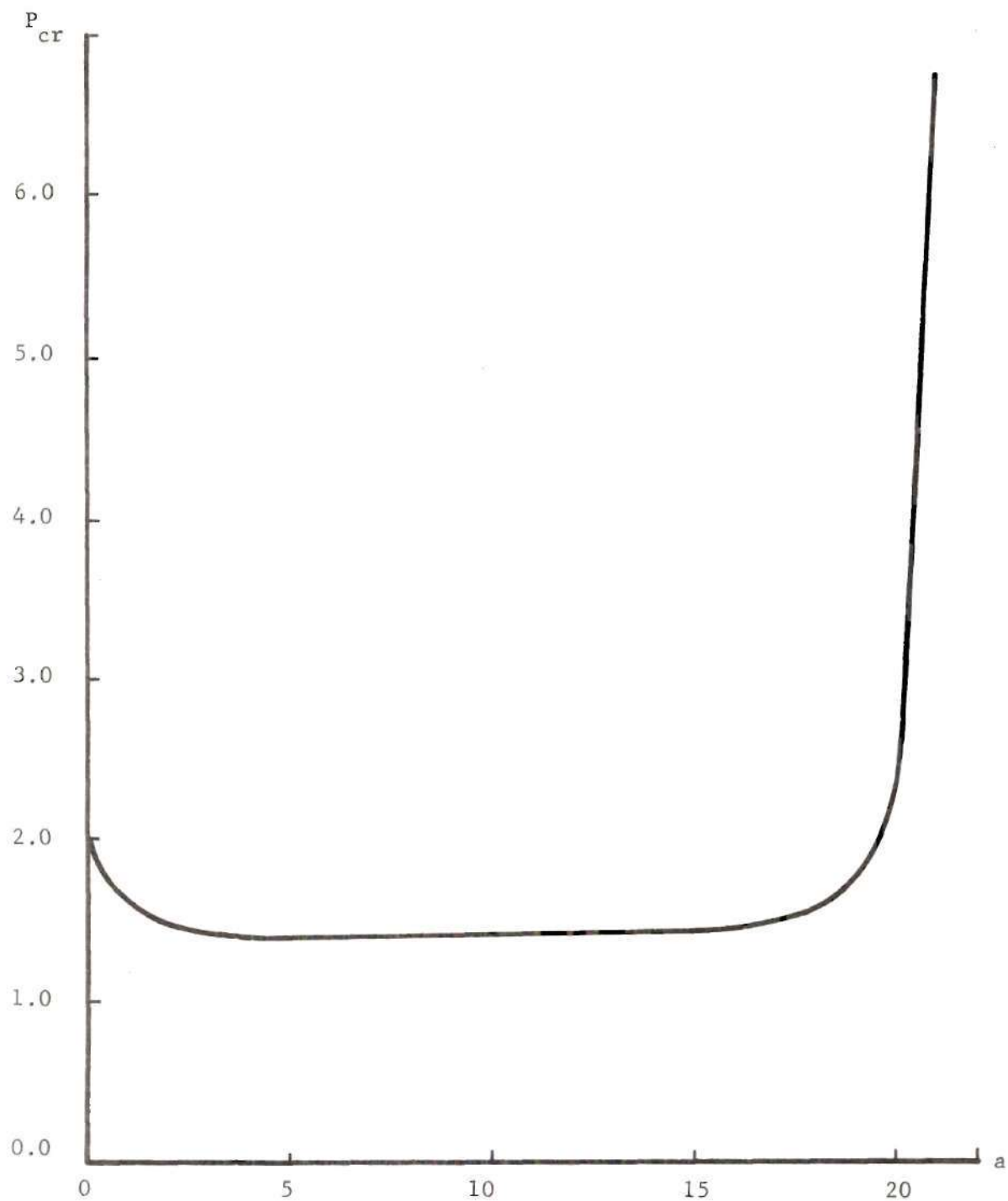


Figure 8. Critical Equilibrium Load Versus Crack Length. $b = 20$.

crack length. After passing through a region where P_{cr} is practically independent of a , it begins to increase rapidly as a approaches and exceeds b .

The shape of the curve in Figure 8 indicates that short initial cracks located within a much longer loaded segment ($a \ll b$) are unstable in the following sense. If a load sufficient to extend the initial crack (i.e. increase a) is applied and maintained, it is more than sufficient to extend longer cracks. On the other hand, the curve also indicates that initial cracks approaching or exceeding the length of the loaded segment are stable because a load sufficient to extend such an initial crack is insufficient to extend the crack when it grows. Figure 7 shows that for loads applied over the entire length of the string, any crack in the tensile foundation is unstable.

In Figure 9, the displacement profile of a mobile equilibrium crack is shown for $a = 5$ and $b = 20$. The forces acting on the string are shown in the same figure. As expected, there is a discontinuity in the total foundation reaction $Q_1 + Q_2$ at the crack tip.

In the nondimensionalization process outlined in the previous section, we used w^* as the characteristic length. The precise value of the "out-of-range" separation for two isolated atoms is not known, but Figure 2 indicates that it is the same order of magnitude as the equilibrium separation. Thus with regard to our model, any crack of practical specific length must be regarded as being very short. In an effort to take into consideration longer cracks, we now study the response of our model when the tensile foundation contains a semi-infinite initial crack.

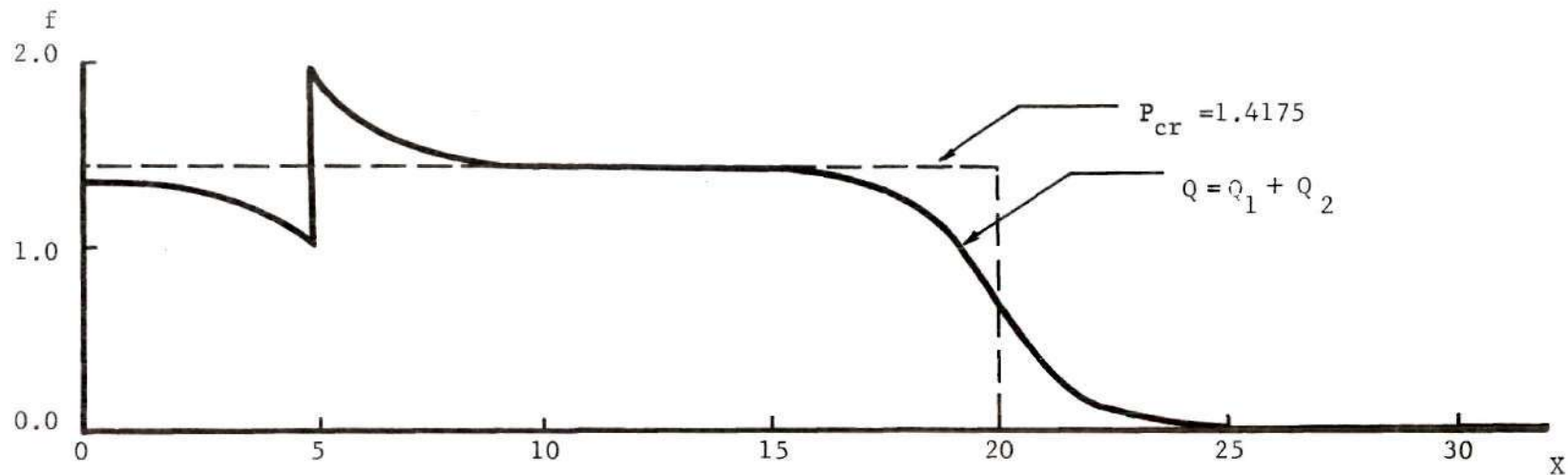


Figure 9a. Distribution of Foundation Reaction and Applied Load.

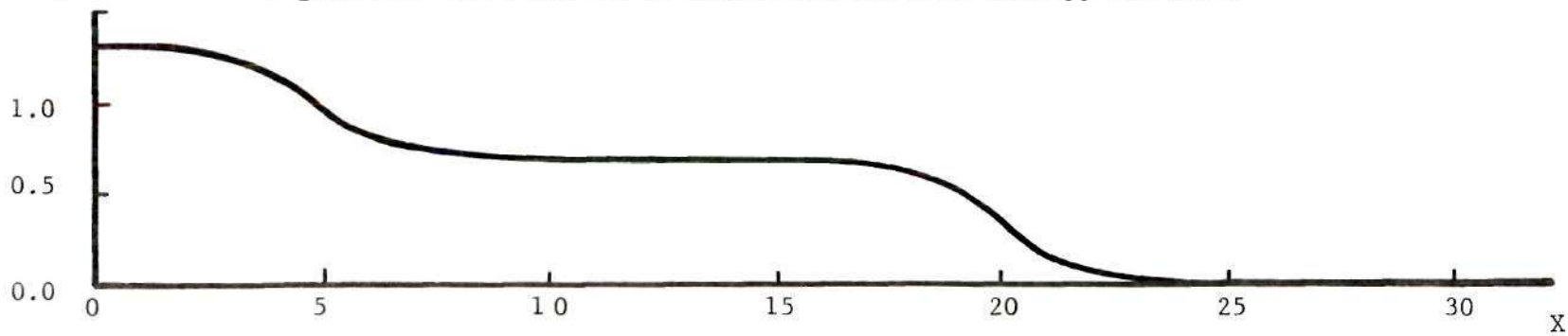


Figure 9b. Critical Equilibrium Profile of the String.

For this situation, the symmetry condition of (13) can no longer be applied, and we require instead that both ends of the string have finite displacement (i.e. $\lim_{X \rightarrow -\infty} W(X)$ exists). This furnishes us enough conditions to solve the problem. For a uniform load applied over the entire string, we have

$$[\sqrt{2} + (1 - \sqrt{2}) e^{MX}] , \quad X \leq 0 \quad (18a)$$

$$W(X) = [\frac{\sqrt{2}}{2} + (1 - \frac{\sqrt{2}}{2}) e^{-\sqrt{2}MX}] , \quad X \geq 0 \quad (18b)$$

and

$$P_{cr} = \sqrt{2} .$$

In Chapter IV the propagation of the semi-infinite crack is studied for several different initial conditions and loading situations.

The Method of Characteristics

After obtaining certain static solutions, we turn now to the problem of solving the equation of motion (7). Such an equation has been treated successfully in the past by employing the method of characteristics. Although the application of this method usually involves numerical integration, it is considerably more straightforward than other methods.⁽¹⁾ The theory of characteristics is well known and will not be discussed in detail here. To apply the method, we first write (7) in a form more convenient for numerical integration. Let

$$V = \frac{\partial W}{\partial T} \quad \text{and} \quad \Theta = \frac{\partial W}{\partial X} . \quad (19)$$

(1) An attempt to solve the initial-boundary value problem analytically using the Rieman-Volterra method is presented in the Appendix.

Then the equation of motion becomes

$$\frac{\partial V}{\partial T} - \frac{\partial \Theta}{\partial X} + M^2(Q - P) = 0 . \quad (20)$$

We shall integrate these three first order partial differential equations rather than the single second-order wave equation. The dependent variables to be determined are W , V and Θ as well as Q_1 and Q_2 , which depend on W through (9) and (10). Physically, V is the velocity of an element of the string and Θ is the slope of the string.

Since the equation of motion is hyperbolic (with constant coefficients) its characteristics are the two families of straight line defined by

$$\frac{dX}{dT} = 1 \quad \text{and} \quad \frac{dX}{dT} = -1 . \quad (21)$$

Along these lines, the dependent variables are governed by the "characteristic" equations

$$\frac{d}{dT} (V - \Theta) + M^2(Q - P) = 0 , \quad \text{along} \quad \frac{dX}{dT} = 1 \quad (22a)$$

$$\frac{d}{dT} (V + \Theta) + M^2(Q - P) = 0 , \quad \text{along} \quad \frac{dX}{dT} = -1 \quad (22b)$$

In addition to the lines defined by $\frac{dX}{dT} = \pm 1$, the vertical lines on the XT plane are of special interest because

$$\frac{dW}{dT} = V \quad \text{along} \quad \frac{dX}{dT} = 0 . \quad (22c)$$

If initial values ($T = 0$) are given, we can determine the values of W , V , Θ and Q at any desired point on the XT plane. To do this, we

first construct a region on the XT plane bounded by the line $T = 0$ and the characteristic lines $\left(\frac{dX}{dT} = \pm 1\right)$ passing through the point in question. Then we integrate equations (22). Numerically, this procedure can be performed by subdividing the region into a grid system consisting of characteristic lines and vertical lines. The integration is performed step by step until the point in question is reached. A brief outline of the numerical procedure follows. Results of various initial-boundary value problems are presented in the next chapter.

We first construct a characteristic net on the XT plane formed by the families of lines $\frac{dX}{dT} = \pm 1$ and $\frac{dX}{dT} = 0$ (see Figure 10). Since the space mesh size is related to the time mesh size, an arbitrary time interval ΔT determines the elementary mesh size. Then we integrate the differential equations (22) along the appropriate lines. To do this, we consider a general square abcd (Figure 10). The sides ad and cd have slopes $+1$ and -1 respectively, and the diagonal bd is vertical. Integration of the characteristic equations yields

$$W_d = W_b + (V_d + V_b) \Delta T, \quad (23a)$$

$$V_d = \frac{1}{2} \{V_a + V_c - \Theta_c - \frac{M^2}{2} (2Q_d + Q_a + Q_c - 2P_d - P_a - P_c) \Delta T\} \quad (23b)$$

and

$$\Theta_a = \frac{1}{2} \{V_c - V_a + \Theta_a - \Theta_c - \frac{M^2}{2} (Q_c - Q_a - P_c + P_a) \Delta T\}, \quad (23c)$$

where the approximation $\int_{\xi_1}^{\xi_2} f(\xi) d\xi = \frac{\Delta \xi}{2} [f(\xi_1) + f(\xi_2)]$ is used to evaluate

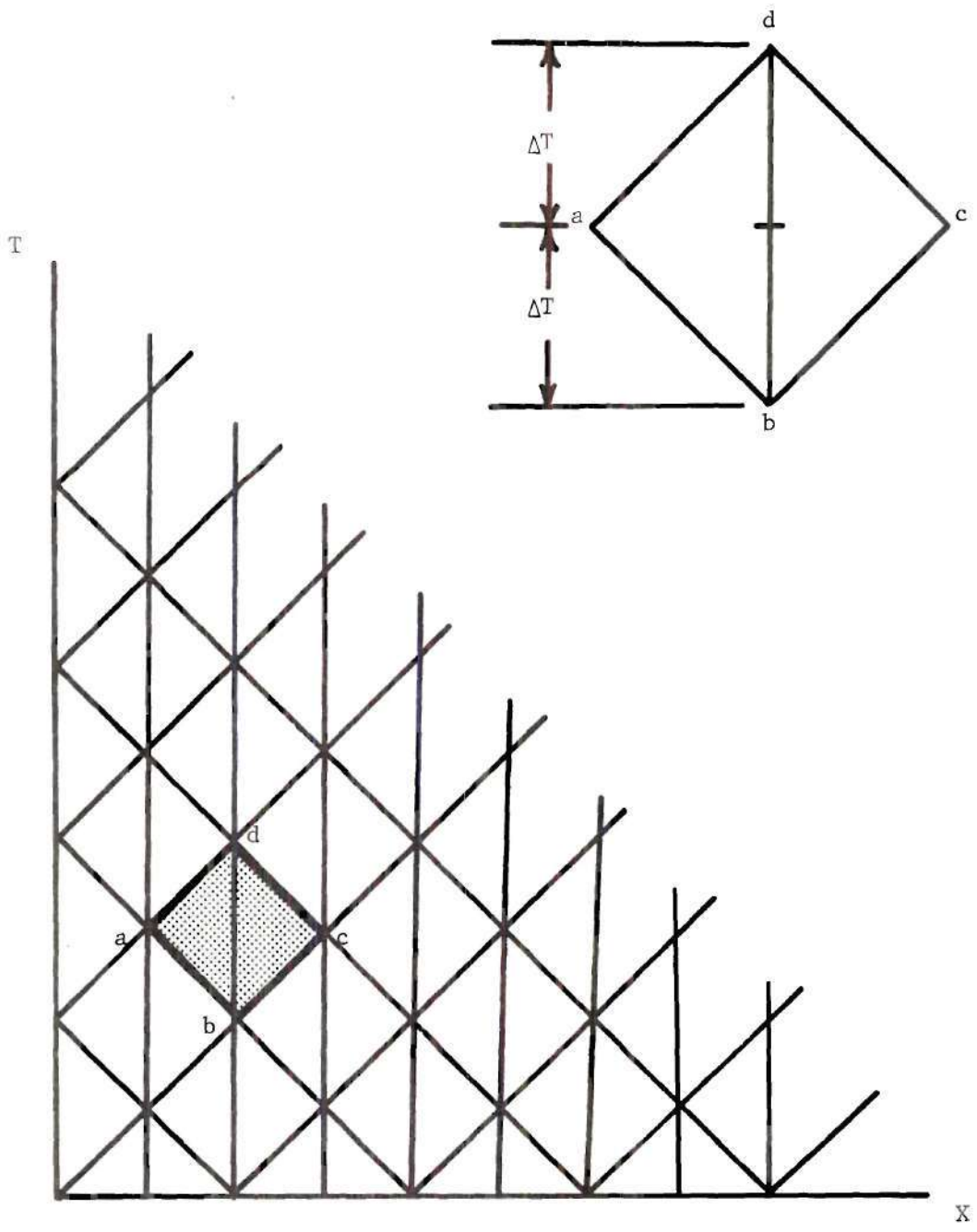


Figure 10. A General Characteristic Net and its Interior Element.

the integrals. In addition to (23), we have

$$Q_d = \begin{cases} W_d, & \text{if } W(W_d, T) \gg 1 \\ 2W_d, & \text{if } W(X_d, T) \leq 1 \end{cases} \quad (24)$$

The numerical calculations are generally started from the line $T = 0$, where the initial data are available. Thus, when the element $abcd$ is under consideration, values of W , V , Θ and Q at points a , b and c are known beforehand. Then equations (23) and (24) form a set of four algebraic equations for the determination of W_d , V_d , Θ_d and Q_d . By repeating the procedure, we can obtain all the values of W , V , Θ and Q throughout the region.

The characteristic net shown in Figure 10 is a form of broad applicability. However for some initial-boundary value problems we shall use nets with slightly different elements. These special cases will be discussed as they occur.

CHAPTER IV

NUMERICAL RESULTS

The method of characteristics discussed at the end of Chapter III will now be used in developing numerical solutions of a series of initial-boundary value problems. The results presented in this chapter describe the effects of four different loading histories - quasi-static, suddenly applied and maintained, impulsive and periodic - and considers some of the consequences of introducing damping in our model.

Disturbed Mobile Equilibrium Crack

In this problem, the string is initially at rest under an externally applied load that is just insufficient to extend an existing crack in the tensile foundation. The string is set in motion when the external load is suddenly increased by a small amount. The initial displacement and slope of the string are taken from the static solutions of Chapter III.

The region of integration is the shaded part of Figure 11a. It is convenient to regard the interior of this region as being composed of triangular elements such as the one shown in Figure 11b. This choice leaves triangular half-elements (Figure 11c) adjacent to the boundary $X = 0$.

The difference equations for any interior element are obtained from (23) and (24) by replacing ΔT by $\Delta T/2$. We now drop the alphabetical (abcd) designation of points in favor of the index coordinates (i,j) indicated in Figure 11.

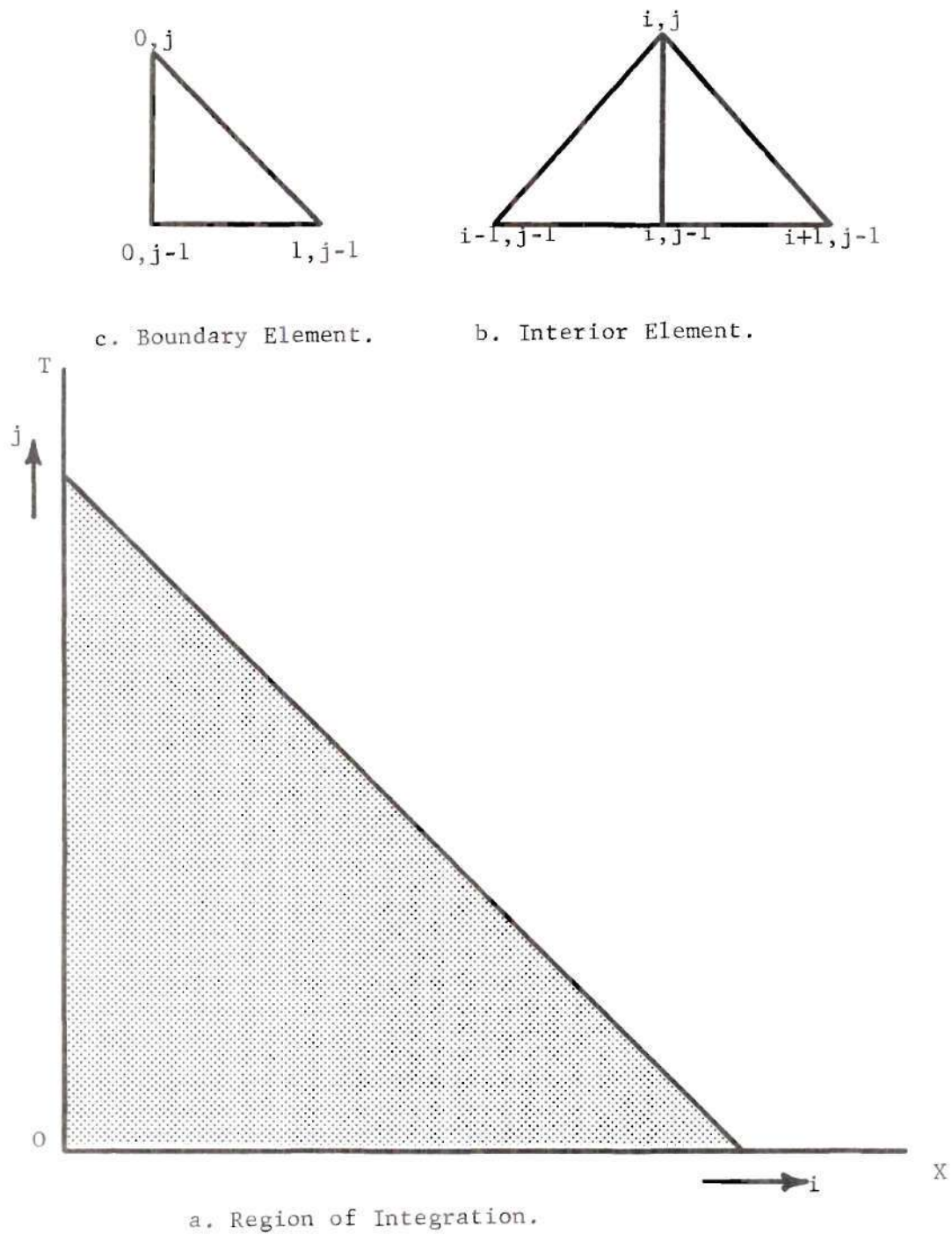


Figure 11. Region of Integration and its Elements.

For points along $X = 0$, the slope of the string is zero due to symmetry; i.e. $\Theta_{0,j} = 0$. Hence only the equations along $\frac{dX}{dT} = -1$ and $\frac{dX}{dT} = 0$ are required to determine the variables for boundary elements. Furthermore, since points on $X = 0$ are always within the cracked segment of the tensile foundation, $Q_{0,j} \equiv W_{0,j}$. This permits the following direct solution of the difference equations for boundary elements.

$$W_{0,j} = \frac{1}{1 + \left(\frac{M\Delta T}{2}\right)^2} \left\{ W_{0,j-1} + \frac{\Delta T}{2} (V_{0,j-1} + V_{1,j-1} + \Theta_{1,j-1}) - \left(\frac{M\Delta T}{2}\right)^2 (Q_{1,j-1} - P_{0,j} - P_{1,j-1}) \right\},$$

$$V_{0,j} = V_{1,j-1} + \Theta_{1,j-1} - \frac{M^2}{2} (W_{0,j} + Q_{1,j-1} - P_{0,j} - P_{1,j-1}) \Delta T,$$

$$Q_{0,j} = W_{0,j} \tag{25}$$

and

$$\Theta_{0,j} = 0$$

We now consider the following two problems separately. A uniform load P is applied over the entire string ($b = \infty$); a uniform load P is applied only over a finite segment of the string ($a < b < \infty$).

$b = \infty$:

In this case, $P_{i,j} \equiv (1 + \epsilon) P_{cr}$, where ϵ is a small positive constant and P_{cr} is given by (15). Initial values of displacement and slope are taken from the limiting form of (14) as $b \rightarrow \infty$. Results for

mobile equilibrium cracks of initial length $a(0) = 5^{(1)}$ and $a(0) = 10$ disturbed by 1% and 5% increases in load are presented in Figures 12-17.

$a < b < \infty$:

For this problem, the external load $P_{i,j}$ can be written

$$P_{i,j} = \begin{cases} P \text{ (constant) ,} & X \leq b \\ 0 & , \\ & X > b \end{cases}$$

where again $P = (1 + \epsilon)P_{cr}$. Initial data and P_{cr} are taken from (17a) and (17c) respectively. The numerical integration was performed for $b = 20$ with $a(0) = 5$ and $a(0) = 10$ subject to critical load excesses of 1% and 5%. The results are presented in Figures 18-26.

The results for the first case ($b = \infty$) indicate that a mobile equilibrium crack begins to extend measurably as soon as the critical load is exceeded (Figure 12). The extension continues although the external load is held constant. The velocity of the crack tip ($\frac{da}{dT}$) builds from zero to a terminal value that is the same order of magnitude as the sound speed of the string. The duration of the acceleration period and, to a lesser extent, the terminal velocity depend on the amount by which the critical load is exceeded (Figure 13). Profiles of the string at $T = 0$, $T = 15$ and $T = 30$ are shown in Figures 14 and 15 for $a(0) = 5$ and $a(0) = 10$. The displacement history of points at $x = a(0)$, $X = a(0) + 10$ and $X = a(0) + 20$ are shown in Figures 16 and 17 for $a(0) = 5$ and $a(0) = 10$.

(1) We have been using the symbol a for the initial length of an existing crack. It is now convenient to let $a(T)$ represent the current length of a crack whose initial length was $a(0)$.

Here we see that, except near the crack tip, points on the string perform small oscillations about their equilibrium positions. A comparison of results for the two different initial crack lengths suggests that the length of the initial crack has little or no influence on the dynamic behavior of the extending crack.

The results for the second case are substantially different as might be predicted on the basis of the stability discussion in Chapter III. The crack begins to propagate in much the same manner as before, but as $a(T)$ approaches b , the velocity drops very quickly to zero (Figures 18 and 19); i.e. the crack stops. To review the reason for this, consider Figures 20-22. Figure 20 shows that for $b = \infty$, any maintained load greater than $P_{cr}[a(0)]$ remains greater than P_{cr} for longer equilibrium cracks. Hence it is sufficient to insure the continued growth of the crack. However in the second case ($a < b < \infty$), Figures 21 and 22 show that loads maintained slightly greater than $P_{cr}[a(0)]$ are not sufficient to extend all longer equilibrium cracks. More specifically, they become insufficient as $a(T)$ approaches b . The propagating crack behaves as if it had some "inertia" since it runs past the "point of insufficiency" by a small distance Δl before stopping. String profiles at selected times and displacement histories of selected points are shown in Figures 23-26. Once again, there is no apparent sensitivity to initial crack length.

Suddenly Applied Load

In this section we consider the response of our model when a uniform load is suddenly applied and maintained. The string is initially at

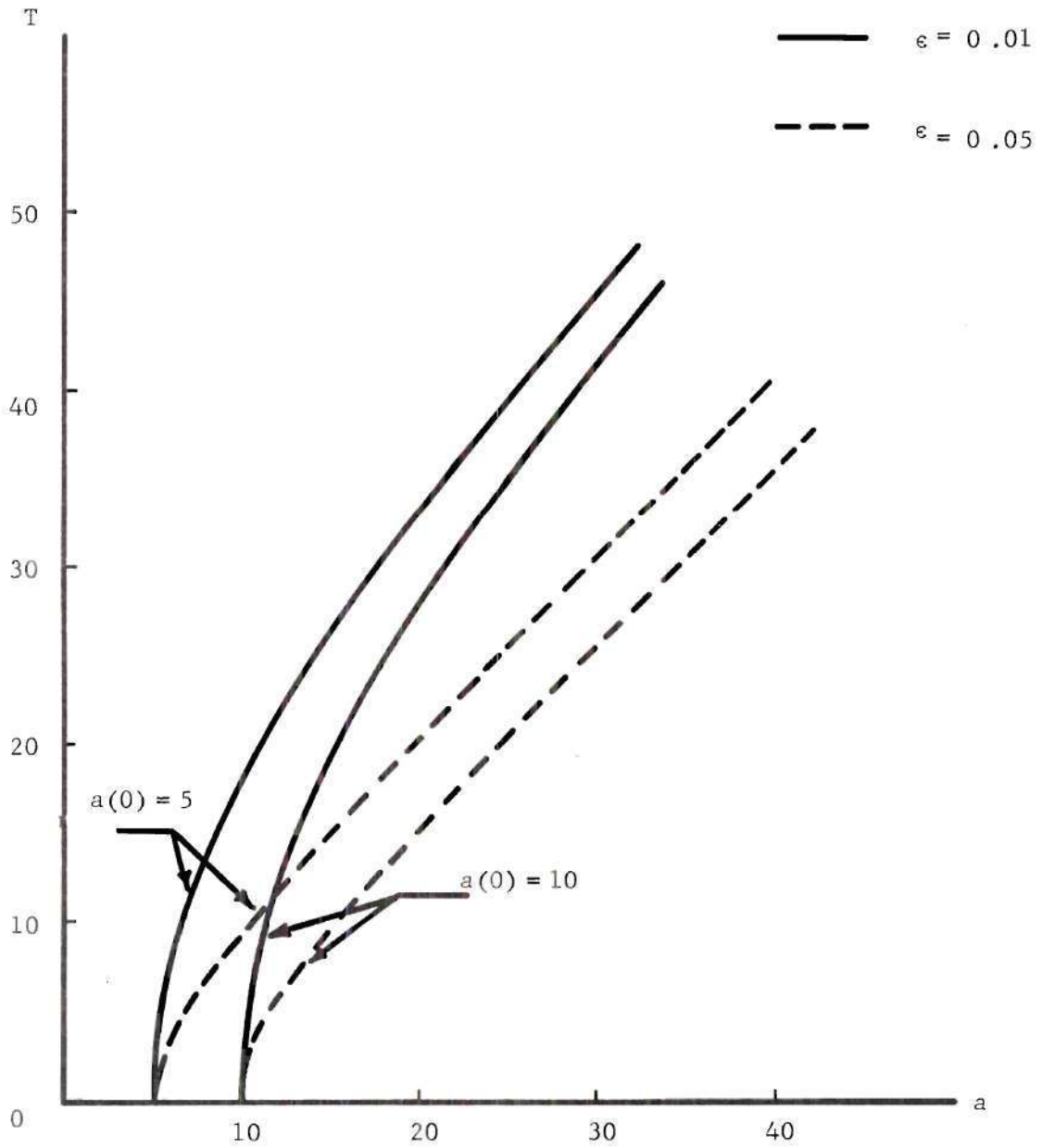


Figure 12. Crack Length Versus Time. $b = \infty$

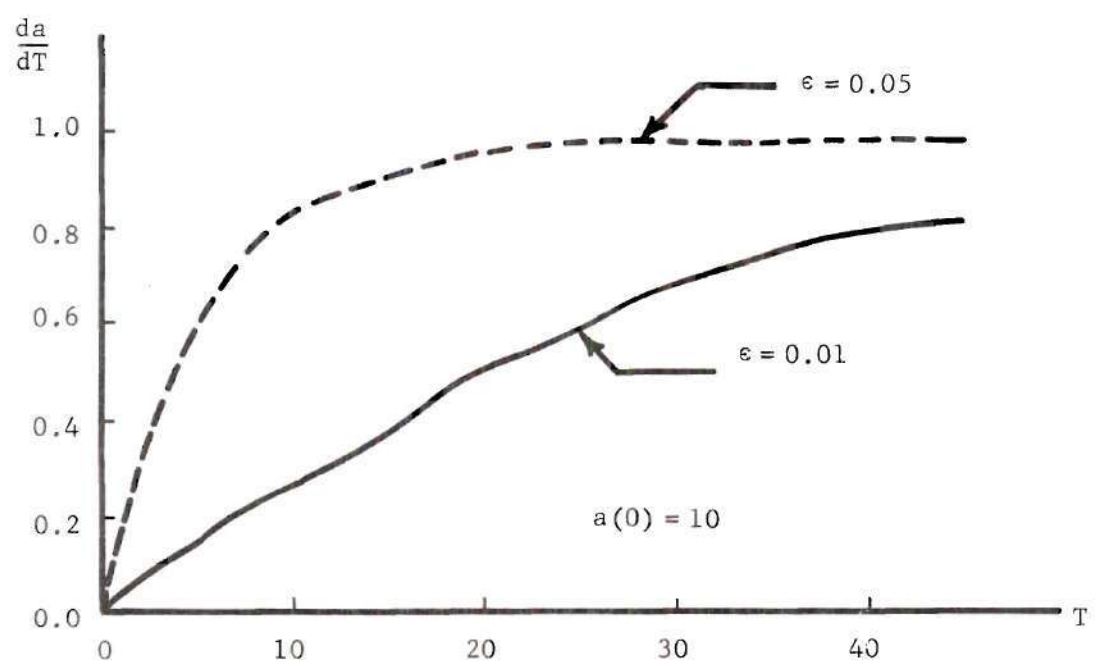
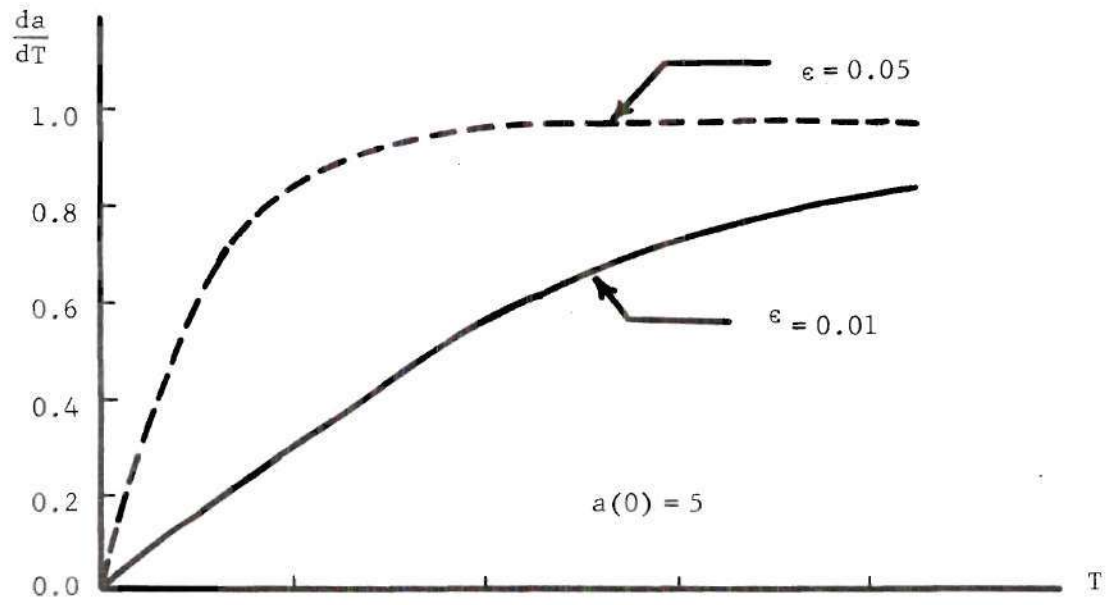


Figure 13. Velocity of Crack Propagation. $b = \infty$

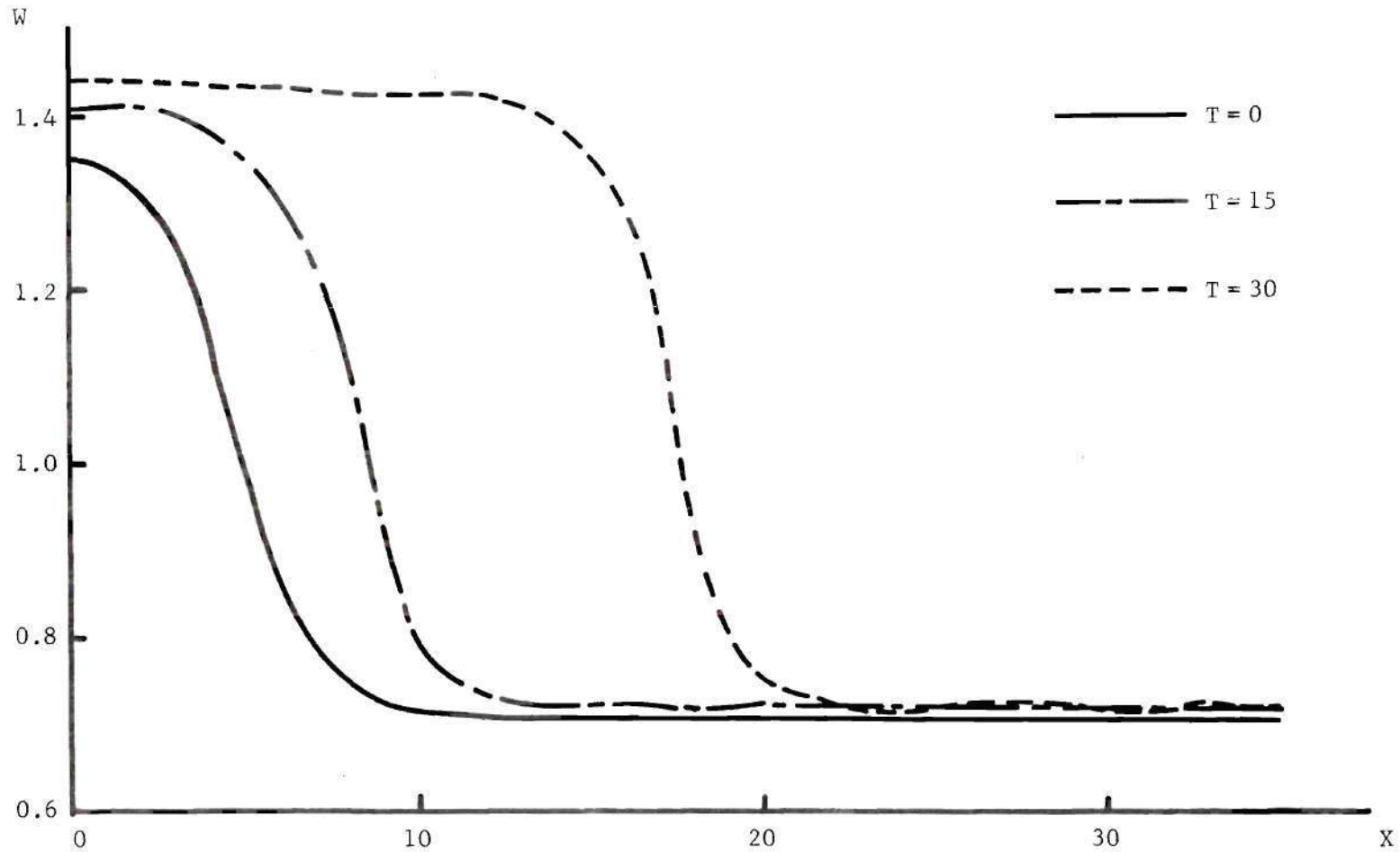


Figure 14. Displacement Profiles of the String at Selected Time.
 $a(0) = 5$, $b = \infty$, $\epsilon = 0.01$.

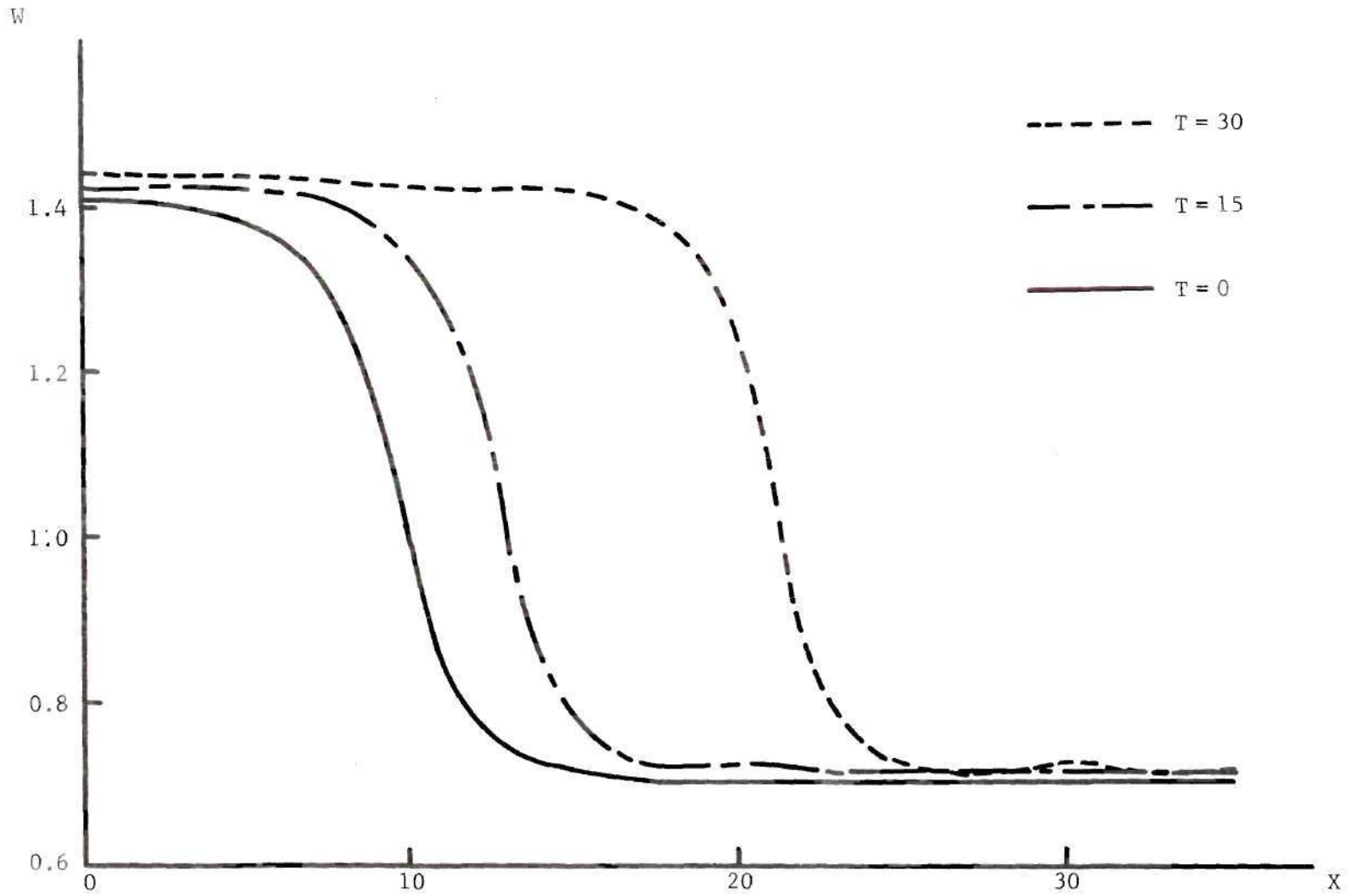


Figure 15. Displacement Profiles of the String at Selected Time .
 $a(0) = 10$, $b = \infty$, $\epsilon = 0.01$.

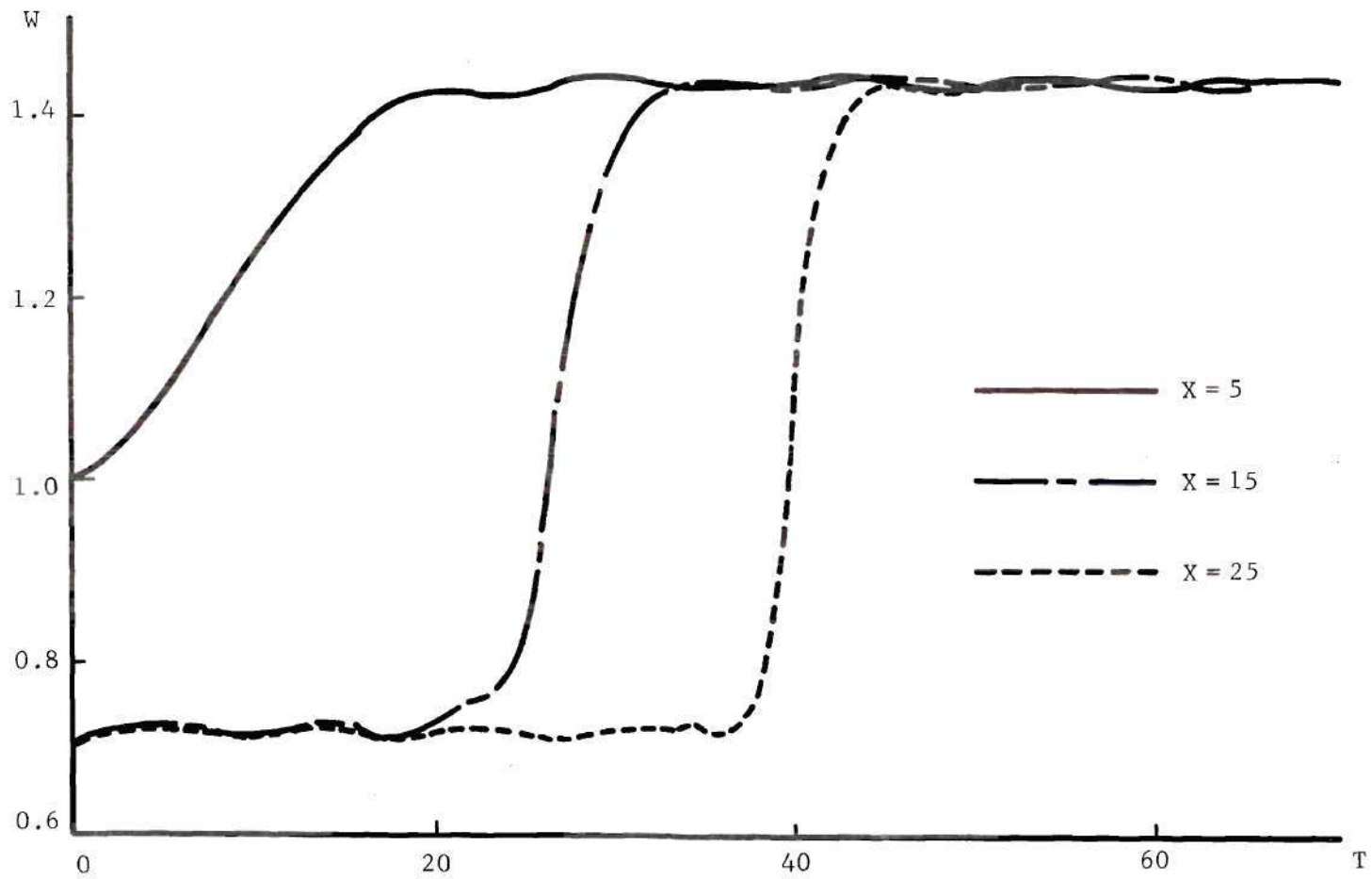


Figure 16. Displacement History at Selected Points on the String.
 $a(0) = 5$, $b = \infty$, $\epsilon = 0.01$.

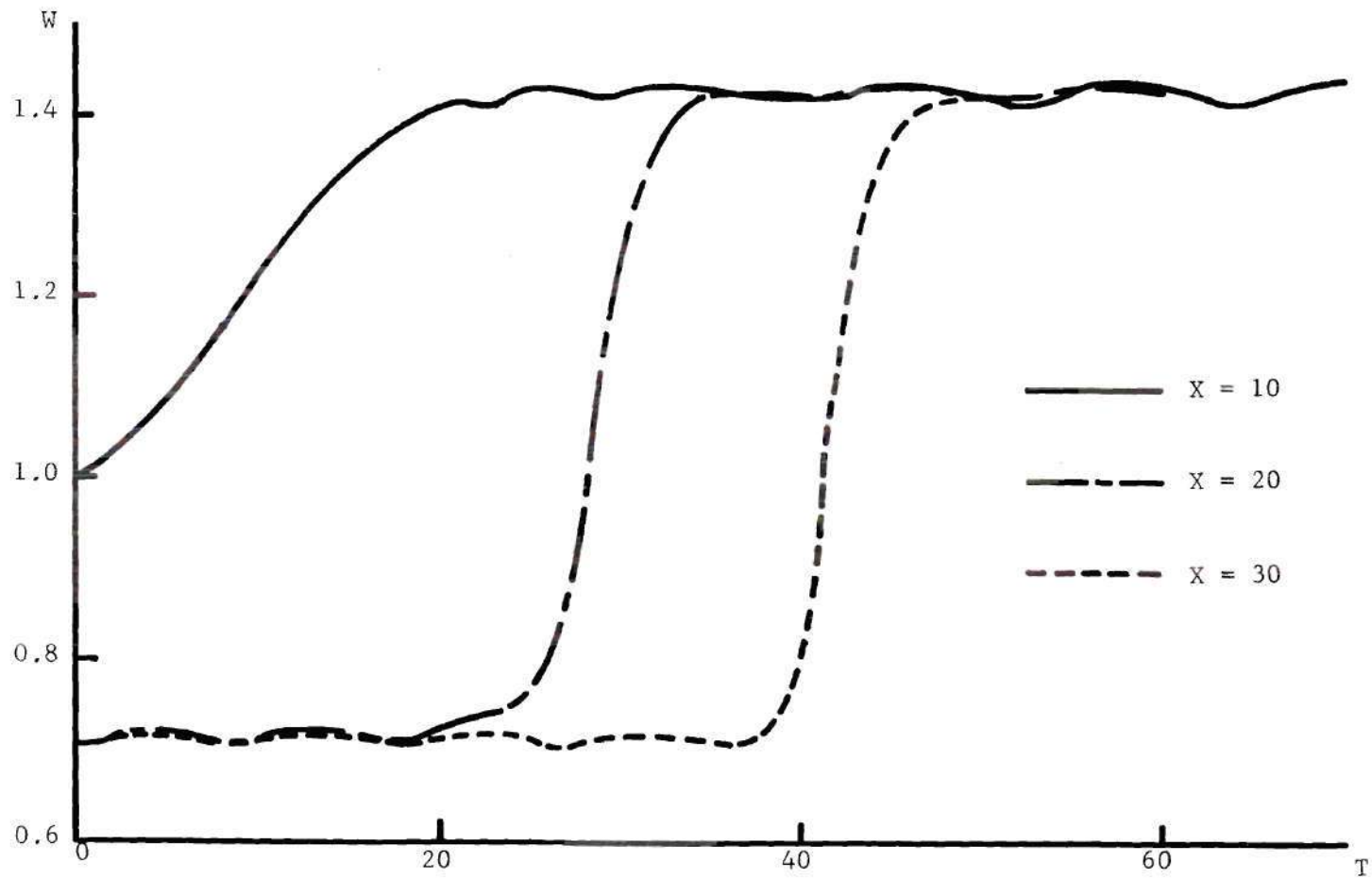


Figure 17. Displacement History at Selected Points on the String.
 $a(0) = 10$, $b = \infty$, $\epsilon = 0.01$.

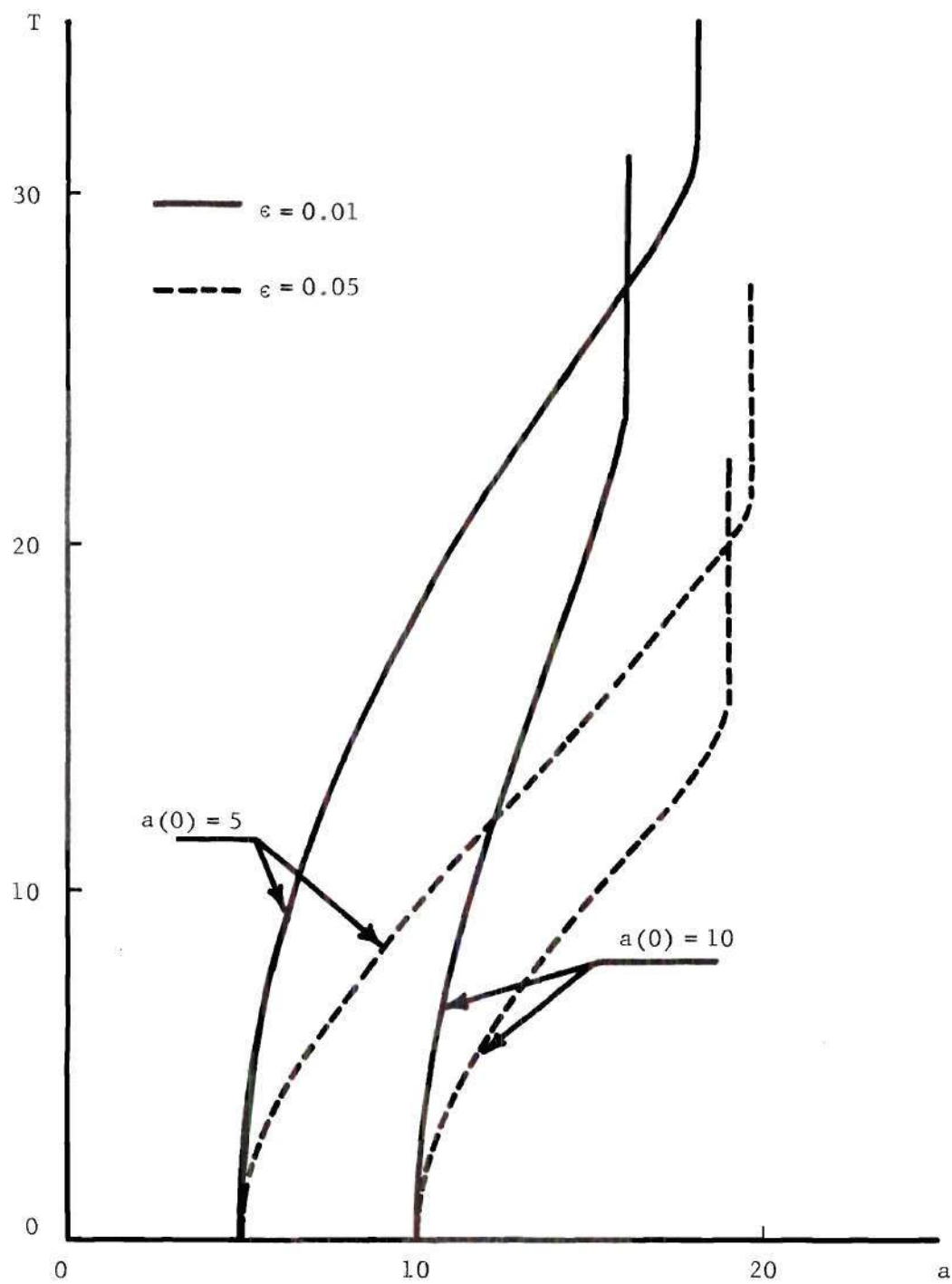


Figure 18. Crack Length Versus Time. $b = 20$.

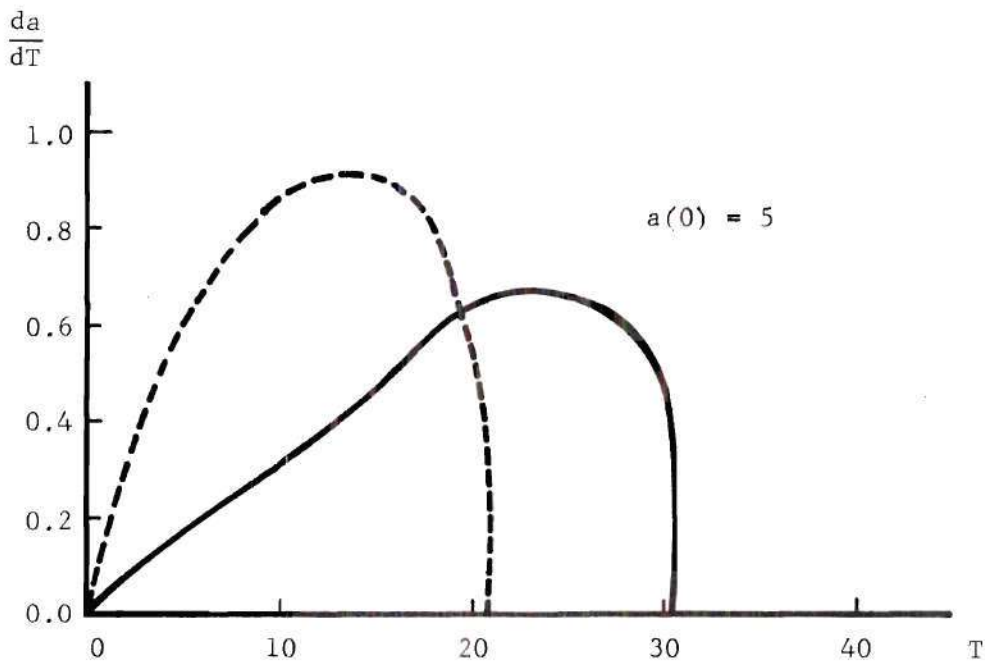
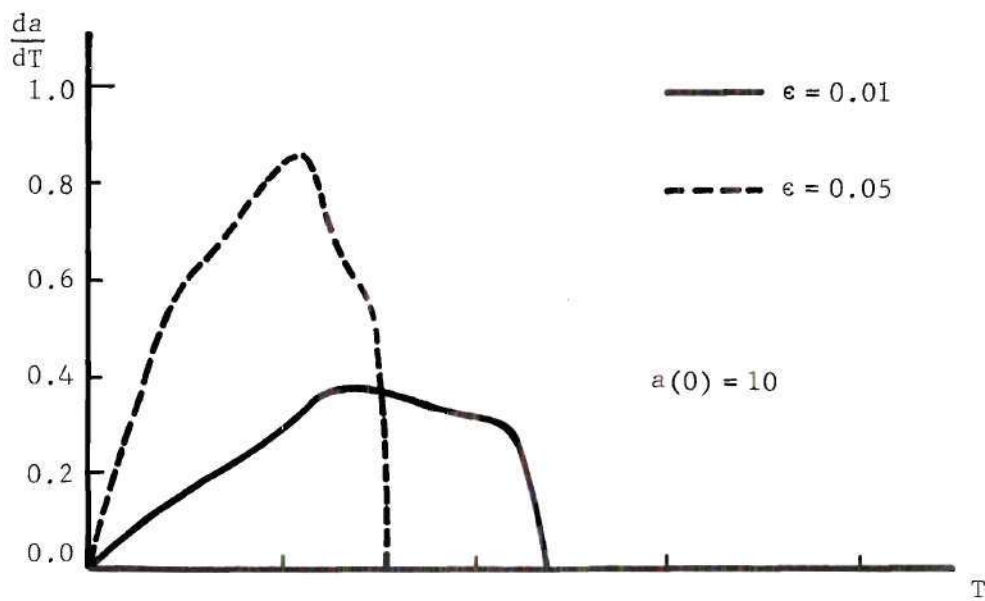


Figure 19. Velocity of Crack Propagation. $b = 20$.

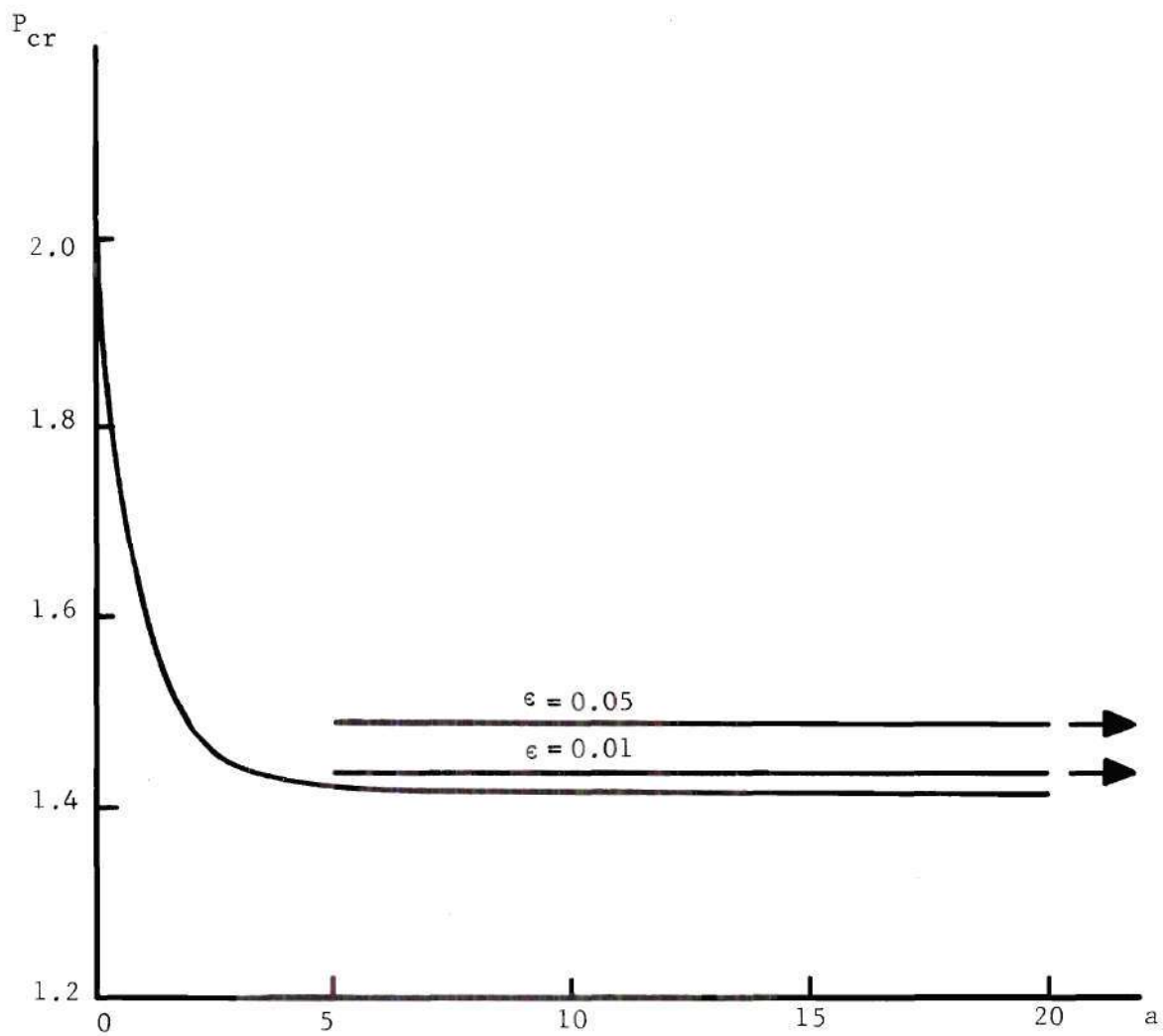


Figure 20. Unstable Crack Propagation. $a(0) = 5$, $b = \infty$.

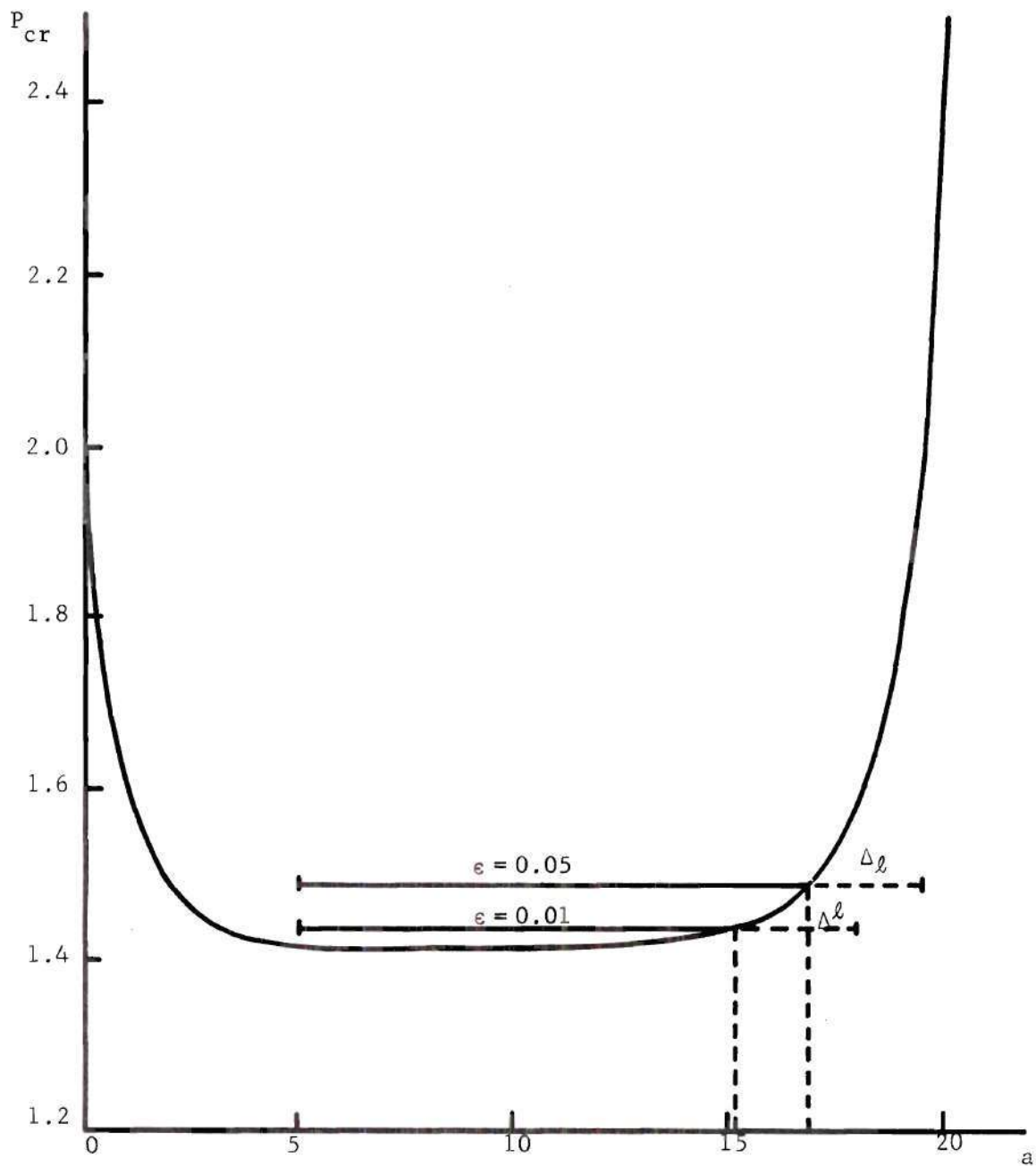


Figure 21. Stable Crack Propagation. $a(0) = 5$, $b = 20$.

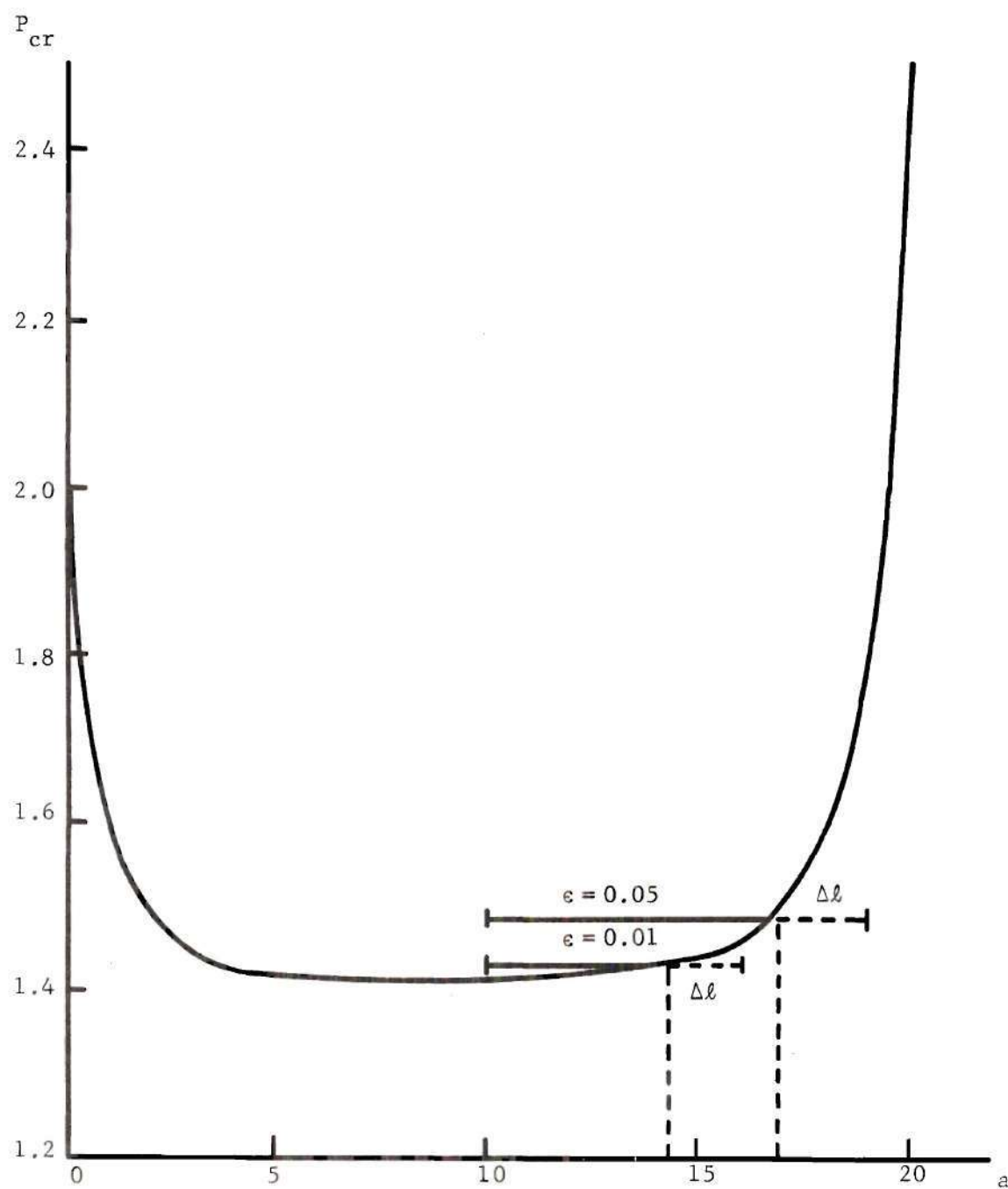


Figure 22. Stable Crack Propagation. $a(0) = 10$, $b = 20$.

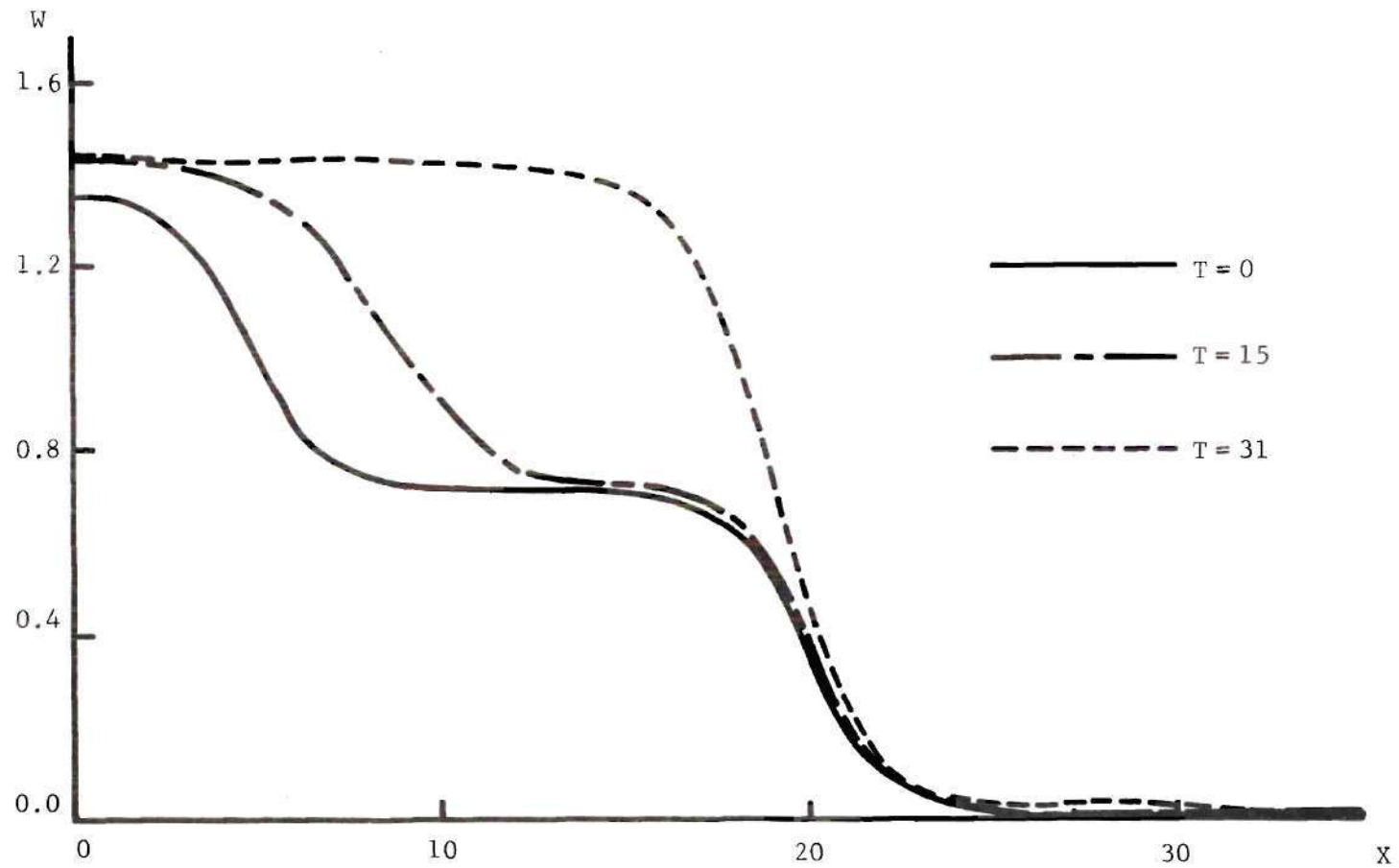


Figure 23. Displacement Profiles of the String at Selected Time. $a(0) = 5$, $b = 20$, $\epsilon = 0.01$.

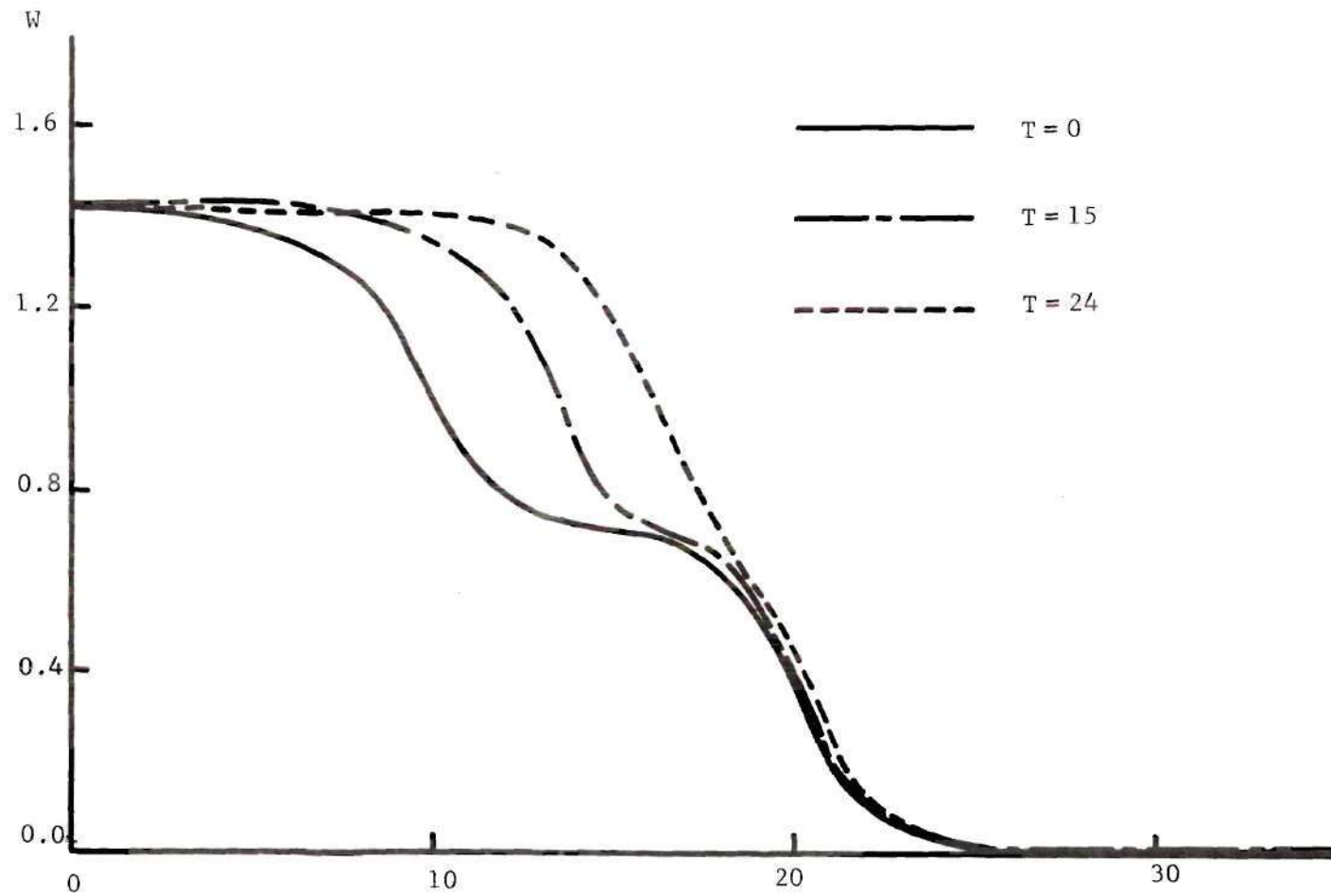


Figure 24. Displacement Profiles of the String at Selected Time. $a(0) = 10$, $b = 20$, $\epsilon = 0.01$.

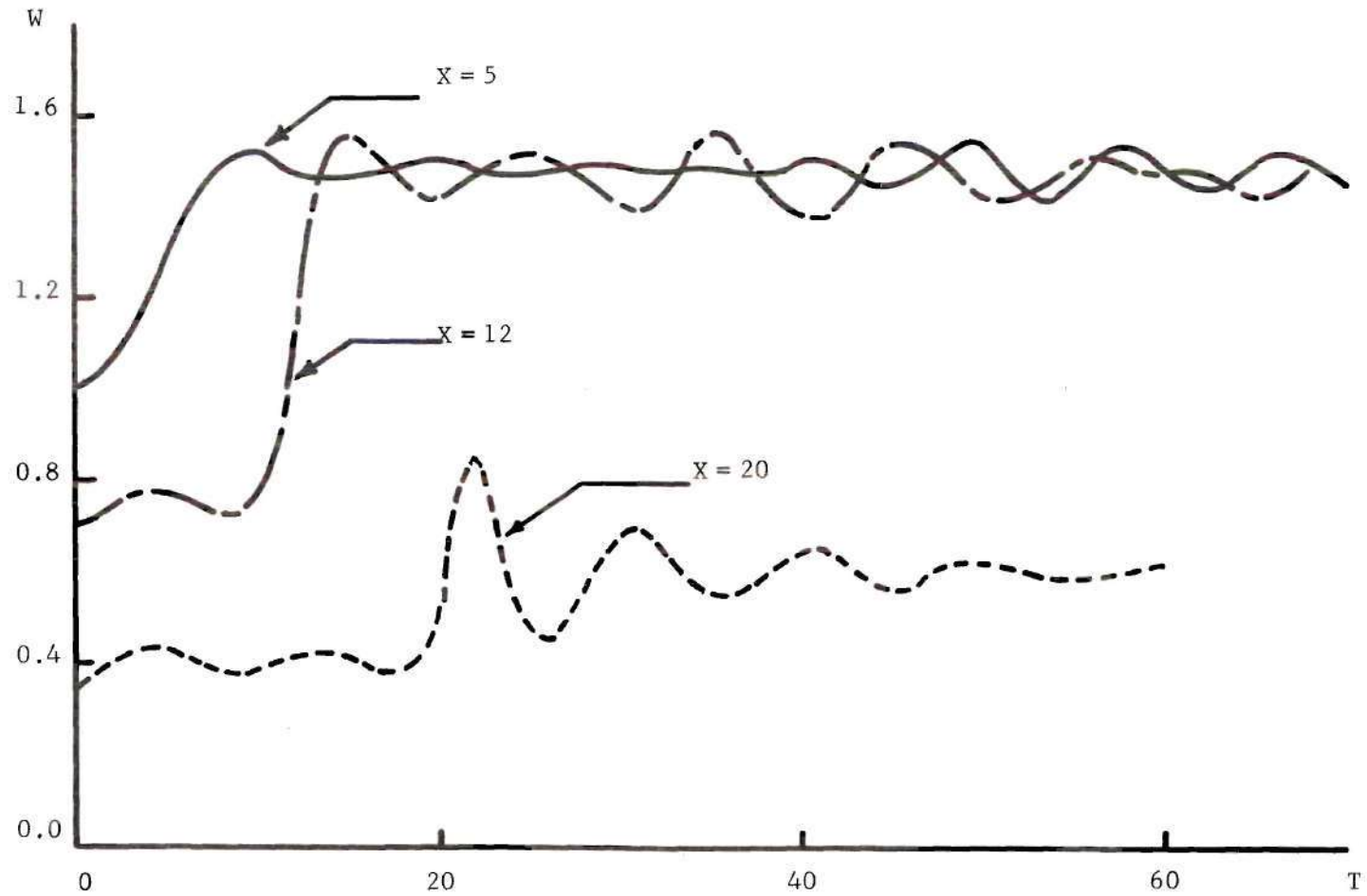


Figure 25. Displacement History at Selected Points on the String. $a(0) = 5$, $b = 20$, $\epsilon = 0.05$.

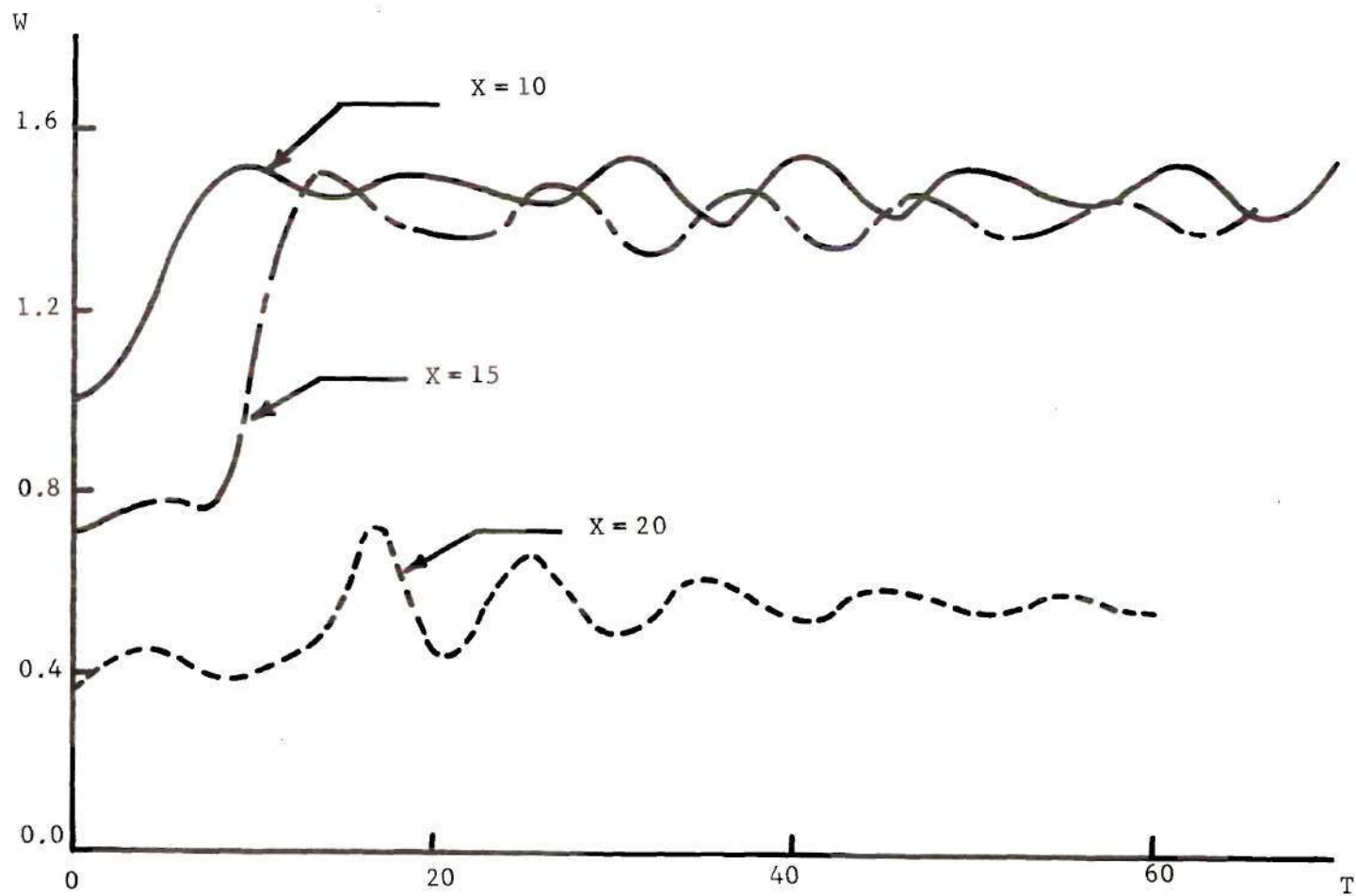


Figure 26. Displacement History at Selected Points on the String. $a(0) = 10, b = 20, \epsilon = 0.05$.

rest under no external load and the tensile foundation contains an initial crack of length $a(0)$.

If there were no crack, the string would perform uniform oscillatory motions (with amplitude dependent on the magnitude of applied load and frequency dependent on the foundation stiffness). Thus points on the string sufficiently far from the crack behave just as a single degree of freedom spring-mass system. Since the effects of the initial crack cannot be transmitted faster than the sound speed of the string, the characteristic line $\frac{dX}{dT} = 1$ passing through the initial position of the crack tip divides the XT plane into regions of uniform and nonuniform motion. Thus the region of integration is reduced to the shaded part of Figure 27a.

For computational purposes, we set up index coordinates (i, j) originating at $X = a(0)$ and $T = 0$; i.e. the original crack tip. The axes i, j are parallel to the characteristic lines $\frac{dX}{dT} = 1$ and $\frac{dX}{dT} = -1$ respectively. Along the line $j = 0$ the motion is governed by

$$\frac{d^2W}{dT^2} + 2M^2W = M^2P \quad (26)$$

with initial conditions

$$W(0) = 0 \quad \text{and} \quad \frac{dW(0)}{dT} = 0 .$$

Thus the dependent variables along $j = 0$ are

$$\begin{aligned} W_{i,0} &= \frac{P}{2} (1 - \cos \sqrt{2} MT) , \\ V_{i,0} &= \frac{\sqrt{2}}{2} MP \sin \sqrt{2} MT) , \end{aligned} \quad (27)$$

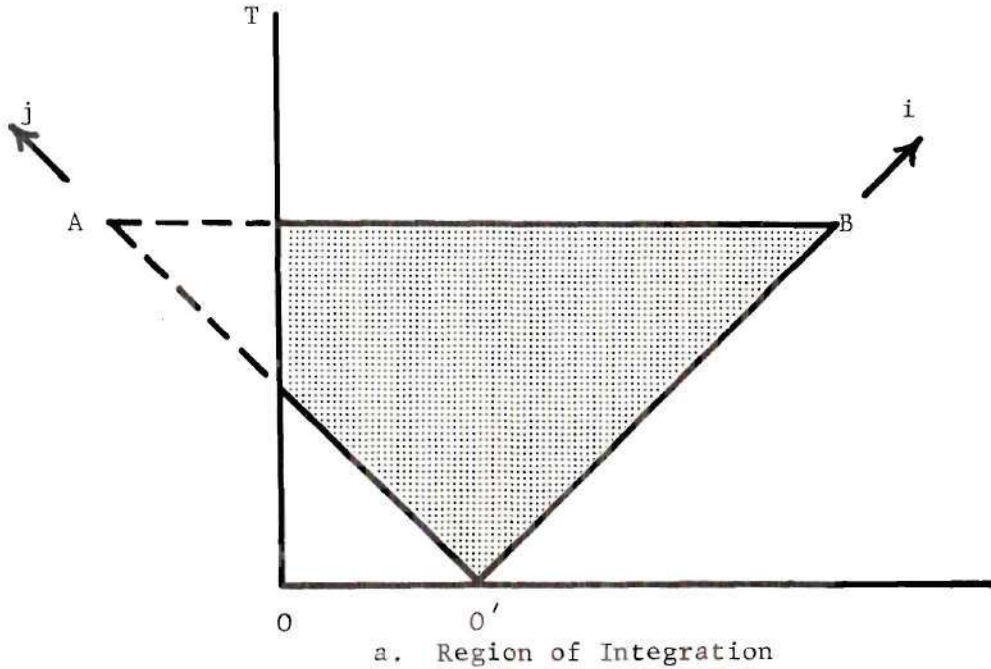
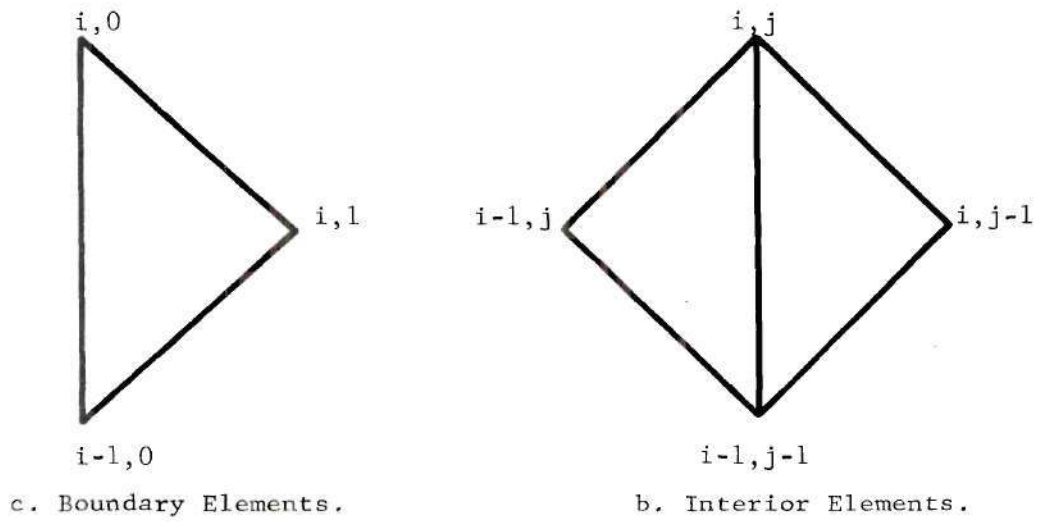


Figure 27. Region of Integration and its Elements.

$$\Theta_{i,0} = 0$$

and

$$Q_{i,0} = 2W_{i,0} .$$

Along the line $i = -j$ ($T=0$) we have the homogeneous initial conditions

$$W_{-j,j} = V_{-j,j} = \Theta_{-j,j} = Q_{-j,j} \equiv 0 .$$

The interior element is shown in Figure 27b; its difference equations are given by (23 and (24). The boundary elements (see Figure 27c) are triangles. With the boundary condition $\Theta = 0$. The treatment of boundary elements is the same as in the previous section, and the solutions are similar to (25).

The uniform load P is taken to be a fraction of the least load that would rupture the perfect tensile foundation. This load can be obtained from (10) by setting the maximum displacement equal to the critical displacement (unity) and solving for P . The least load was found to be unity.

To insure that the existing crack extends, the load P must be greater than a certain minimum value that cannot be found directly. Numerically it is approximately 0.76. If P is less than this value, the initial crack does not extend.

In this section, we also consider a semi-infinite crack. For this case, it is convenient to take the origin of the XT plane at the initial position of the crack tip; i.e. move O to O' in Figure 27a. Thus the index coordinates and the XT coordinates have a common origin. The region of integration is the triangle $O'AB$.

Along $i = 0$ ($O'A$) the dependent variables are

$$\begin{aligned} W_{0,j} &= P(1 - \cos MT) , \\ V_{0,j} &= MP \sin MT , \\ \Theta_{0,j} &= 0 \end{aligned} \quad (28)$$

and

$$Q_{0,j} = W_{0,j} .$$

All elements are square (Figure 27b) with difference equations given again by (23) and (24). Numerical results for both the finite and semi-infinite initial cracks are presented in Figures 28-37.

Figure 28 shows how the crack tip displacement depends on the magnitude of the applied load. When P is small, the crack tip displacement remains below the critical value and the crack does not extend. The amplitude of the crack tip displacement increases with increasing P . and at $P \approx 0.76$, the maximum crack tip displacement exceeds the critical value and the crack extends.

We take this value as the lowest suddenly applied and maintained uniform load that will extend any existing crack of initial length greater than 5. It is approximately 54% of the static critical load P_{cr} .

Figures 29, 33, 34 and 35 show an unexpected feature of crack propagation due to suddenly applied load. The crack does not propagate continuously. When $P > 0.76$, the initial crack extends, but its extension is accompanied by the formation of new and separate cracks. We shall call these new cracks "secondary cracks". As time increases, they grow in

size and continue to increase in number. The length of the secondary cracks seems to be limited.

In comparing the figures, we conclude that the effect of the original crack length is small. The relative positions of the secondary cracks are very much the same and the corresponding secondary cracks are formed approximately at the same time. The only influence of initial crack length seems to be in the extension of the primary (initial) crack. Longer initial cracks ($a(0) = \infty$ in Figure 29 and $a(0) = 20$ in Figure 35) stop extending at an earlier stage than shorter initial cracks ($a(0) = 5$ in Figure 33 and $a(0) = 10$ in Figure 34). The shorter initial cracks continue to grow slowly until, for $a(0) = 5$ (Figure 33), the primary crack and the nearest secondary crack coalesce.

Displacement profiles before and after the occurrence of secondary cracks are shown in Figure 30. In Figure 31 we show successive displacement profiles for the string segment from $X = 0$ to $X = 12$. Here we see a local maximum displacement in front of the original crack tip building up and finally forming a secondary crack.

To understand how these small secondary cracks are formed, it is helpful to decompose the displacement history of a point within such a cracked segment into two parts. The first part, which we shall refer to as the remote response, would be the response of the point if the foundation were perfect. The remaining part of the response is due to the disturbing effect of the crack. This is zero until a signal travels from the crack tip to the point in question. Shortly after the signal arrives, this part of the displacement remains small compared to the remote response, but its amplitude increases with time. When it is large enough

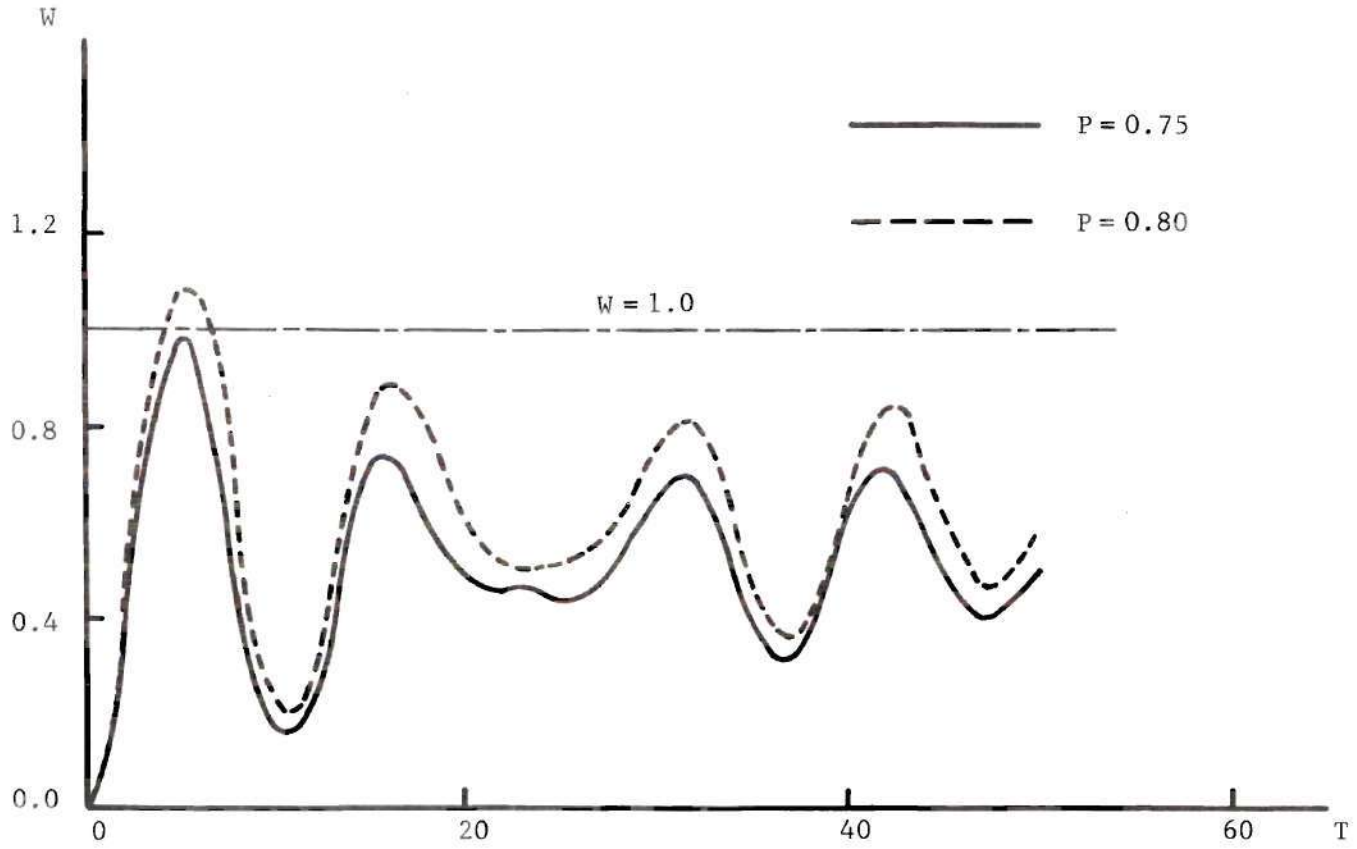


Figure 28. Displacement History of the Initial Crack Tip. $a(0) = \infty$.

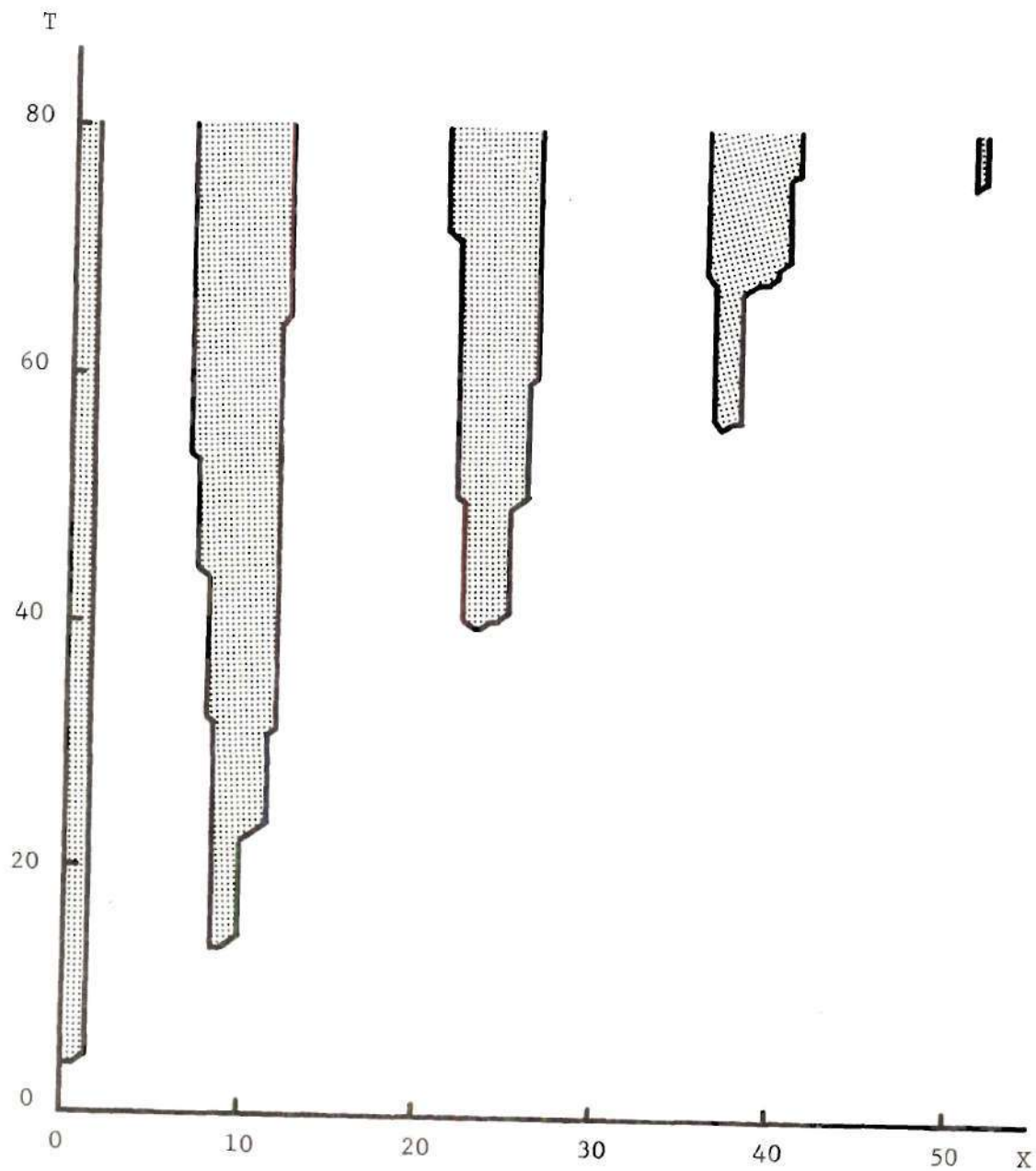


Figure 29. Location of the Cracks. $a(0) = \infty$, $P = 0.95$.

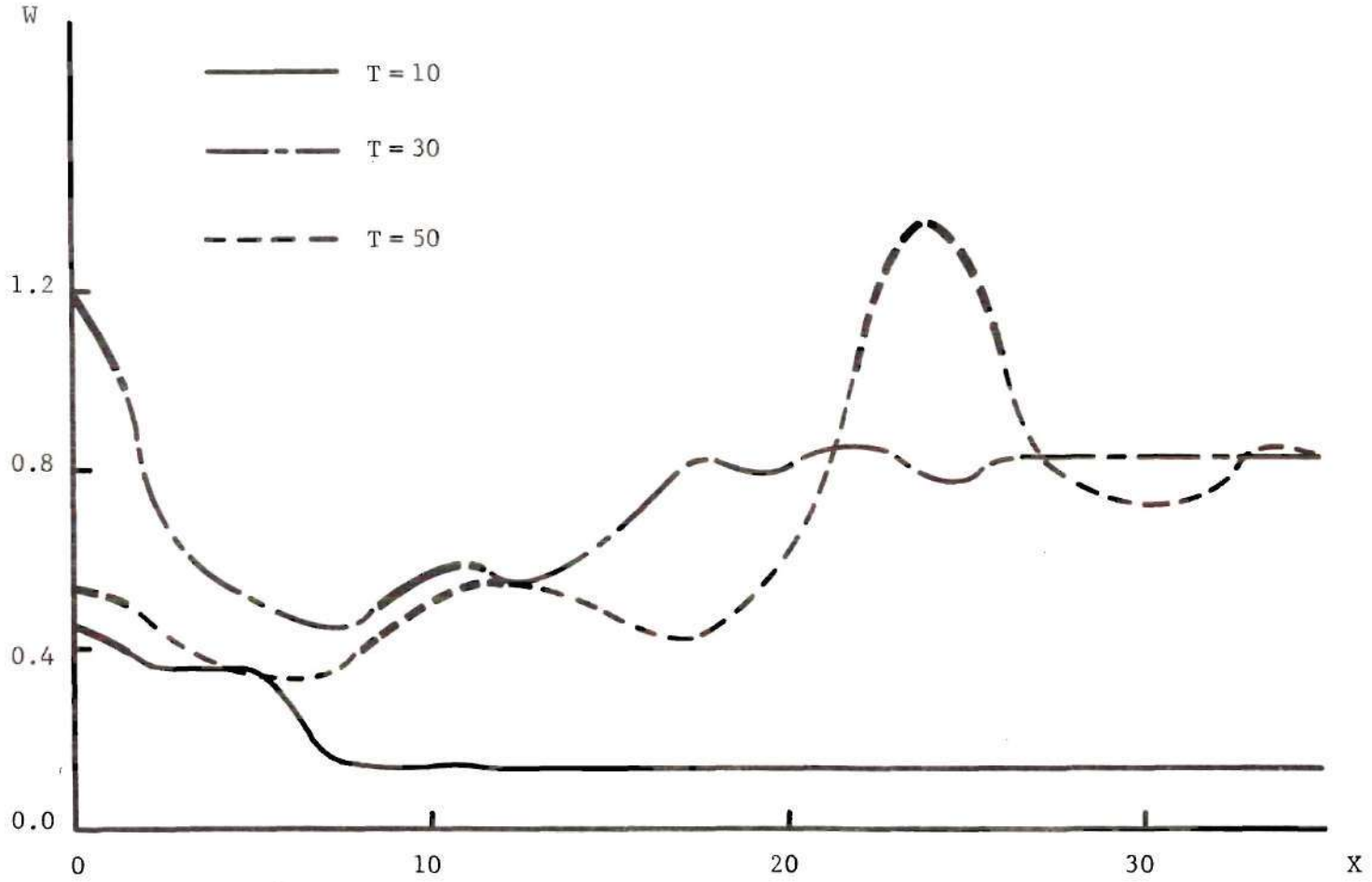


Figure 30. Displacement Profiles of the String at Selected Time. $a(0) = \infty$, $P = 0.95$.
 (Boldface lines indicate the positions of cracks)

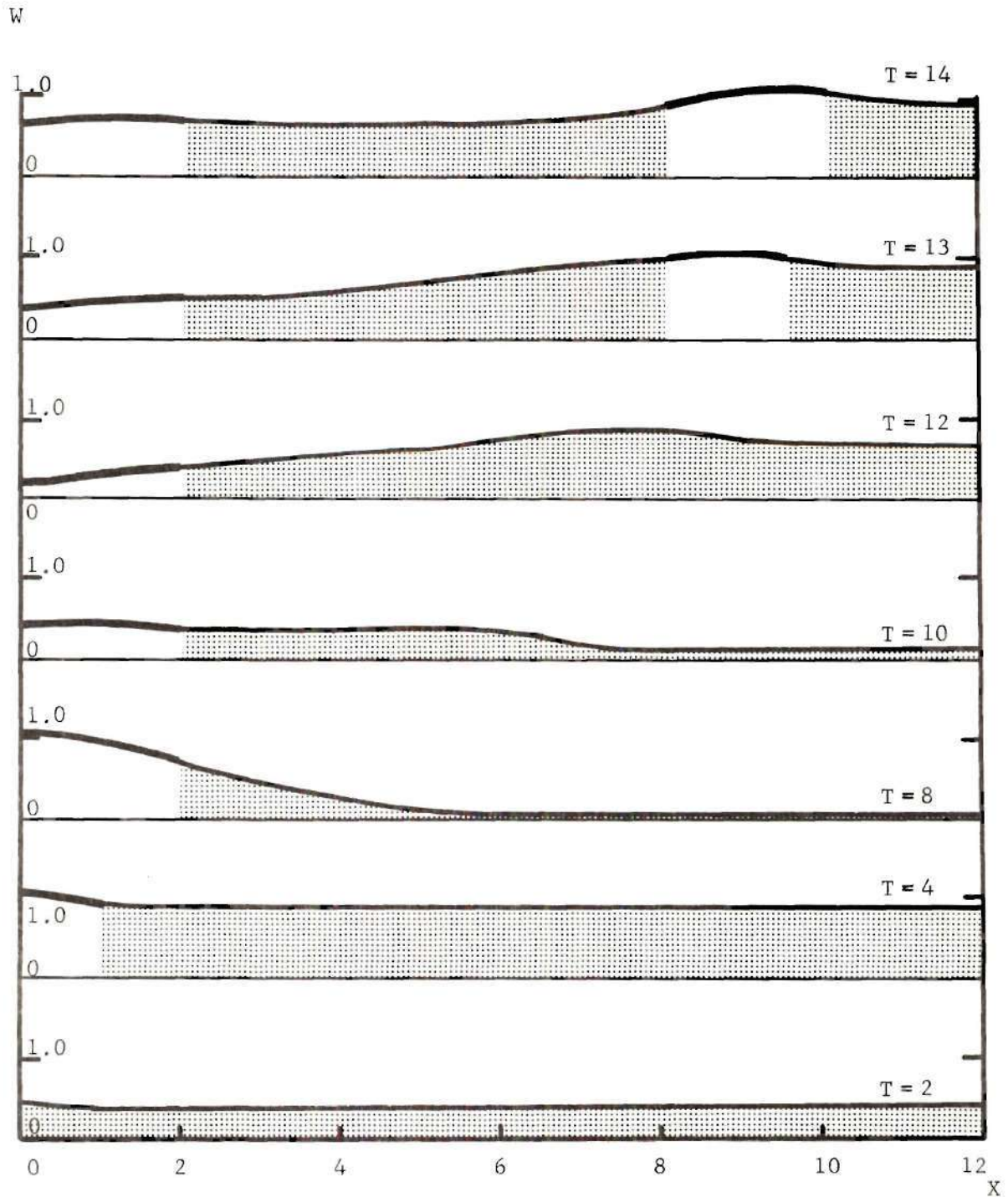


Figure 31. Successive Displacement Profiles Show Forming of a Secondary Crack. $a(0) = \infty$, $P = 0.95$.

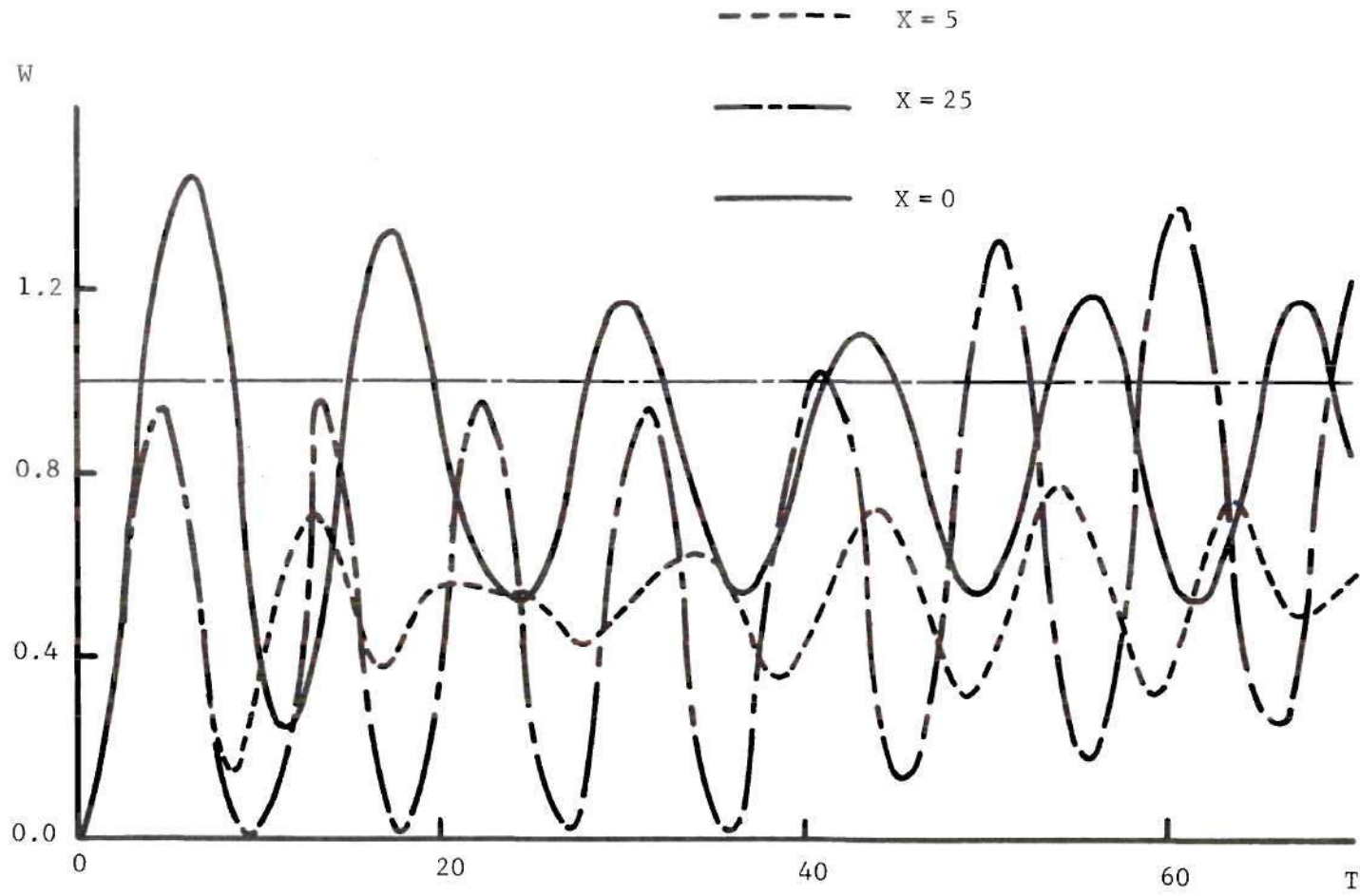


Figure 32. Displacement History at Selected Points on the String. $a(0) = \infty$, $p = 0.95$.

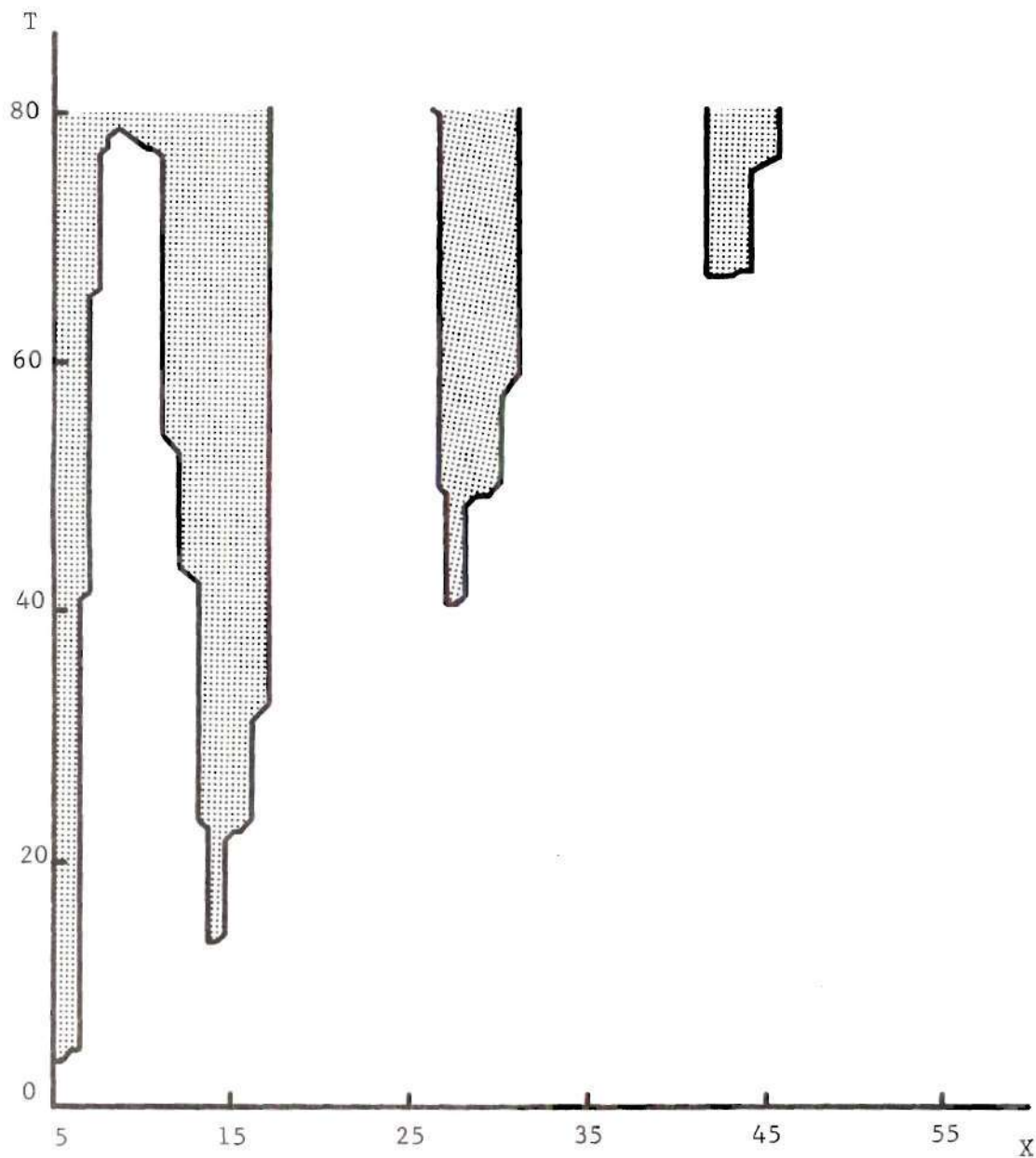


Figure 33. Location of the Cracks. $a(0) = 5$, $P = 0.95$.

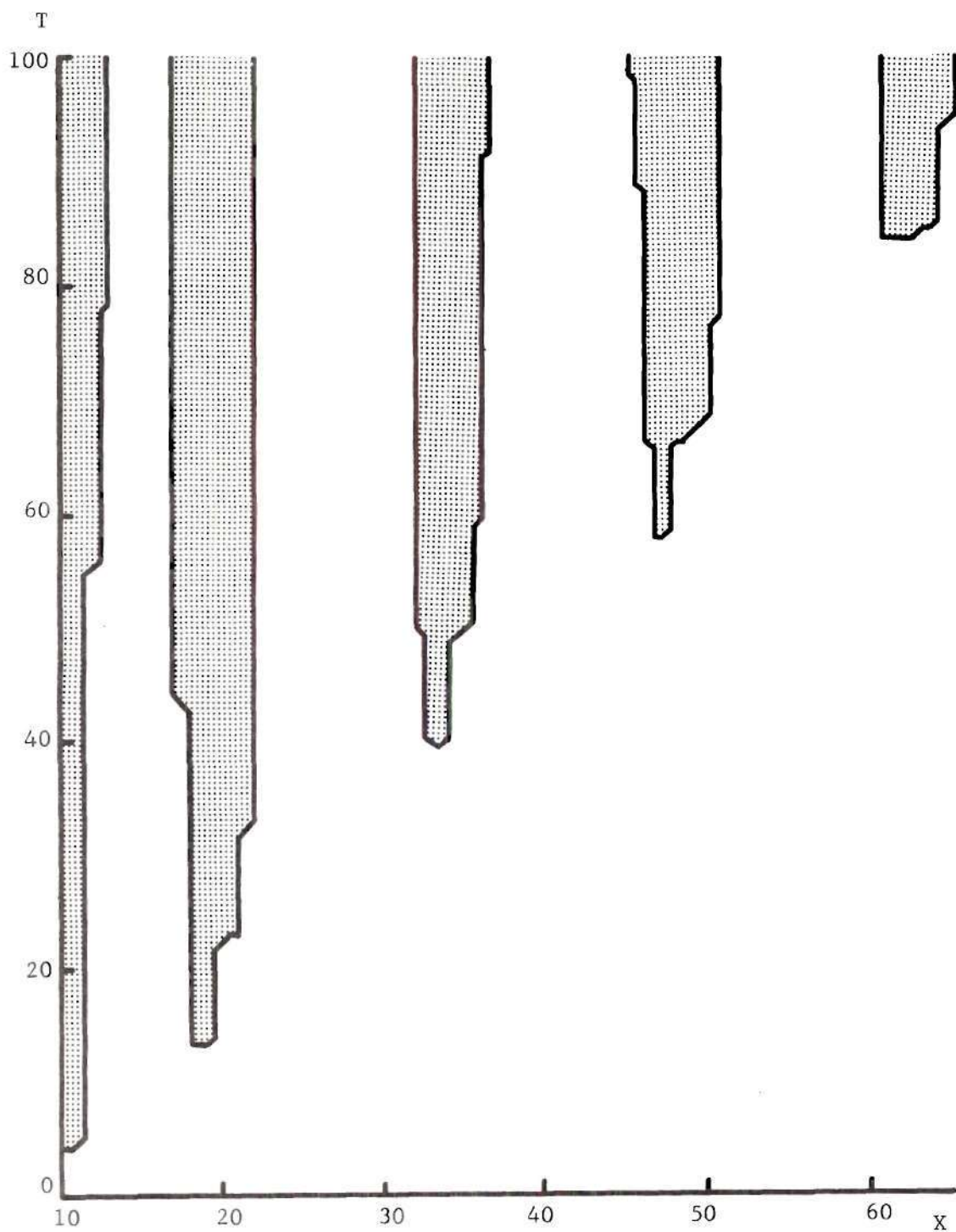


Figure 34. Location of the Cracks. $a(0) = 10$, $P = 0.95$.

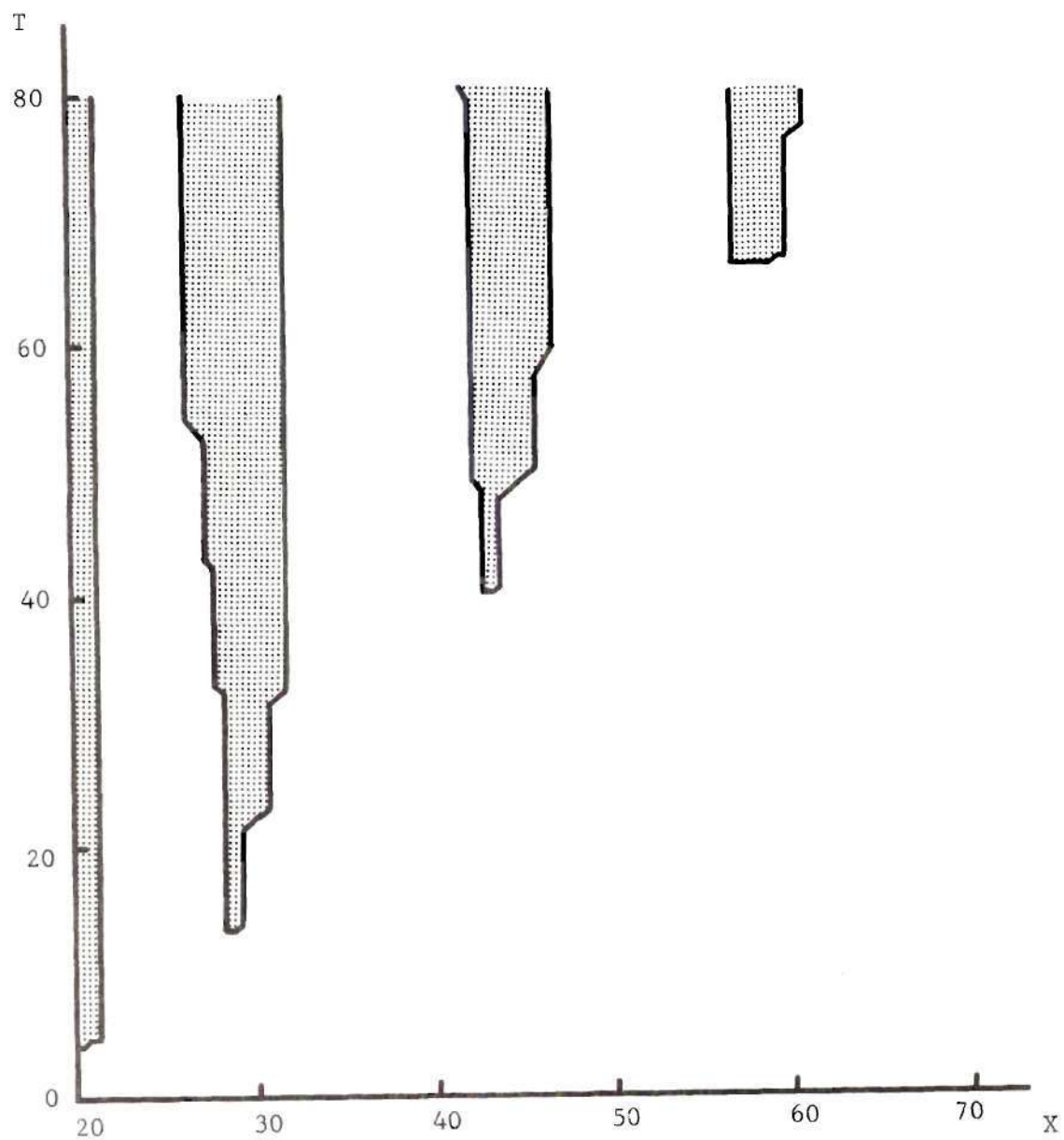


Figure 35. Location of the Cracks. $a(0) = 20$, $P = 0.95$.

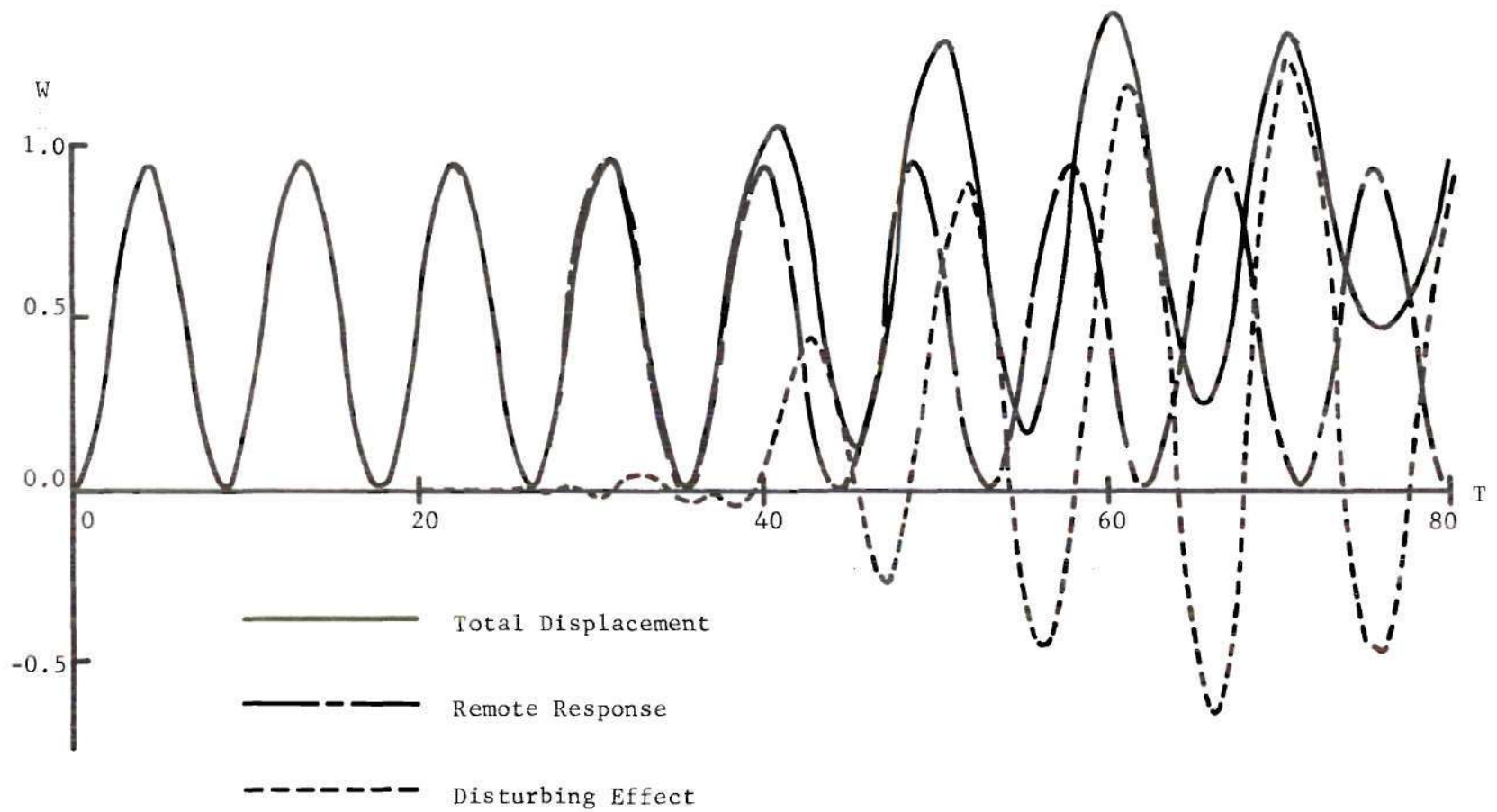


Figure 36. Decomposition of Displacement History. $a(0) = \infty$, $P = 0.95$, $X = 25$.

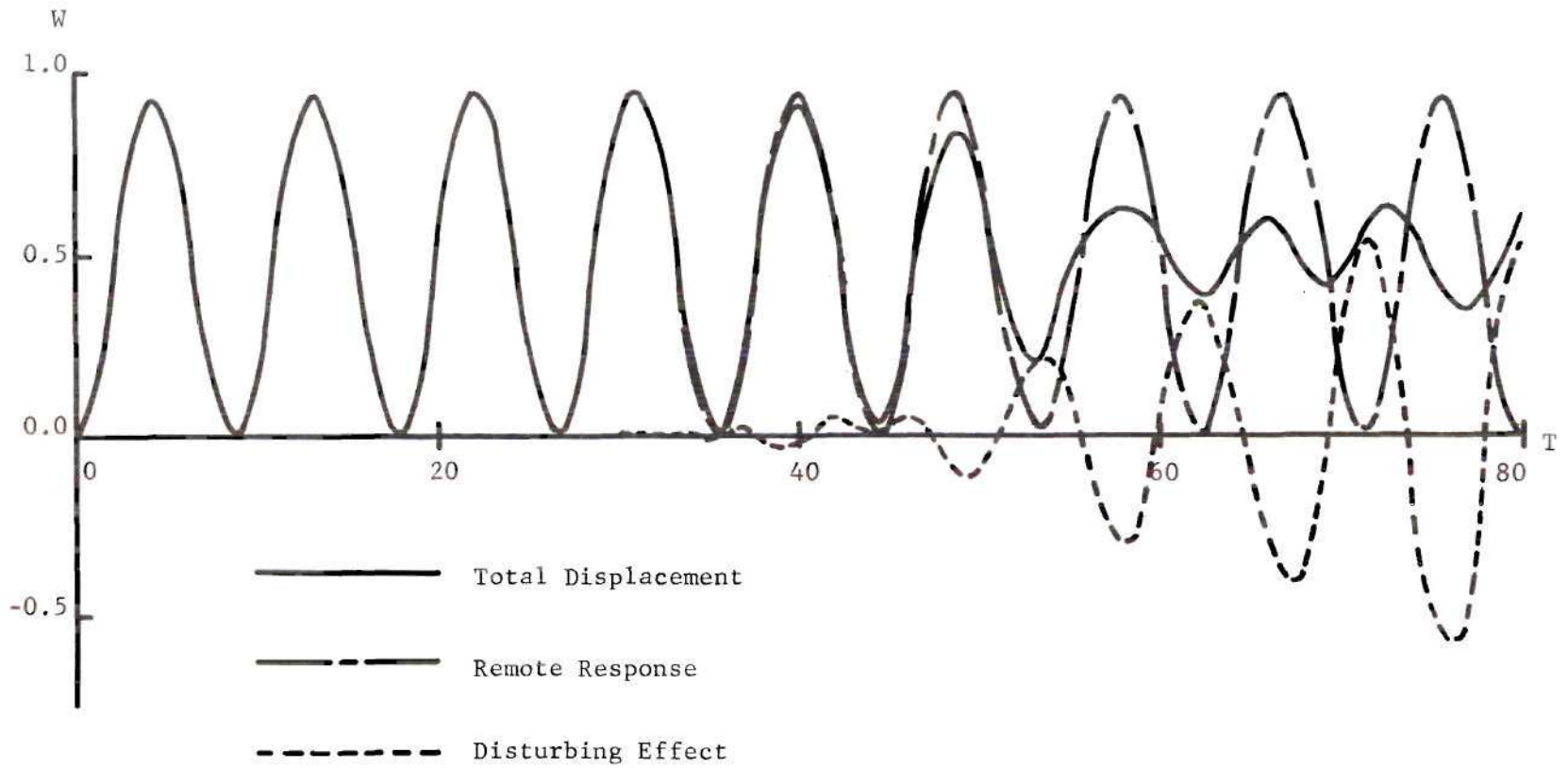


Figure 37. Decomposition of Displacement History. $a(0) = \infty$, $P = 0.95$, $X = 30$.

and additive to the remote response, the total displacement exceeds the critical value and a secondary crack is formed. Figure 36 shows this happening 25 units downstream from the tip of the semi-infinite crack.

Figure 37 shows the displacement history of a point 30 units downstream. Here the response due to the presence of the crack is out of phase with the remote response and no secondary crack is formed.

Initial Velocity Problem

The string is initially at rest under no external load. At $T = 0$, every point of the string is given the same transverse velocity V_0 by the application of a uniform impulse over the entire string. There is an initial crack of half-length $a(0)$ in the tensile foundation.

The numerical calculations for this case are similar to those of the suddenly-applied-load problem. The region of integration shaded in Figure 27a is used again here. Along the line $X = T + a(0)$ (or $j = 0$), the solution is known,

$$W_{i,0} = \frac{V_0}{\sqrt{2} M} \sin \sqrt{2} MT ,$$

$$V_{i,0} = V_0 \cos \sqrt{2} MT , \quad (29)$$

$$Q_{i,0} = 2 W_{i,0}$$

and

$$\Theta_{i,0} = 0 .$$

If the maximum displacement of the remote part of the string is to remain less than the critical value, there is an upper limit for V_0 .

Setting the maximum $W_{i,0}$ in (29) equal to unity, we find that the upper limit for V_0 is $\sqrt{2} M$. The least V_0 extending an initial crack is approximately 0.62 for $M^2 = \frac{1}{4}$ (Figure 38).

The semi-infinite crack is also considered for this loading. The region of integration and elements used in the computation are the same as those used for the corresponding problem in the previous section (Figure 27).

For the remote part of the string ($X = -T$), the solution is

$$\begin{aligned} W_{0,j} &= \frac{V_0}{M} \sin MT, \\ V_{0,j} &= V_0 \cos MT, \end{aligned} \tag{30}$$

$$Q_{0,j} = W_{0,j}$$

and

$$\Theta_{0,j} = 0.$$

Results for this problem are shown in Figures 38-43. These figures show that the crack propagates in much the same manner as it would under a suddenly applied and maintained load. For $V_0 = 0.67$, separate secondary cracks are formed. In contrast to the suddenly applied load problem, however, the secondary cracks in the present problem do not tend to coalesce even when very short initial cracks are considered (Figures 42 and 43).

Periodic Loading

When a time dependent uniform load is applied to the string, the disturbing effect of an existing crack can also cause the formation of

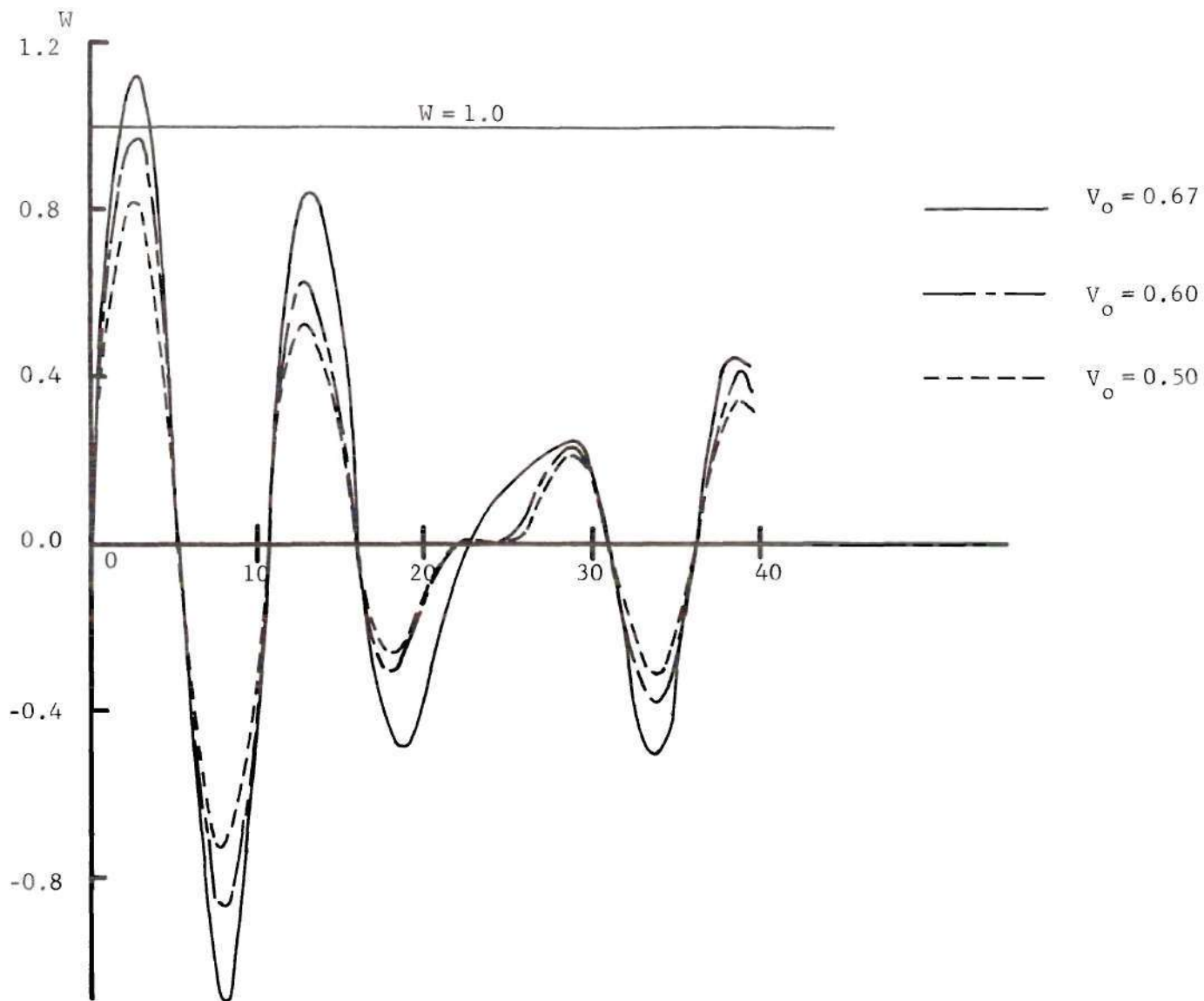


Figure 38. Displacement History of the Initial Crack Tip. $a(0) = \infty$.

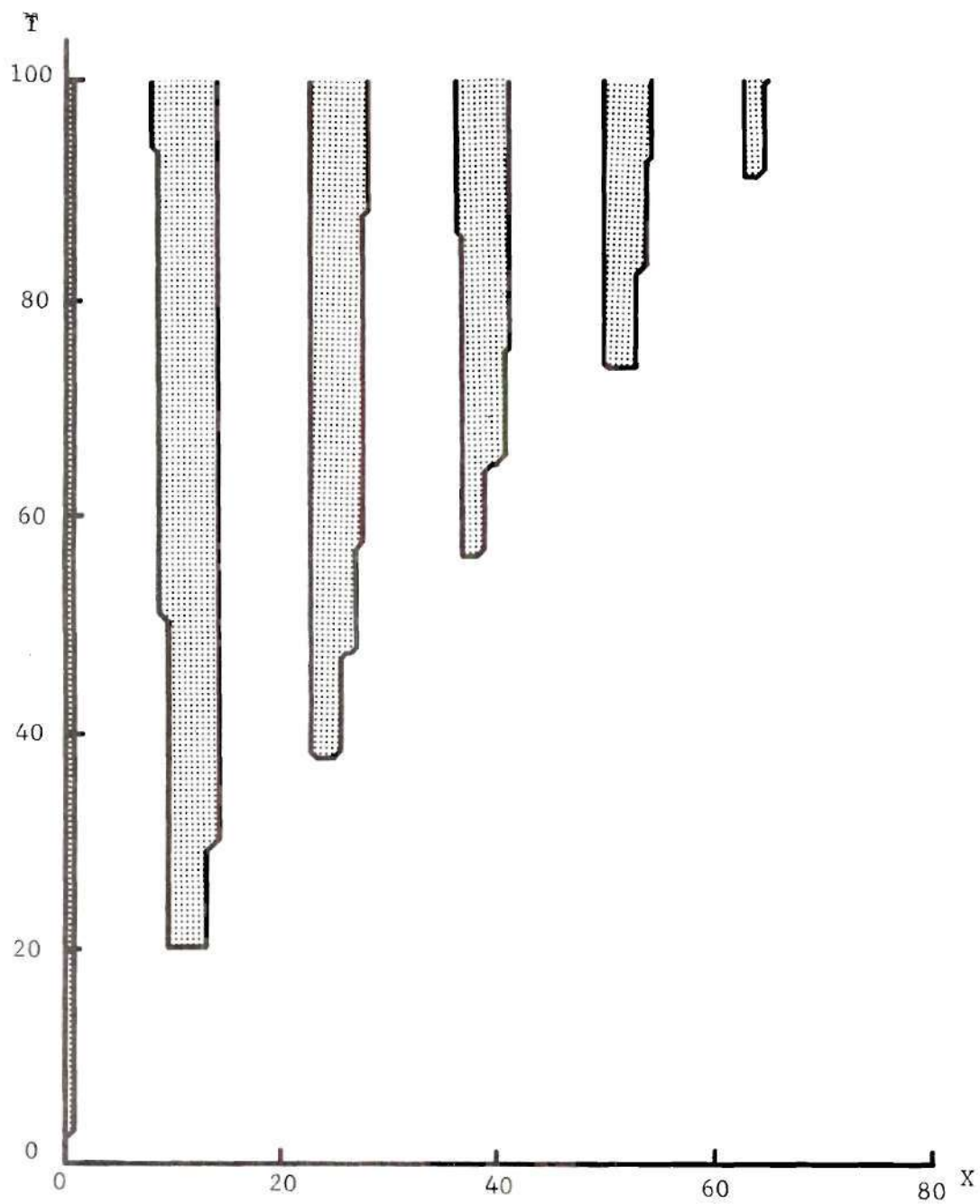


Figure 39. Location of the Cracks. $a(0) = \infty$, $V_0 = 0.67$.

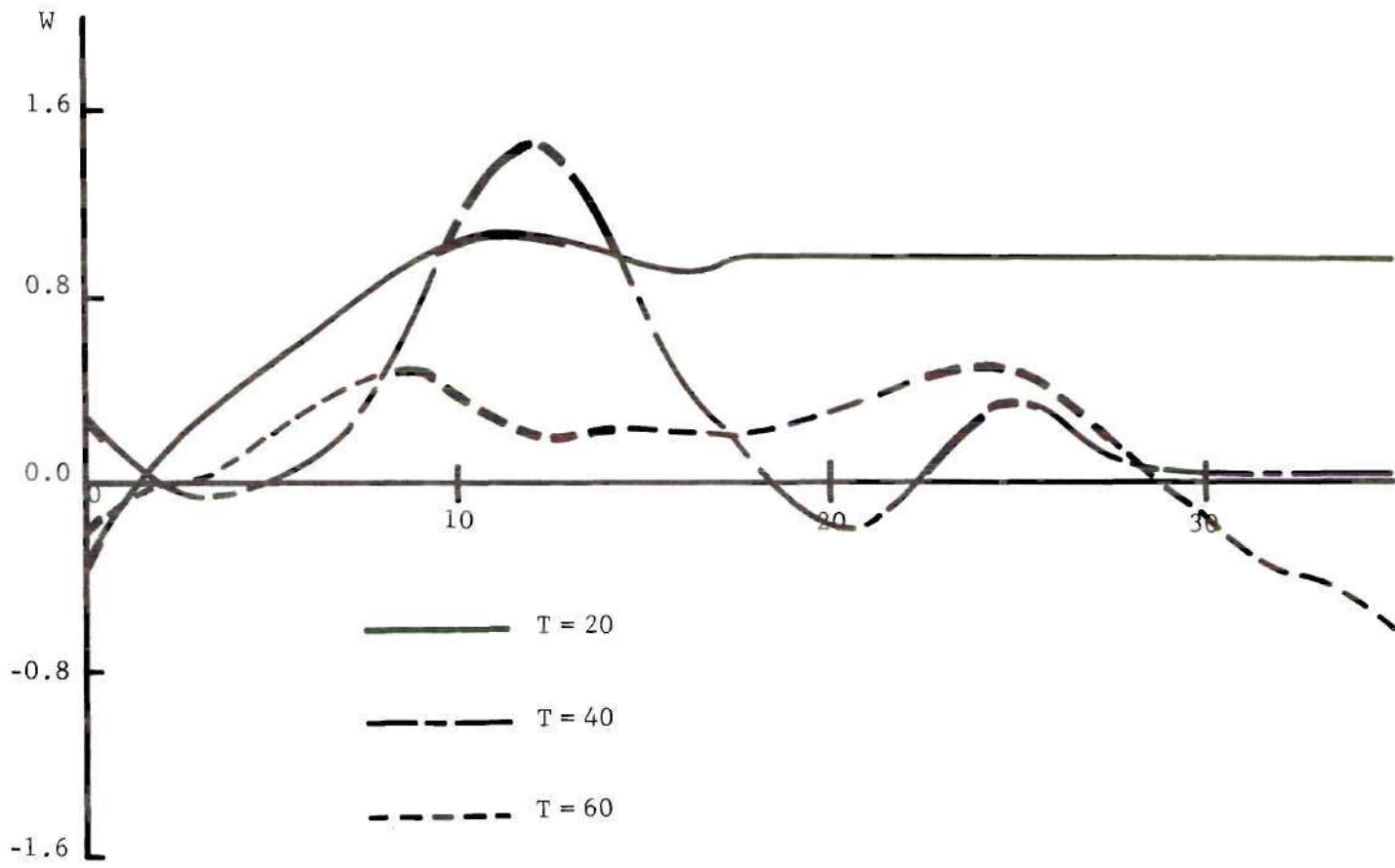


Figure 40. Displacement Profiles of the String at Selected Time. $a(0) = \infty, V_0 = 0.67$.

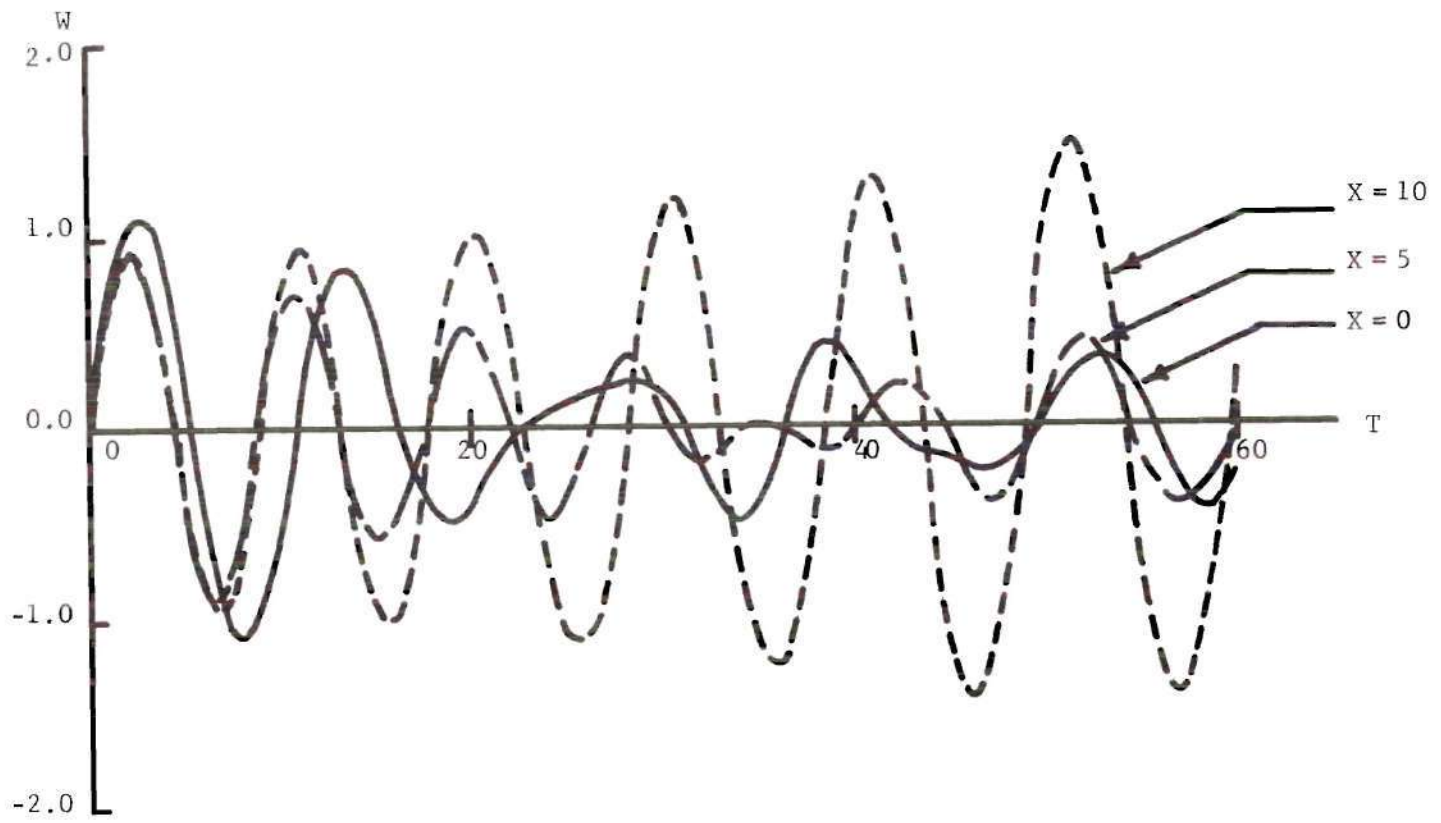


Figure 41. Displacement History at Selected Points on the String. $a(0) = \infty$, $V_0 = 0.67$.

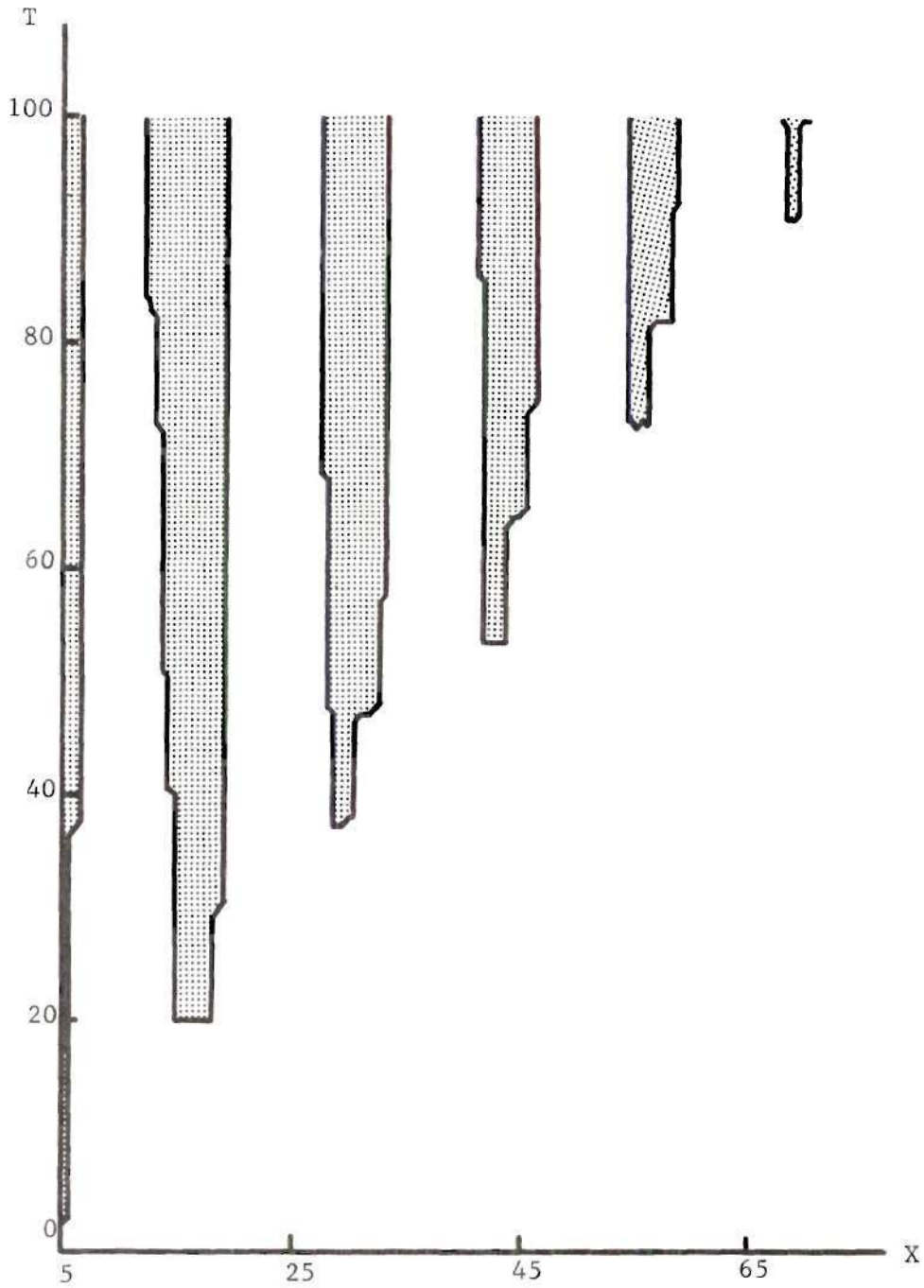


Figure 42. Location of the Cracks. $a(0) = 5$, $V_0 = 0.67$.

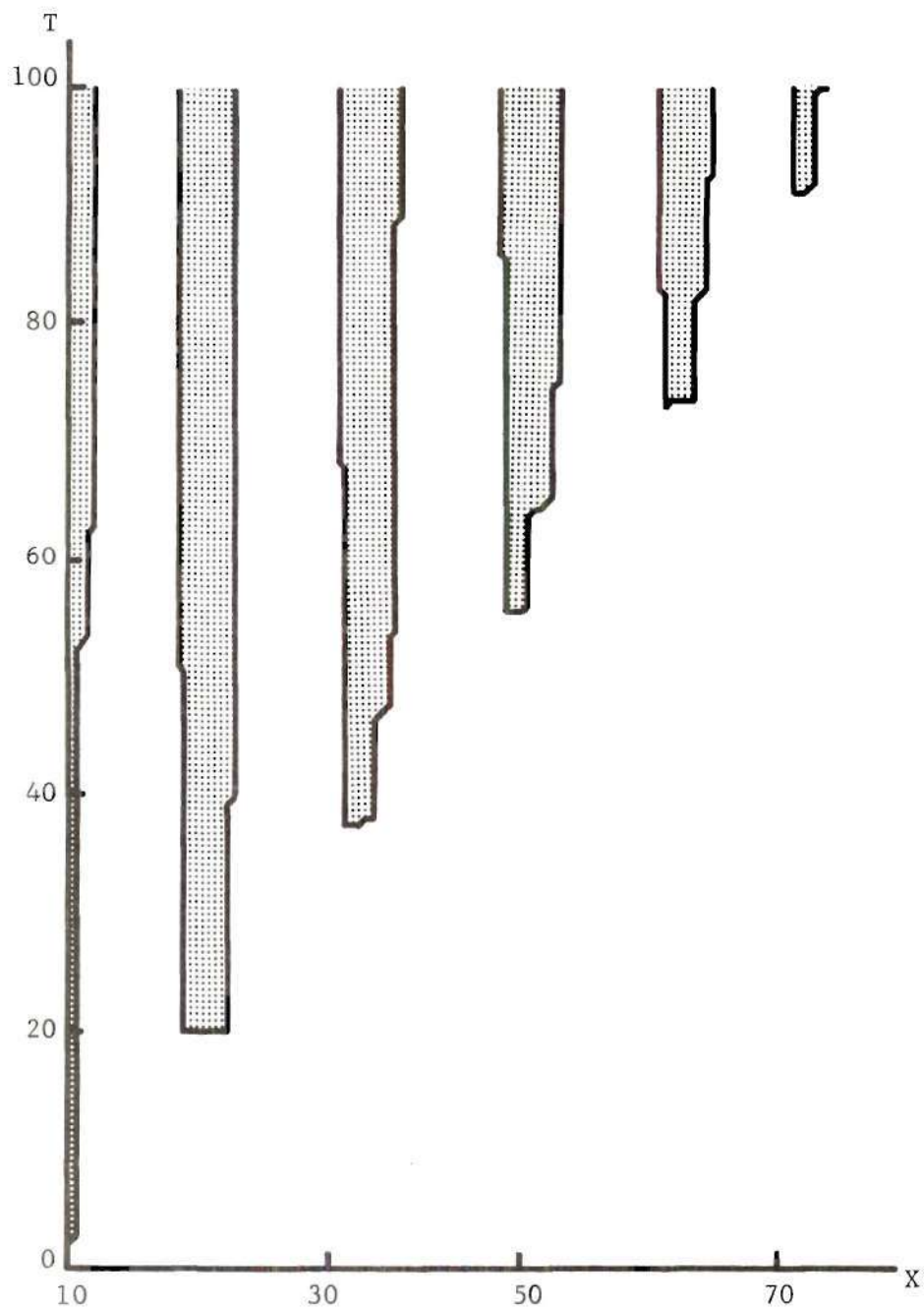


Figure 43. Location of the Cracks. $a(0) = 10$, $v_o = 0.67$.

secondary cracks. In this section we consider the problem of a semi-infinite crack under a spatially-uniform load $P \cos \omega T$, where ω is the frequency of the driving force and P is a constant.

The value of P is selected so that the displacement in the remote part of the string ($X \leq T$) remains less than the critical value. This part of the string performs a uniform forced vibration governed by

$$\frac{d^2 W}{dT^2} + 2M^2 W = M^2 P \cos \omega T, \quad (31)$$

which has the solution

$$W = \frac{M^2 P}{2M^2 - \omega^2} (\cos \omega T - \cos \sqrt{2} MT). \quad (32)$$

Now, for $W < 1$ we have

$$\frac{M^2 P}{2M^2 - \omega^2} (\cos \omega T - \cos \sqrt{2} MT) \leq \frac{2M^2 P}{2M^2 - \omega^2} < 1;$$

i.e. we require

$$P < \frac{2M^2 - \omega^2}{2M^2} = 1 - \frac{\omega^2}{2M^2}. \quad (33)$$

The critical amplitude defined by $P_{cr}^{(1)} = 1 - \frac{\omega^2}{2M^2}$ becomes $1 - 2\omega^2$ for $M^2 = \frac{1}{4}$.

The region O'AB in Figure 27a is again employed for the numerical

(1) P_{cr} has been used earlier to denote critical static load. It is convenient in this section to use the same symbol for the critical amplitude of the periodic load.

computations. The known values along the line $X = T$ (or $j = 0$) and $X = -T$ (or $i = 0$) are:

$$W_{i,0} = \frac{M^2 P}{2M^2 - \omega^2} (\cos \omega T - \cos \sqrt{2} MT) ;$$

$$V_{i,0} = \frac{M^2 P}{2M^2 - \omega^2} (\sqrt{2} M \sin \sqrt{2} MT - \omega \sin \omega T) ; \quad (35)$$

$$\Theta_{i,0} = 0 ;$$

$$Q_{i,0} = 2 W_{i,0} ;$$

and

$$W_{0,j} = \frac{M^2 P}{M^2 - \omega^2} (\cos \omega T - \cos MT) ;$$

$$V_{0,j} = \frac{M^2 P}{M^2 - \omega^2} (M \sin MT - \omega \sin \omega T) ; \quad (35)$$

$$\Theta_{0,j} = 0 ;$$

$$Q_{0,j} = W_{0,j} .$$

It is seen from the above expressions that there are two "resonant" frequencies corresponding to the natural frequencies of the perfect and cracked foundations. They are $\sqrt{2}M$ and M respectively. These resonant frequencies are avoided in the computations. The frequencies of the applied loads considered are above ($\omega = 1.0$ and 0.8), between (0.65 and 0.577) and below (0.4 , 0.2 and 0.1) the resonant frequencies. Higher

frequencies are not considered here because they require finer grid size and consequently longer computation time.

The results (Figures 44-48) show that cracks propagate mainly by the spreading of small secondary cracks. The primary crack extends by a small amount under some driving frequencies whereas on certain occasions it does not extend (See Figure 45). Two basic factors determining the pattern of secondary cracks are the driving frequency ω and the force ratio P/P_{cr} . The frequency has the effect of locating the secondary cracks (Figure 45), and the force ratio seems to dictate their number and size (Figure 44). When the frequency is fixed, it is found that the process of forming new cracks is very sensitive to the ratio P/P_{cr} (Figure 44). Furthermore, there is only a narrow band of load ratios that lead to the formation of secondary cracks. Beneath this band no crack propagation of any form is detected; beyond it, the tensile foundation is completely ruptured. To illustrate this, Figure 44 shows the pattern of secondary cracks for $\omega = 1$ under varying load ratios after approximately 12.7 cycles of the loading. From this figure, we see that below $P = 0.895$ no secondary cracks are formed, nor does the primary crack extend. And, $P = 1$ is the critical value of P which causes the entire foundation to rupture.

In Figure 45 we see the pattern of secondary cracks for fixed P/P_{cr} (0.95) while the driving frequency is varied. For $\omega = 0$ the results coincide with those of suddenly applied load, as expected. When the frequency increases, the pattern changes considerably; as ω goes beyond the lower resonant frequency ($\omega = \frac{1}{2}$), the main crack does not extend and only secondary cracks are formed. Typical displacement histories, string

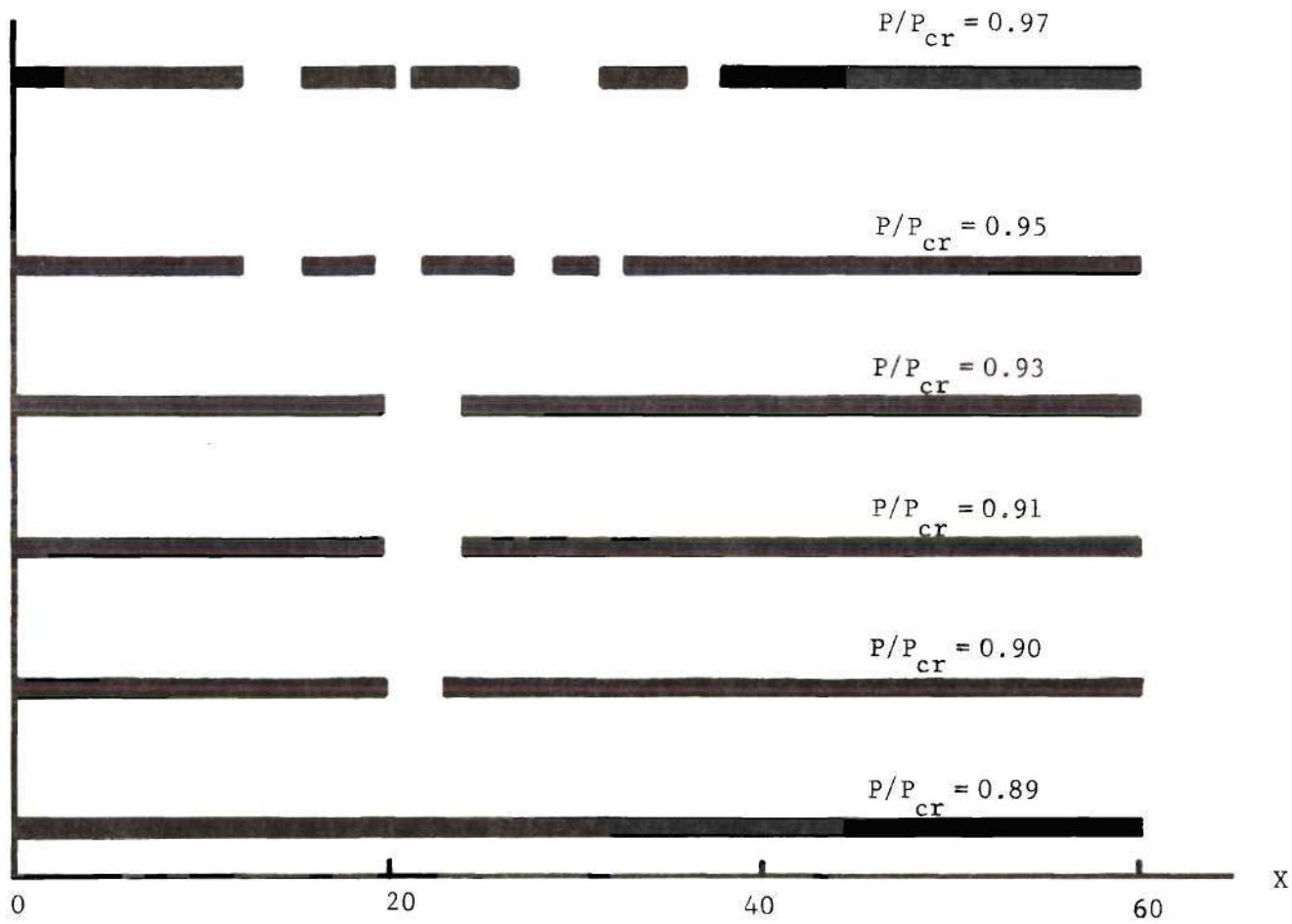


Figure 44. Pattern of Secondary Cracks Under Varying Load Ratios. $\omega = 1$, $T = 80$.

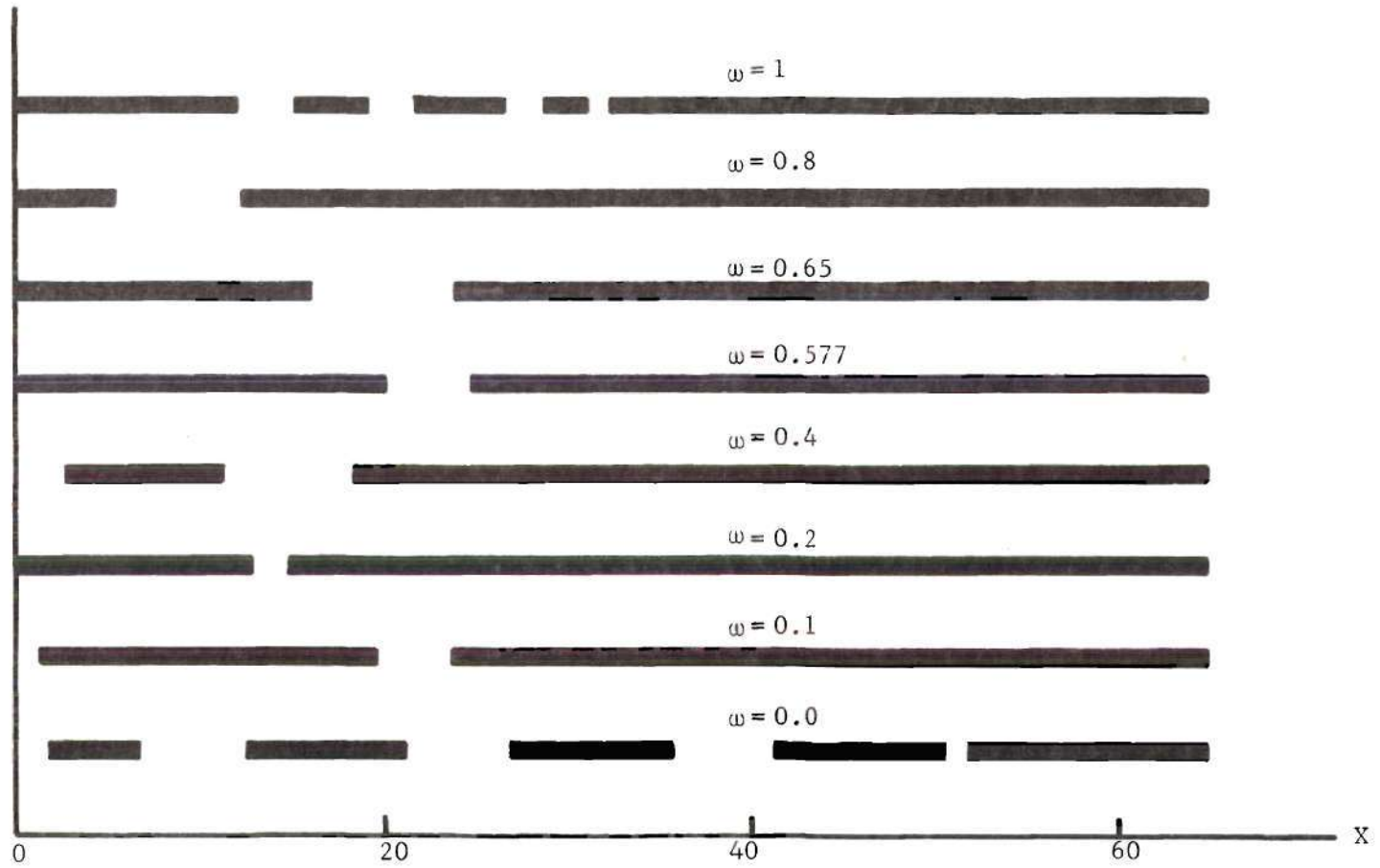


Figure 45. Pattern of Secondary Cracks Under Varying Driving Frequencies.
 $P/P_{cr} = 0.95$, $T = 80$.

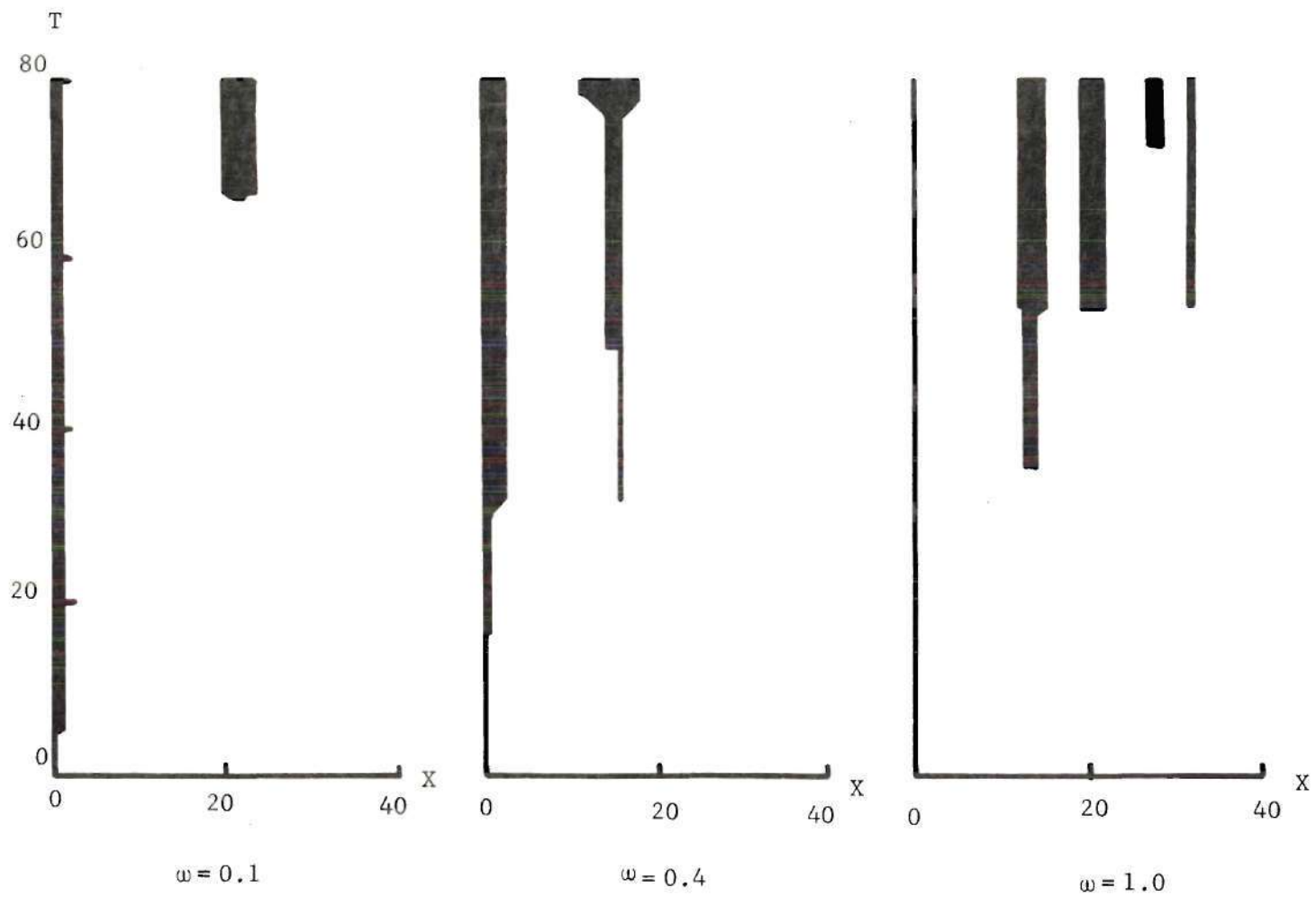


Figure 46. Location of the Cracks. $P/P_{cr} = 0.95$.

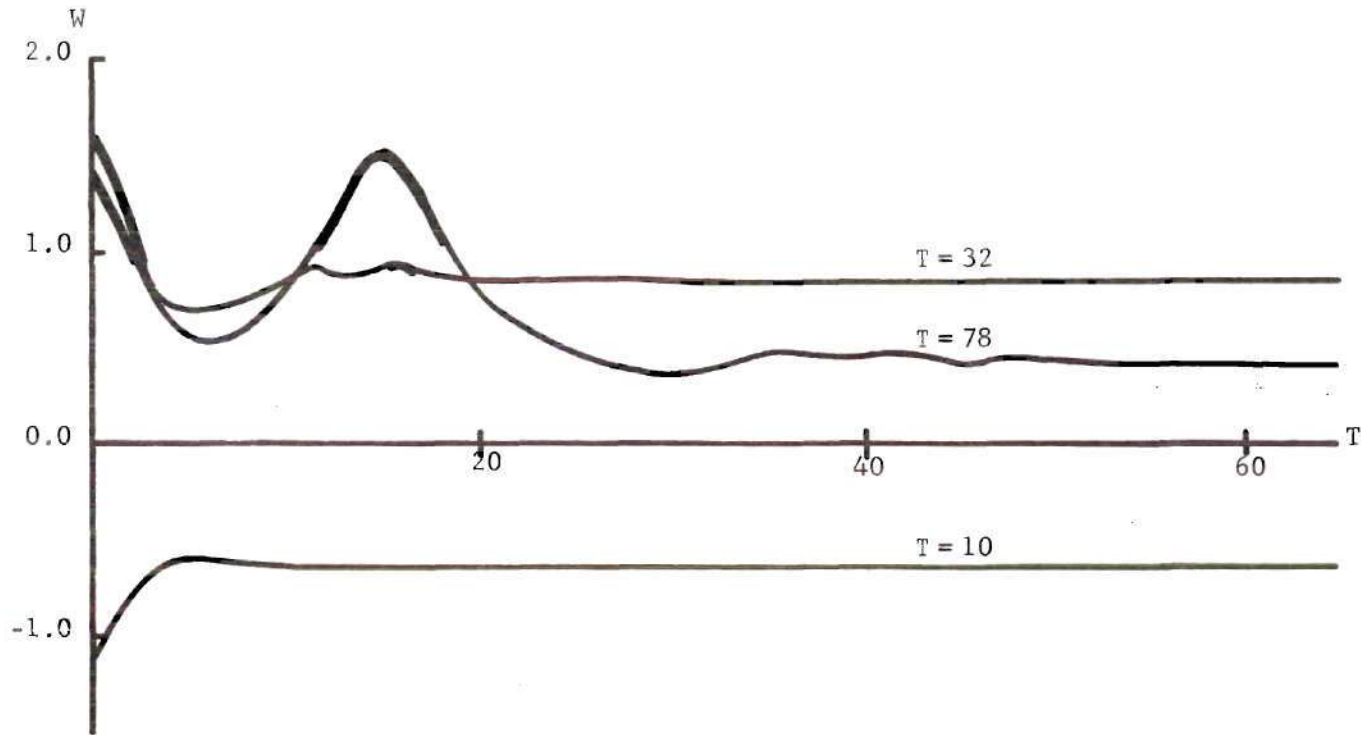


Figure 47. Displacement Profiles of the String at Selected Time. $\omega = 0.4$, $P/P_{cr} = 0.95$.

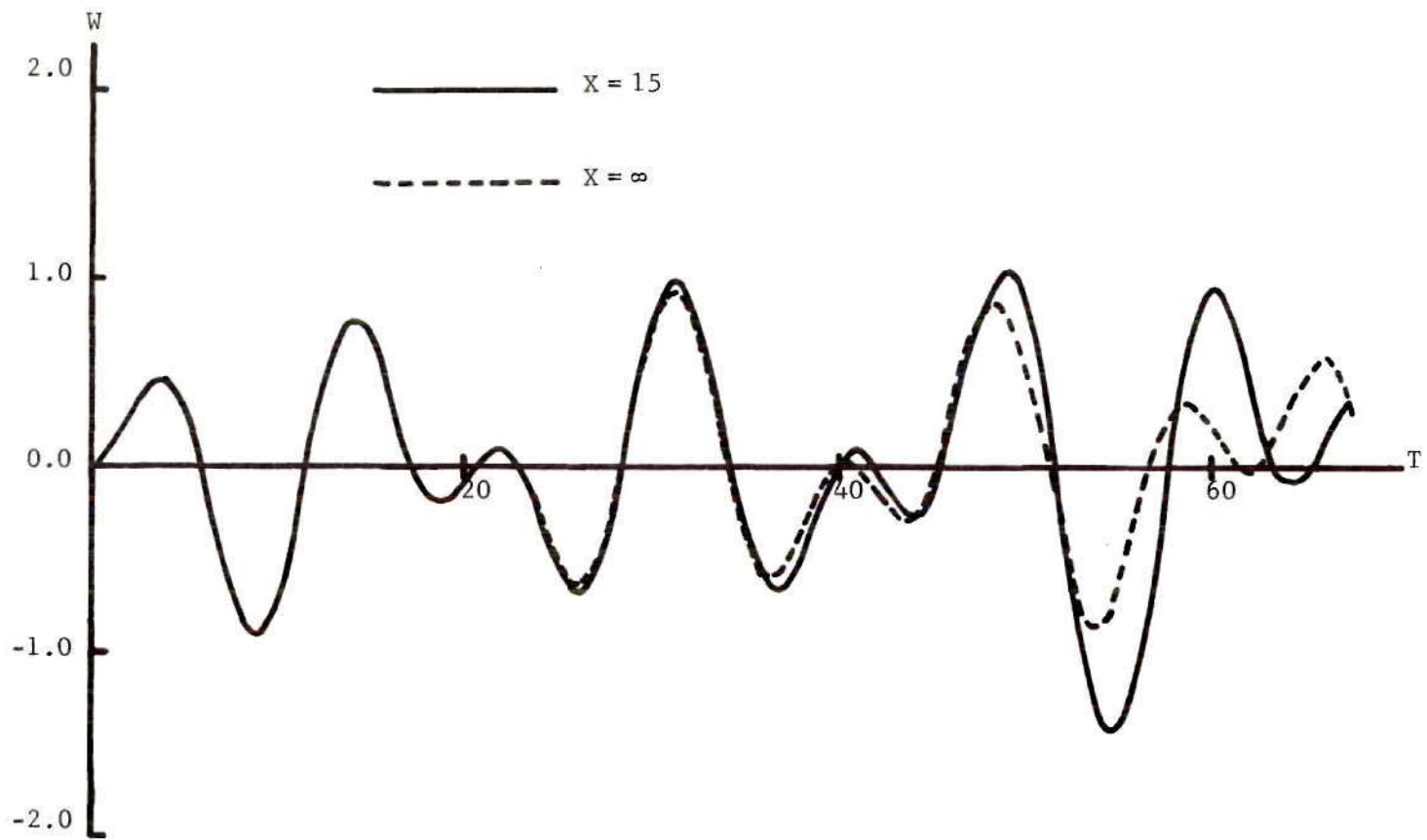


Figure 48. Displacement History at Selected Points on the String. $\omega = 0.4$, $P/P_{cr} = 0.95$.

profiles and crack formations and extensions in the XT plane are indicated in Figures 46-48.

Effects of Small Damping

Most materials exhibit the property of energy dissipation because of internal friction or damping. To take this into consideration for our model we modify the foundations by introducing dashpots as indicated in Figure 49.

If each dashpot has a coefficient of viscosity β' and its corresponding dimensionless parameter is $\beta = \frac{\beta' c w^*}{S}$, then the equation of motion becomes

$$\frac{\partial^2 W}{\partial X^2} - \frac{\partial^2 W}{\partial T^2} = M^2 (2W - P) + 2\beta \frac{\partial W}{\partial T}, \text{ for perfect foundation}$$

$$M^2 (W - P) + \beta \frac{\partial W}{\partial T}, \text{ for fractured foundation}$$
(36)

Thus the dashpot of the tensile foundation ceases to affect the string as soon as the corresponding spring is broken.

For a semi-infinite crack under a suddenly applied load, we can consider the motion of the remote string as a spring-mass-dashpot system. Parts of the string for which $X \geq T$ have the equation of motion

$$\frac{d^2 W}{dT^2} + 2\beta \frac{dW}{dT} + 2M^2 W = M^2 P .$$
(37)

Solutions of this equation depend on the values of β and M . From the theory of vibrations, the critical damping factor β_{cr} is found to be $\beta_{cr}^2 = 2M^2$. For $M^2 = \frac{1}{4}$ we have $\beta_{cr} = \sqrt{2}/2$. Since we are considering the

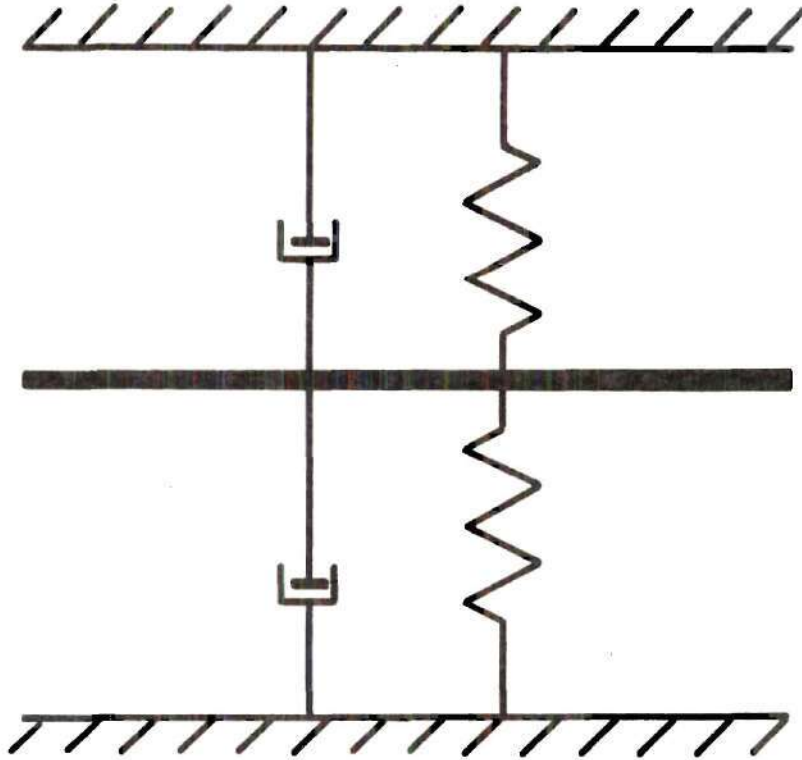


Figure 49. A Modified Model Showing Material Damping Effect.

effects of material damping, the damping factor should be far below β_{cr} .

Therefore, the solution of (37) has the form

$$W = \frac{P}{2} \left\{ 1 - e^{-\beta T} \left(\cos \sqrt{2M^2 - \beta^2} T + \frac{\beta}{\sqrt{2M^2 - \beta^2}} \sin \sqrt{2M^2 - \beta^2} T \right) \right\}$$

and

$$V = \frac{dW}{dT} = \frac{M^2 P}{\sqrt{2M^2 - \beta^2}} e^{-\beta T} \sin \sqrt{2M^2 - \beta^2} T \quad (38)$$

A similar solution for the left hand side of the string ($X \leq -T$) can be obtained.

The amplitude of W decays with increasing time, and we find W has a maximum value at $T = \pi / \sqrt{2M^2 - \beta^2}$. Thus, to satisfy the condition that this displacement in (38) remains less than the critical value, take

$$\frac{P}{2} \left(1 + e^{-\frac{\beta \pi}{\sqrt{2M^2 - \beta^2}}} \right) < 1$$

or

$$P_{cr} = \frac{2}{1 + e^{-\frac{\beta \pi}{\sqrt{2M^2 - \beta^2}}}}$$

In the numerical integration, again we use the region $O'AB$ shown in Figure 27a. We have taken P to be 95% of the critical load given above, for $\beta = 4\%$, 1% , 0.4% and 0.1% of β_{cr} and $M^2 = \frac{1}{4}$. Figures 50-52 show typical results.

Figure 53 indicates the effects of damping on the extension of an existing crack and the formation of new cracks. For the larger values of β , the dynamic response becomes small as time increases (39.3% of it has

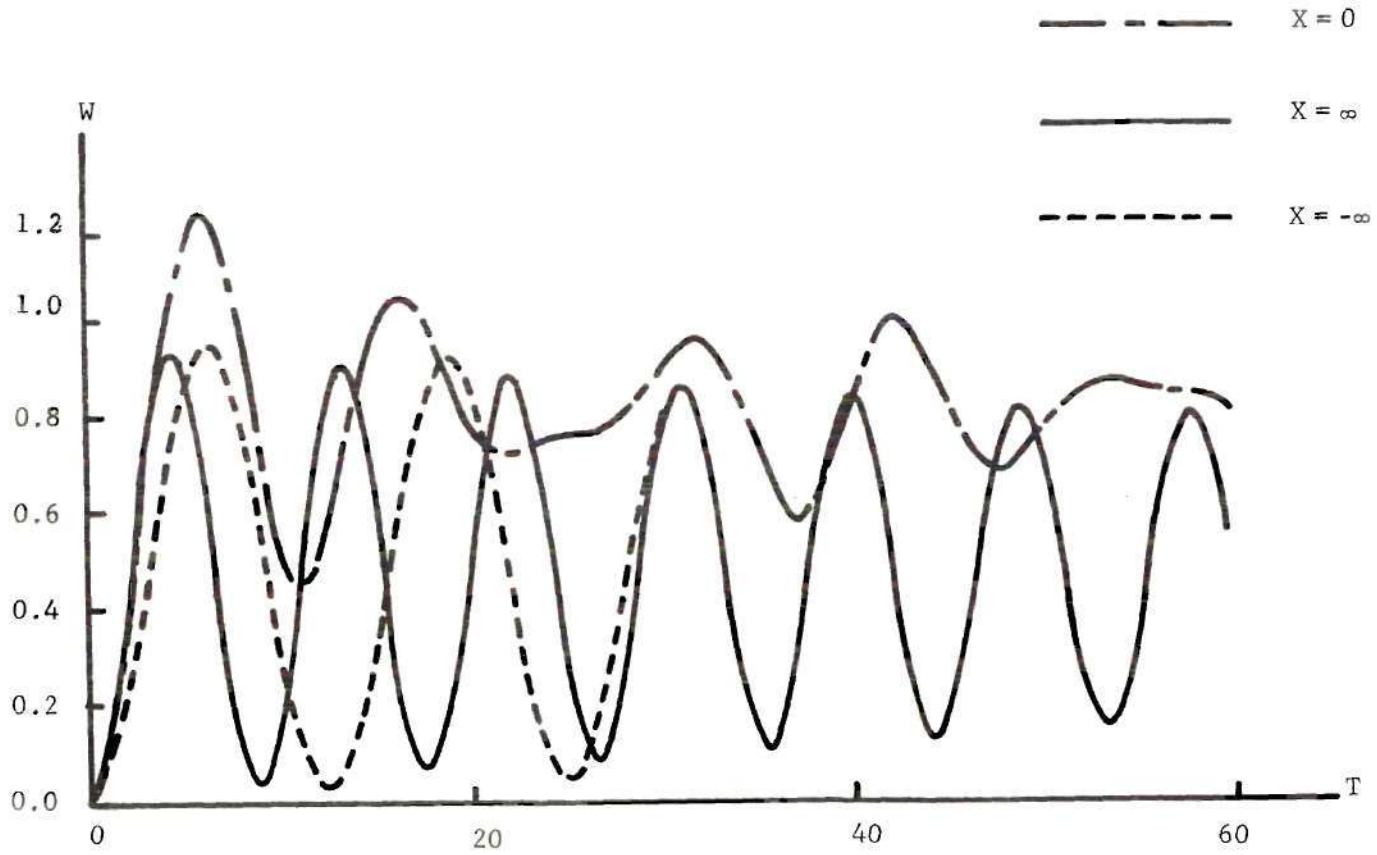


Figure 50. Displacement History at Selected Points on the String. $\beta = 0.01\beta_{cr}$, $P/P_{cr} = 0.95$.

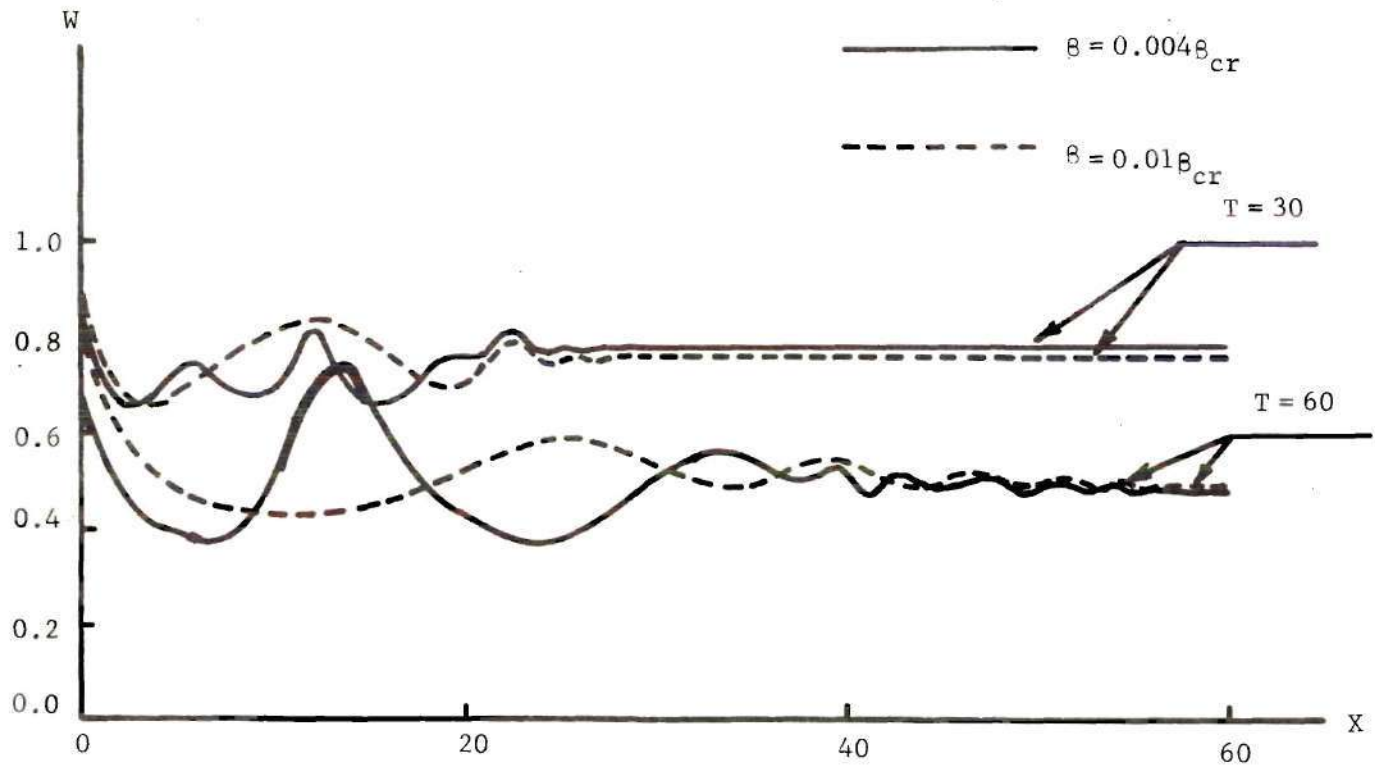


Figure 51. Displacement Profiles of the String at Selected Time. $P/P_{cr} = 0.95$.

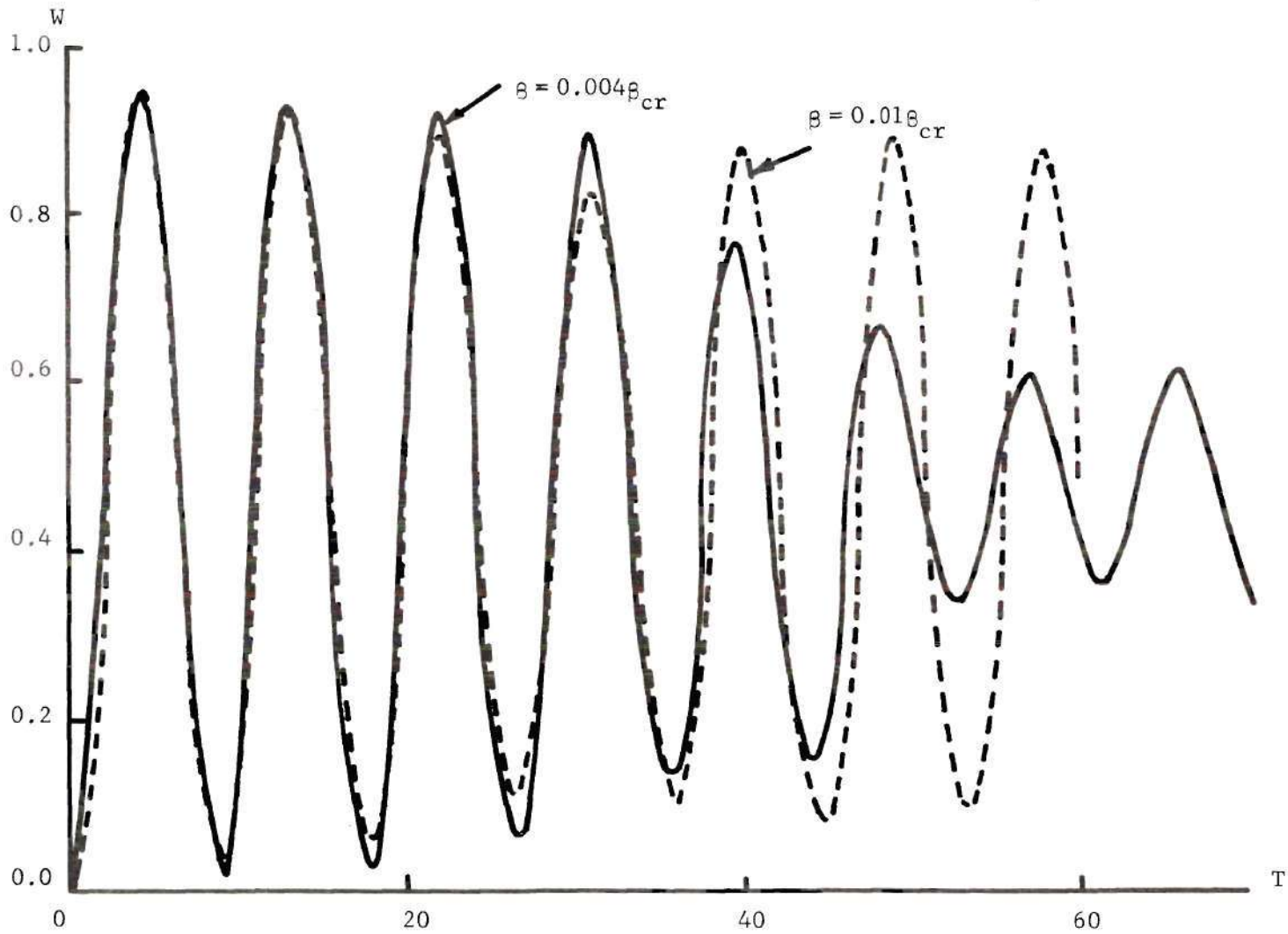


Figure 52. Displacement History at $X = 20$. $P/P_{cr} = 0.95$.

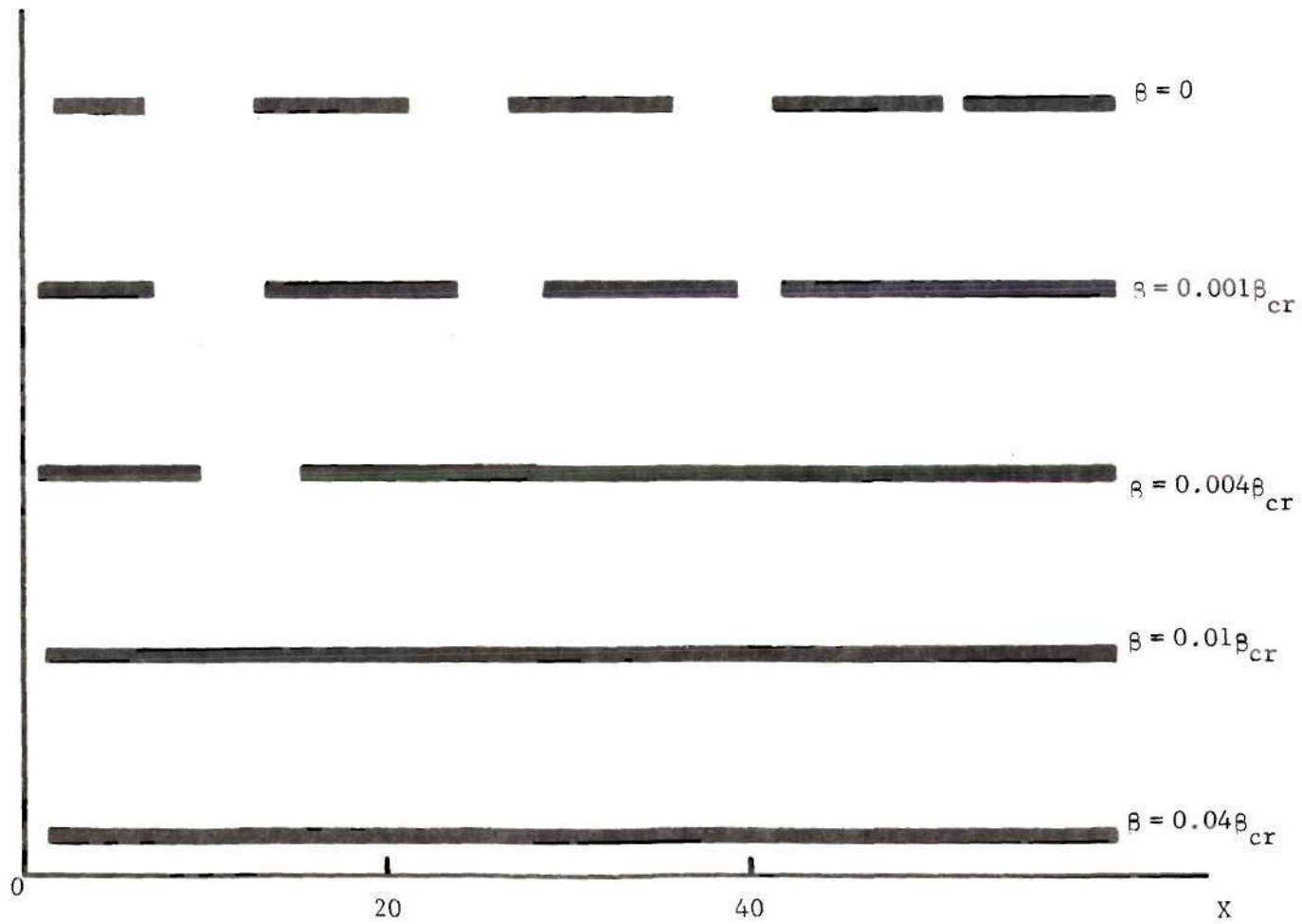


Figure 53. Effect of Damping on the Pattern of Secondary Cracks. $P/P_{cr} = 0.95$. $T = 80$.

been damped out at $T = 76$ for $\beta = 4\%$ of β_{cr}). Thus secondary cracks can hardly be expected to appear. After the main crack has been extended for a small distance, it stops, and the string tends to its equilibrium configuration corresponding to the new crack length. When β is smaller, say 0.1% of β_{cr} , the response tends to that of no damping (only 2.48% of the dynamic response has been damped at $T = 76$). The secondary cracks appear at approximately the same time and place as they did for no damping ($\beta = 0$). To compare these results, we list the data in Table 2.

Table 2. Effect of Damping on the Pattern of Crack Propagation.

$$P = 0.95 P_{cr}$$

$$\beta = 0.004 \beta_{cr}$$

$$\beta = 0.001 \beta_{cr}$$

$$\beta = 0$$

		$\beta = 0.004 \beta_{cr}$					$\beta = 0.001 \beta_{cr}$					$\beta = 0$							
Primary	X	0	0.5				0	0.5				0	0.5	1	1.5				
Crack	T	4.5	5				4.5	5				4	4	4.5	4.5				
Secondary	X	10	11	12	13	14	15	8	9	10	11	12	13	7	8	9	10	11	12
Crack (1)	T	63	31.5	22	22.5	31.5	41.5	53	32	22.5	22.5	22.5	32	53.5	33	13	14	22.4	32
Secondary	X	None					24	25	26	27	28	22	23	24	25	26			
Crack (2)	T	None					59	48.5	49	49.5	59	50	39.5	40	40.5	50			
Secondary	X	None					40	41	36	37	38	39	40	41					
Crack (3)	T	None					75.5	75.5	67.5	57.5	58.5	67	67.5	77.5					
Secondary	X	None					None					51	51.5						
Crack (4)	T	None					None					75.5	76						

CHAPTER V

SUMMARY AND CONCLUSIONS

One of the purposes of this study was to investigate the differences between dynamic and static (or quasi-static) cleavage crack propagation. From the numerical results reported in the preceding chapter, we found that, for the proposed model, an existing crack may propagate in significantly different ways depending on the loading condition.

Continuous crack propagation is obtained when the string is disturbed from its mobile equilibrium position. In this case, when small disturbances are given, the dynamic response is small and the entire process is dominated by the initial configuration. When the load is applied dynamically, the dynamic response becomes more and more important. An existing crack is not likely to propagate continuously.

Crack propagation in real material under dynamic loading is indeed a very complicated phenomenon. Literature dealing with analytical aspects is almost nonexistent. Past researches, such as the works of Yoffe, Craggs and Broberg, emphasized Griffith's work. In fact, all these analyses are based on the assumption that under a critical load an existing crack can propagate continuously at a constant speed. This constant speed of crack propagation is assumed to be achieved independently of how the critical load is originally applied. However, for the present model, the transient state of crack extension, which depends on the loading situation, seems important to the subsequent propagation,

and continuous crack propagation may not be attained.

In the case of dynamic loading, we find from Chapter IV that the critical loads are far below the quasi-static one. As an example, for the semi-infinite crack problem the quasi-static critical load is 1.414; on the other hand, if the load is suddenly applied and maintained it is 0.76. Furthermore, when $P = 1$, the entire foundation will be ruptured. By comparing these critical loads, we may conclude that under dynamic loading, although a crack can be extended a very short distance, the total energy input is not sufficient for further propagation of the crack. But the dynamic response superimposed with the waves emitted from the crack tip may cause the formation of secondary cracks in front of the primary crack. Once these secondary cracks are formed, they themselves emit waves which further complicate the process.

Cracks that do not propagate continuously have been detected experimentally. Van Elst [17] shows in his research that the emission of stress waves by a brittle crack seems only conceivable if the fracture propagates by discrete steps. In an analysis of his photographs, Van Elst suggests that a brittle fracture does not propagate continuously but rather intermittently as a sequence of individual steps with the contour of the crack appearing as a broken line instead of a smooth line. Evidence of spreading microcracks ahead of a primary crack has also been found by Pratt and Stock [18] in their experiments concerning crack propagation in semi-brittle materials. In more recent research of crack propagation in composite materials, Daniel [19] found hairline traces extending beyond the ends of a visible crack. An explanation of

these traces is that molecular bonds are broken in the region due to the high dynamic stress.

In the Appendix, we have attempted to solve the equation of motion analytically. In view of the existence of secondary cracks, we may conclude that Kostrov's method is not applicable to the present problem. From the resulting integral equation of this analysis, and if we expect secondary cracks to form during the process, we can see that the integral is along an undefined path of crack propagation which is not continuous in the XT plane. Furthermore, if the crack extends as a sequence of individual steps, the displacement at the crack tip varies with time. Thus the assumption, that the crack tip displacement is always the critical value, of Equation (A-20) is not valid. Under these circumstances, a solution of the integral equation is likely to be very difficult to obtain.

The method of characteristics employed in Chapter IV allows numerical solution of the problem. Since the fracture criterion is built into the model, the crack is found to extend or new cracks are found to form by detecting the displacement history. Thus, the character of the crack propagation is obtained as a result and not prescribed in advance.

To determine the accuracy of the numerical integration, we compared the displacement and velocity of the remote part of the string with the exact solution for a single spring-mass system. We found that the grid size of the characteristic net, which is governed by the elementary time ΔT , dominates the accuracy of the numerical integration. For example, in the periodic loading cases, for $\Delta T = 1$ the error is

about four per cent per cycle. This is a large discrepancy, because the error is cumulative as the region of integration expands to cover several cycles of vibration. Such an error will completely change the pattern of the string motion and consequently the crack propagation. To overcome this, we reduced the grid size. With $\Delta T = 1/4$, the error diminished to less than 0.1%. Further shrinkage of the grid size would further improve the results, but at a price of a significant increase in computation time, since the number of computations is inversely proportional to the square of ΔT . In the actual computation, we adjusted the values of dependent variables in the remote part of the string by prescribing the exact solutions. By so doing, the number of computations was considerably reduced.

In Chapter II, we discussed two possible forms of the foundation law, but in the later development, only the linear-with-cut-off law was used because static solutions for the sine law are difficult to evaluate. In order to examine the importance of different foundation laws, a solution for the sine law for a suddenly applied and maintained load was obtained by numerical integration. For this foundation law, the critical displacement is $\pi/2$ and the corresponding critical load is approximately 1.14. When loads of magnitude between 1.00 and 1.10 are applied, we found that the dominant features of crack propagation do not change significantly. When the load is small, the primary crack extends only a small distance. If the load is increased, in addition to this extension, we found secondary cracks. This indicates that different foundation laws may affect the value of the critical load and the location of the secondary cracks. But the overall character of the crack propagation

is similar to that predicted by linear law.

When viscous damping was introduced in our model, we found that if it was sufficiently large, the secondary cracks did not appear and the dynamic loading caused the main crack to extend for only a small distance. As the damping was reduced, the secondary cracks were found again. The crack propagation features tended to those with no damping as the damping factor approached zero.

To examine two-dimensional crack propagation in brittle crystalline solids, the Goodier-Kanninen model may be a useful tool for analysis. Hovis [20] has investigated a dynamic crack propagation problem by employing such a model. But his problem is steady like Yoffe's; i.e. a crack of constant length travels through an infinite plate with prescribed constant speed. We suggest formulating an unsteady problem based on the Goodier-Kanninen model and attempting a solution through the two-dimensional (space) method of characteristics.

APPENDIX

A FORMAL SOLUTION OF THE EQUATION OF MOTION

In this appendix we attempt to obtain an analytical solution of the equation of motion. Through the method of Riemann-Volterra, this equation can be transformed into the form of an integral equation.

Consider the nondimensional equation of motion

$$\frac{\partial^2 W}{\partial X^2} - \frac{\partial^2 W}{\partial T^2} - M^2(Q_1 + Q_2 - P) = 0. \quad (A-1)$$

Since the reaction of the compressive foundation can always be written as $Q_2 = W$, we can write this equation as

$$\frac{\partial^2 W}{\partial X^2} - \frac{\partial^2 W}{\partial T^2} - M^2 W = M^2 K, \quad (A-2)$$

where $K = Q_1 - P$ is the resultant lineal force of the tensile foundation reaction and the applied load. The loading function P here and throughout this section is considered as constant. Suppose that K is an unknown function of the independent variables X and T ; i.e. $K = K(X, T)$.

Equation (A-2) is a hyperbolic partial differential equation; its normal form can be obtained through the transformations

$$\alpha = M(T + X) \quad \text{and} \quad \beta = M(T - X). \quad (A-3)$$

The transformed equation is

$$\frac{\partial^2 W}{\partial \alpha \partial \beta} + \frac{W}{4} = -\frac{K}{4}. \quad (A-4)$$

Equation (A-4) is known as the normal form of a Telegraphist's equation with a nonhomogeneous part $-\frac{K}{4}$ ⁽¹⁾. The characteristics of this equation in the $\alpha\beta$ plane are found to be

$$\alpha = \text{constant} \quad \text{and} \quad \beta = \text{constant} . \quad (\text{A-5})$$

Now define a differential operator L by

$$L = \frac{\partial^2}{\partial\alpha\partial\beta} + \frac{1}{4} . \quad (\text{A-6})$$

Then the equation of motion becomes

$$L(W) = -\frac{K}{4} . \quad (\text{A-7})$$

Let N be the adjoint operator of L. Since (A-4) is self-adjoint, $L \equiv N$. The Green's formula can be written as

$$\begin{aligned} & \iint_R [u L(W) - W N(u)] \, d\alpha d\beta \\ &= \int_{\Gamma} \left\{ \frac{W}{2} \left[\frac{\partial u}{\partial\beta} \cos(n\alpha) + \frac{\partial u}{\partial\alpha} \cos(n\beta) \right] \right. \\ & \quad \left. - \frac{u}{2} \left[\frac{\partial W}{\partial\beta} \cos(n\alpha) + \frac{\partial W}{\partial\alpha} \cos(n\beta) \right] \right\} ds, \quad (\text{A-8}) \end{aligned}$$

in which u is a solution of the adjoint differential equation. Γ is a closed contour formed by the characteristics and a curve on which sufficient data are given. In the present case this curve is $\alpha = -\beta$ ($T = 0$) and the given data are initial conditions. R represents the region

(1) See A. G. Webster, "Partial Differential Equations of Mathematical Physics", 2nd Edition, Dover Publications, 1955. Chapter VI.

bounded by Γ ; n is the inward normal of Γ and s is the line segment along Γ in counterclockwise sense. Figure A-1 shows such a region.

Referring to Figure A-1, we write

$$\int_{\Gamma} \left\{ \quad \right\} ds = \int_{\rho}^A + \int_A^B + \int_B^{\rho}, \quad (\text{A-9})$$

where the integrands are identical to those inside the line integral in (A-8). The integrals can now be evaluated separately as follows. Along ρA we have $d\beta = 0$ and $ds = -d\alpha$ so that

$$\cos(n\alpha) = 0 \quad \text{and} \quad \cos(n\beta) = -1. \quad (\text{A-9})$$

$$\begin{aligned} \int_{\rho}^A \left\{ \quad \right\} dr &= \frac{1}{2} \int_{\rho}^A \left(W \frac{\partial u}{\partial \alpha} - u \frac{\partial W}{\partial \alpha} \right) d\alpha \\ &= \frac{1}{2} \left[\int_{\rho}^A W \frac{\partial u}{\partial \alpha} d\alpha - uW \Big|_{\rho}^A + \int_{\rho}^A W \frac{\partial u}{\partial \alpha} d\alpha \right] \\ &= \frac{1}{2} \left[u(\rho)W(\rho) - u(A)W(A) \right] + \int_{\rho}^A W \frac{\partial u}{\partial \alpha} d\alpha. \end{aligned} \quad (\text{a})$$

Similarly,

$$\int_A^B \left\{ \quad \right\} dp = \frac{1}{2} \int_A^B \left\{ W \left(\frac{\partial u}{\partial \beta} + \frac{\partial u}{\partial \alpha} \right) - u \left(\frac{\partial W}{\partial \beta} + \frac{\partial W}{\partial \alpha} \right) \right\} d\alpha, \quad (\text{b})$$

and

$$\int_B^{\rho} \left\{ \quad \right\} dp = \frac{1}{2} \left[u(\rho)W(\rho) - u(B)W(B) \right] - \int_B^{\rho} W \frac{\partial u}{\partial \beta} d\beta. \quad (\text{c})$$

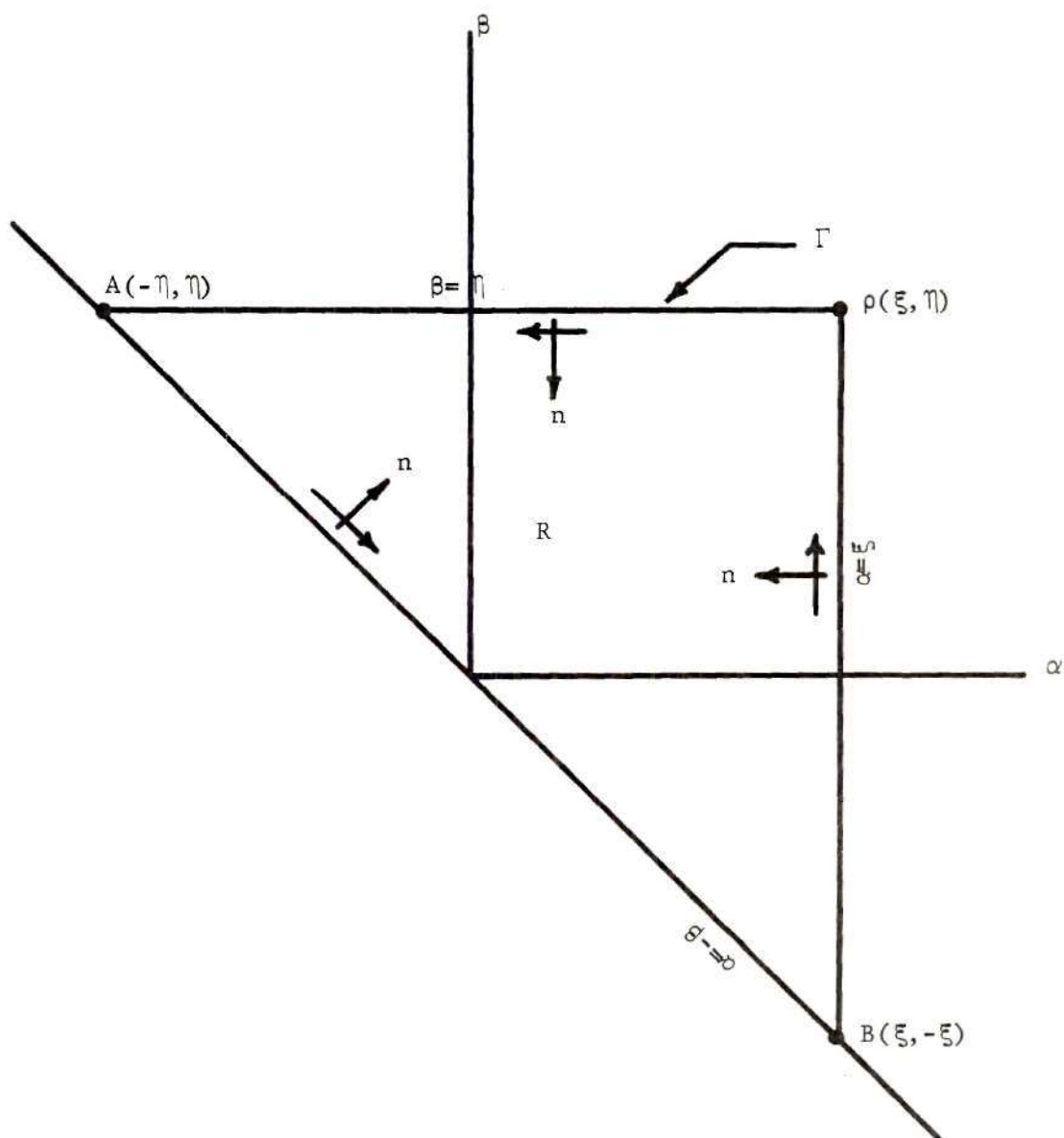


Figure A-1 Region of Integration for Equation (A-8).

Substituting (a), (b) and (c) into (A-8) we have

$$\begin{aligned}
 & \iint_R [uL(W) - WN(u)] d\alpha d\beta \\
 &= U(\rho)W(\rho) - \frac{1}{2}[u(A)W(A) + u(B)W(B)] \\
 & \quad + \int_{\rho}^A W \frac{\partial u}{\partial \alpha} d\alpha - \int_B^{\rho} W \frac{\partial u}{\partial \beta} d\alpha \\
 & + \frac{1}{2} \int_A^B \left\{ W \left(\frac{\partial u}{\partial \beta} + \frac{\partial u}{\partial \alpha} \right) - u \left(\frac{\partial W}{\partial \beta} + \frac{\partial W}{\partial \alpha} \right) \right\} d\alpha . \tag{A-10}
 \end{aligned}$$

Now let u be a particular solution of the adjoint homogeneous equation

$$N(u) = 0 . \tag{A-11}$$

Without losing any generality, we now choose a particular solution, G , satisfying the following conditions:

$$\frac{\partial G}{\partial \alpha} = 0 \quad , \quad \text{along } \rho A \quad ; \tag{d}$$

$$\frac{\partial G}{\partial \beta} = 0 \quad , \quad \text{along } B\rho \quad ; \tag{e}$$

$$G(\xi, \eta) = 1 \quad , \quad \text{at } \rho(\xi, \eta) . \tag{f}$$

A function of $\varphi = (\xi - \alpha)(\eta - \beta)$ satisfies (d) and (e) identically. To satisfy (A-11), we let $G = G(\varphi)$. Then (A-11) becomes

$$\varphi \frac{d^2 G}{d\varphi^2} + \frac{dG}{d\varphi} + \frac{G}{4} = 0 . \tag{A-12}$$

(A-12) is an ordinary differential equation for G . To solve this equation, we make another transformation by letting

$$\varphi = \psi^2 .$$

Equation (A-12) now becomes a Bessel's equation of zero order; i.e.

$$\frac{d^2 G}{d\Psi^2} + \frac{1}{\Psi} \frac{dG}{d\Psi} + G = 0 . \quad (\text{A-13})$$

The solution of this equation is

$$G = J_0(\psi) = J_0\left(\sqrt{(\xi-\alpha)(\eta-\beta)}\right). \quad (\text{A-14})$$

Note that the condition (f) is now satisfied.

Suppose that the initial conditions can be written as

$$W(X, 0) = h(X) \quad (\text{A-15})$$

and

$$\frac{\partial W}{\partial T}(X, 0) = g(X).$$

Then after certain algebraic manipulations and transforming back to the original variable (X and T), we have

$$\begin{aligned} W(\lambda, \tau) &= \frac{1}{2}[h(\lambda-\tau) + h(\lambda+\tau)] \\ &+ \frac{M\tau}{2} \int_{\lambda-\lambda}^{\lambda+\tau} h(X) \frac{J_0' \left(M \sqrt{(\tau-T)^2 - (\lambda-X)^2} \right)}{\sqrt{(\tau-T)^2 - (\lambda-X)^2}} dX \\ &+ \frac{1}{2} \int_{\lambda-\tau}^{\lambda+\tau} g(X) J_0 \left(M \sqrt{(\tau-T)^2 - (\lambda-X)^2} \right) dX \\ &- \frac{1}{4} \iint_R K J_0 \left(M \sqrt{(\tau-T)^2 - (\lambda-X)^2} \right) dXdT , \end{aligned} \quad (\text{A-16})$$

where λ and τ are the corresponding coordinates of ξ and η in the XT plane.

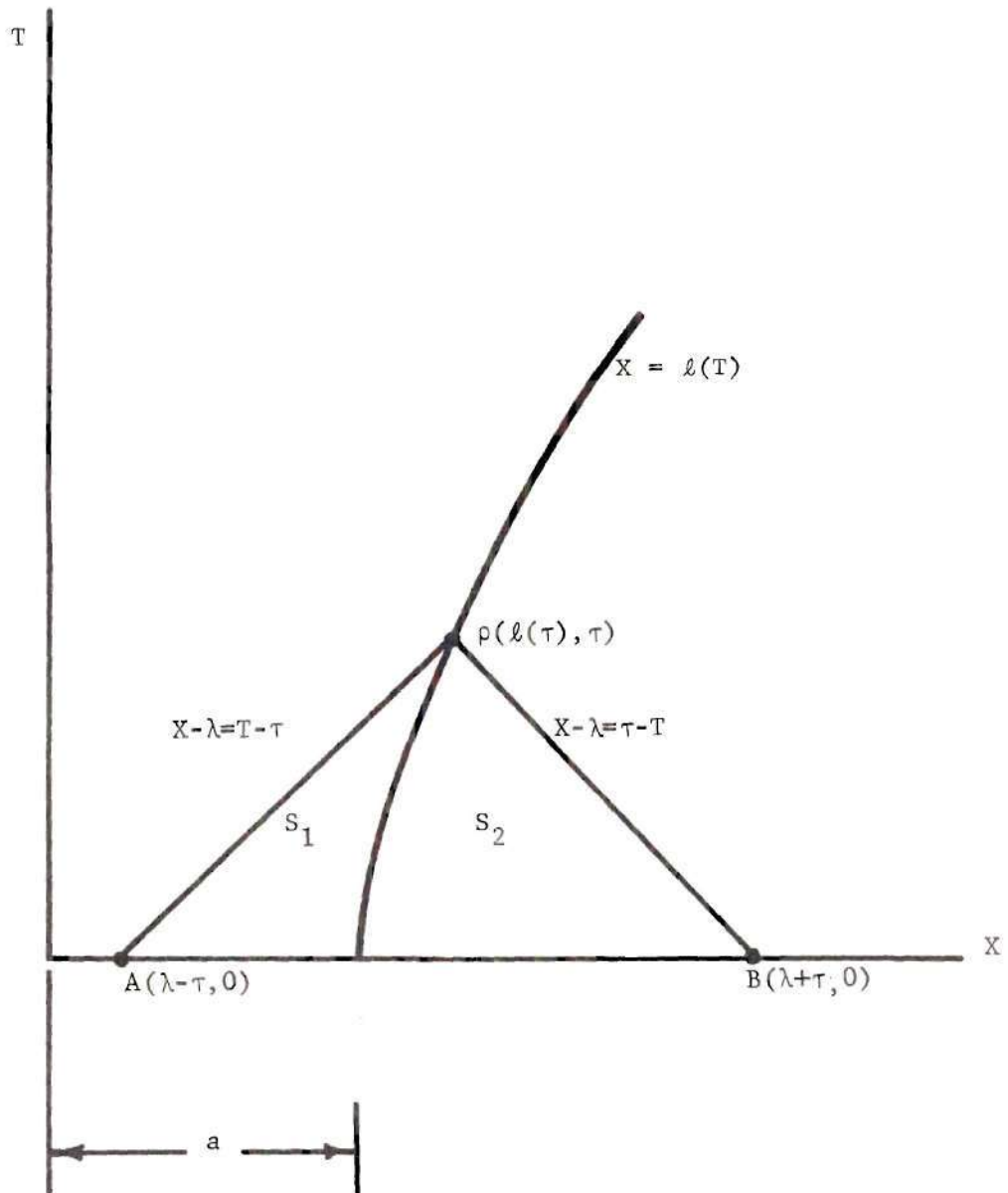


Figure A-2 The Path of the Crack Tip Divides R into S_1 and S_2 .

Consider now that there exists an initial crack and it propagates continuously so that the crack tip traces a curve represented by $X = \ell(T)$ in Figure A-2. If we fix the point under consideration, $\rho(X, T)$, at the crack tip, then $\lambda = \ell(\tau)$ and $\rho = \rho(\ell(\tau), \tau)$. In Figure A-2, the curve $X = \ell(T)$ divides the region R into two subregions S_1 and S_2 . In S_1 the tensile foundation is fractured. Whereas in S_2 , we have $Q_1 = W$. Thus

$$\begin{aligned} K_1 &= P, & \text{in } S_1 \\ K &= & \\ k_2 &= P + W, & \text{in } S_2 \end{aligned} \quad (A-17)$$

The surface integral in (A-16) can then be written as

$$\begin{aligned} \iint_R K J_0(\sqrt{\varphi}) \, dXdT &= P \iint_R J_0(\sqrt{\varphi}) \, dXdT + \iint_S W J_0(\sqrt{\varphi}) \, dXdT \\ &= P \int_0^\tau \int_{\ell(\tau) - \tau + T}^{\ell(\tau) + \tau - T} J_0(\sqrt{\varphi}) \, dXdT \\ &\quad + \int_0^\tau \int_{\ell(\tau)}^{\ell(\tau) + \tau - T} W(X, T) J_0(\sqrt{\varphi}) \, dXdT. \end{aligned} \quad (A-18)$$

In (A-17), the function φ , has been transformed to the XT plane which has the form

$$\varphi(X, T) = M^2 [(\tau - T)^2 - (\lambda - X)^2].$$

When the surface integral of (A-18) is substituted into (A-16) we finally obtain an integral equation for the displacement function $W(X, T)$. If the functions $h(X)$ and $g(X)$ are given, one may expect a solution of W in terms of the crack length $\ell(\tau)$. But since $\ell(\tau)$ is not a prescribed

function, the solution can not be considered as complete. Since the purpose of this section is not to obtain a complete solution of the equation of motion, we limit our analysis to the formal solution in the form of an integral equation (A-16).

Since the anti-plane crack problem is governed by a single wave equation similar to the present equation of motion, it is interesting to compare these two problems. Kostrov treated the wave equation analytically by the method of Volterra which is similar to the method discussed in this section. He obtained a formal solution of the displacement function, w , in terms of the unknown shear stress τ . His solution is given below.

$$w(x_0, t_0) = \frac{1}{\pi} \iint_{S_0} \tau(x, t) \frac{dxdt}{\sqrt{(t_0-t)^2 - (x_0-x)^2}} \quad (A-19)$$

Kostrov transformed this equation into Abel's integral equation, invoked Barenblatt's crack extension criterion and obtained numerical results for two special problems.

In order to compare the two problems, we introduce a special case by assuming that the crack tip moves continuously, so that its displacement always assumes the critical value; i.e. $W(\ell(\tau), \tau) \equiv 1$. As in Kostrov's problem, if we take the initial values to be

$$f(X) \equiv 0 \quad \text{and} \quad g(X) \equiv 0 ,$$

then Equations (A-16) and (A-18) reduce to

$$\frac{P}{4} \int_0^{\tau} \int_{\ell(\tau)}^{\ell(\tau) + \tau - T} \int_0^{\tau} \int_{\ell(\tau) - \tau + T} J_0(\sqrt{\varphi}) \, dXdT$$

$$+ \frac{1}{4} \int_0^{\tau} \int_{\ell(\tau)}^{\ell(\tau) + \tau - T} W(X,T) J_0(\sqrt{\varphi}) \, dXdT = -1 . \quad (\text{A-20})$$

Even in this simple form, obtaining a solution of Equation (A-20) is a formidable task. Because not only is $W(X,T)$ an unknown function but also $\ell(\tau)$, which appears in the integration limits. After obtaining Equation (A-18), Kostrov treated his problem by employing two additional conditions. They are: (1) the anti-symmetry of the displacement, that is w is identically zero at points on the prolongation of the crack; and (2) the general Barenblatt criterion, which ignores the actual distribution of the cohesive forces near the crack tip. In the present problem, however, these conditions are not applicable, since W is not known beforehand at any point, except perhaps at the crack tip as in (A-20). Furthermore, the foundation reactions and therefore the displacement must be known at all points because the criterion of crack extension is defined by a critical value of displacement.

LITERATURE CITED

1. Griffith, A. A., The Phenomena of Rupture and Flow in Solids, Philosophical Transactions, Royal Society (London), Series A., Vol. 221, 1920, pp. 163-198.
2. Inglis, C. E., Stresses in a Plate due to the Presence of Cracks and Sharp Corners, Transactions, Institution of Naval Architects, Vol. 60, 1913, pp. 219-230.
3. Goodier, J. N., Mathematical Theory of Equilibrium Cracks, in Fracture, (H. Liebowitz, ed.) Vol. II, Academic Press, 1968, pp. 1-66.
4. Irwin, G. R., Fracture Dynamics, in Fracture of Metals, ASM, Cleveland, Ohio, 1948, pp. 147-166.
5. Orowan, E. O., Fundamentals of Brittle Behavior of Metals, in Fatigue and Fracture of Metals, (W. M. Murray, ed.), Wiley, N. Y., 1950. pp. 139-167.
6. Barenblatt, G. I., The Mathematical Theory of Equilibrium Cracks in Brittle Fracture, Advances in Applied Mechanics, Vol. 7, Academic Press, 1962, pp. 55-129.
7. Goodier, J. N. and Kanninen, M. F., Crack Propagation in a Continuum Model with Nonlinear Atomic Separation Laws, ONR Tech. Report, No. 165, 1966.
8. Mott, N. F., Fracture of Metals: Theoretical Considerations, Engineering, Vol. 165, 1948, pp. 16-18.
9. Yoffe, E. H., The Moving Griffith Crack, Philosophical Magazine, Vol. 42, Series M, 1950, pp. 739-750.
10. Broberg, K. B., The Propagation of a Brittle Crack, Arkiv For Fysik, Vol. 18, 1960, pp. 159-192.
11. Craggs, J. W., On the Propagation of a Crack in an Elastic-Brittle Material, Journal of the Mechanics and Physics of Solids, Vol. 8, 1960, pp. 66-75.
12. Ang, D. D., Elastic Waves Generated by a Force Moving Along a Crack, Journal of Mathematics and Physics, Vol. 38, 1960, pp. 246-256.
13. Baker, B. R., Dynamic Stresses Created by a Moving Crack, Journal of Applied Mechanics, Vol. 29, Transactions, ASME, Vol. 84, Series 3, 1962, pp. 449-454.

14. Erdogan, F., Crack Propagation Theories, in Fracture, (H. Liebowitz, ed.), Vol. II, Academic Press, 1968, pp. 497-560.
15. Kostrov, B. V., Unsteady Propagation of Longitudinal Shear Cracks, Journal of Applied Mathematics and Mechanics, Vol. 30, No. 6, 1966, pp. 1042-1049.
16. Eshelby, J. D., The Elastic Field of a Crack Extending Non-uniformly Under General Anti-plane Loading, Journal of the Mechanics and Physics of Solids, Vol. 17, 1969, pp. 177-199.
17. Van Elst, H. C., The Intermittent Propagation of Brittle Fracture in Steel, Transactions of the Metallurgical Society of AIME, Vol. 230(3), 1964, pp. 460-469.
18. Pratt, P. L. and Stock, T. C. A., The Distribution of Strain about a Running Crack, Proceedings, Royal Society, Vol. 285(A), 1965, pp. 73-82.
19. Daniel, I. M., Photoelastic Study of Crack Propagation in Composite Models, Journal of Composite Materials, Vol. 4, Apr. 1970, pp 178-190.
20. Hovis, D. W., Dynamic Crack Propagation According to Nonlinear Atomic Separation Laws, Ph.D. Thesis, Stanford University, 1969.

VITA

Han Pin Kan was born in Kwang-Tung, China, on August 10, 1940. He received his Bachelor of Science degree in Hydraulic Engineering from Taiwan Provincial Cheng-Kung University in June 1963. He enlisted in the Chinese Army in November 1963 and served for one year. He enrolled as a graduate student at Tennessee Technological University in September, 1965, and received a Master of Science degree in Engineering Mechanics in December 1966. He has pursued graduate study in the School of Engineering Science and Mechanics at the Georgia Institute of Technology since March, 1967.

On December 24, 1969, he married Della Min-Tze Chen of Taiwan, China.